HUMAN WHARTON'S JELLY STEM CELLS AND/OR ITS EXTRACT FOR THE MANAGEMENT OF HEMATOLOGICAL MALIGNANCIES AND BLOOD DISORDERS

LIN HAO DANIEL

(*B.Sci.Hons.*), NTU

A THESIS SUBMITTED FOR THE DEGREE OF

DOCTOR OF PHILOSOPHY

DEPARTMENT OF OBSTETRICS AND GYNAECOLOGY

NATIONAL UNIVERSITY OF SINGAPORE

2015

DECLARATION

I hereby declare that the thesis is my original work and it has been written by me in its entirety.

I have duly acknowledged all the sources of information which have been used in the thesis.

This thesis has also not been submitted for any degree in any university previously.

_____

LIN HAO DANIEL

16th January 2015

ACKNOWLEDGEMENTS

The work presented in this thesis describes the laboratory research undertaken by me at the Department of Obstetrics and Gynecology, Yong Loo Lin School of Medicine, National University of Singapore (NUS), from January 2011 to January 2015. Throughout this period of time, I was supported by a research scholarship from NUS, and funding from National Medical Research Council, Singapore.

Firstly, I would like to express my deepest gratitude and appreciation to my supervisors Associate Professor Fong Chui Yee, Associate Professor Mahesh Choolani and Dr Kalamegam Gauthaman (ex-supervisor) for their continuous guidance, support and trust over the last four years. I am also deeply grateful to my Thesis Advisory Committee Chairman, Professor Ariff Bongso, for his continuous encouragement, knowledge sharing and invaluable advice all the time.

Secondly, I would like to thank my laboratory colleagues, Arjunan Subramanian, Huang Zhouwei, Kimerberly Tam, Suganya C.A. and Akshaya Srinivasan for their help, support and wonderful times in the laboratory. I would also like to thank all other staff and students in the Department of Obstetrics and Gynecology for their kind help throughout the four years.

Finally, special thanks to my parents, family and friends for their encouragement and support throughout my candidature.

TABLE OF CONTENTS

SUMMARY

A novel primitive stem cell from the Wharton's jelly of the human umbilical cord (hWJSCs) has been derived and characterized. Although these hWJSCs share the same developmental origins as adult human bone marrow mesenchymal stem cells (BMMSCs) and possess low level expression of embryonic stem cell markers, they do not induce tumorigenesis in laboratory animals, primates and humans and do not transform to tumor-associated fibroblasts. There have been no reports of any toxicity or side effects when hWJSCs were injected into laboratory animals, non-human primates and in human clinical trials for the treatment of aplastic anemia, leukemia, type 1 diabetes mellitus, heart failure and neurological disorders. This suggests that hWJSCs or its extracts have the potential to be used clinically. Numerous independent reports have confirmed hWJSCs paradoxical tumoricidal properties both *in vitro* and *in vivo* on mammary adenocarcinoma, ovarian carcinoma, osteosarcoma, cholangiocarcinoma and bladder carcinoma. Being similar to BMMSCs, hWJSCs could also provide the structural and physiological support for self renewal, expansion and homing of hematopoietic stem cells (HSCs). Furthermore, hWJSCs express and secrete a high level of adhesion molecules and extracellular matrix components like glycosaminoglycans, osteopontin, MCP-1 and ICAM-1 which are inherent constituents of the hematopoietic stem cell niche that help regulate the expansion and maintenance of HSCs. As such, this thesis hypothesize that hWJSCs and/or its extracts can be used to enhance the treatment of hematological malignancies and blood disorders. The approach to the hypothesis was to evaluate (1) the tumoricidal effect of hWJSCs or its extracts on hematological malignancies and (2) to use hWJSCs or its extracts to enhance the numbers and freeze thaw survival of hematopoietic stem cells (HSC).

In summary, the tumoricidal effect of hWJSCs or its extracts on lymphoma cancer cell lines was evaluated in this thesis. The tumoricidal effect of hWJSCs or its extracts was not restricted to solid tumors but also non-solid tumors. hWJSCs engulfed lymphoma cell lines when co-cultured while its extracts attenuated cell growth and induced lymphoma cell death. In addition, the tumoricidal effect was cancer cell specific as hWJSCs did not engulf control fibroblasts while its extracts did not induce cellular death in control adult BMMSCs. It has also been demonstrated that the effective agents in hWJSC-conditioned medium (hWJSC-CM) were 3kDa and above. In addition, the 3kDa hWJSC-CM concentrate modulated the activities of key oxidative stress enzymes involved in hydrogen peroxide metabolism in lymphoma cell lines. Treatment of lymphoma cell lines with 3kDa hWJSC-CM concentrate increased hydrogen peroxide level, oxidative stress and lipid peroxidation. The ability of the 3kDa hWJSC-CM concentrate to induce immunogenic cell death to lymphomas, osteosarcomas and breast adenocarcinomas was also evaluated in the thesis. All three cancer cell lines expressed increased danger associated molecular pattern (DAMPs)-ecto-CRT, ecto-Hsp90, extracellular ATP and HMGB1 which are molecular hallmarks for immunogenic cell death after exposure to the 3kDa hWJSC-CM concentrate. Lastly, similar to BMMSCs, hWJSCs or hWJSC-CM could also be used for the expansion of cord blood CD34+ cells *ex vivo*. It is also possible to isolate and expand CD34+ cells using autologous hWJSCs within 24 hours of umbilical cord and cord blood collection. Moreover, addition of hWJSC-CM into the freezing media during freezing could enhance the freeze-thaw survival of cord blood CD34+ cells.

Collectively, the findings in the thesis support the storage of hWJSCs in public cord blood banks and their use in improving the efficiency in the clinical management of hematological malignancies and blood disorders.

LIST OF PUBLICATIONS

Fong CY, Gauthaman K, Cheyyatraivendran S, **Lin HD**, Biswas A, Bongso A. 2012. Human umbilical cord Wharton's jelly stem cells and its conditioned medium support hematopoietic stem cell expansion ex vivo. J Cell Biochem 113:658-68.

Lin HD, Bongso A, Gauthaman K, Biswas A, Choolani M, Fong CY. 2013. Human Wharton's jelly stem cell conditioned medium enhances freeze-thaw survival and expansion of cryopreserved CD34+ cells. Stem Cell Rev 9:172-83.

Lin HD, Fong CY, Biswas A, Choolani M, Bongso A. 2014. Human Wharton's Jelly Stem Cells, its Conditioned Medium and Cell-Free Lysate Inhibit the Growth of Human Lymphoma Cells. Stem Cell Rev 10(4):573-86.

Lin HD, Fong CY, Biswas A, Choolani M, Bongso. The 3kDA MWCO concentrate of human Wharton's jelly stem cell conditioned medium induces tumoricidal effects on lymphoma cells through hydrogen peroxide mediation. (Manuscript in preparation)

Lin HD, Fong CY, Biswas A, Choolani M, Bongso. 3kDA MWCO concentrate of human Wharton's jelly stem cell conditioned medium induces immunogenic cell death in lymphoma, osteosarcomas and breast adenocarcinomas (Manuscript in preparation)

LIST OF PATENTS FILED

Fong CY, Bongso A., **Lin HD.** 2014. Method of Freezing Stem Cells US20140120615 A1

LIST OF FIGURES

LIST OF TABLES

ABBREVIATIONS

AGM	Aorta-gonadal mesonephros
ATP	Adenosine triphosphate
BFU-E	Burst-forming unit erythroid
BM	Bone marrow
BrdU	Bromodeoxyuridine
CFU-E	Colony-forming unit erythroid
CFU-GEMM	Colony-forming unit granulocyte/erythroid/macrophage/megakaryocyte
CFU-GM	Colony-forming unit granulocyte/macrophage
CRT	Calreticulin
Da	Dalton
DAMPs	Danger associated molecular patterns
DCs	Dendritic cells
ECM	Extracellular Matrix
ER	Endoplasmic reticulum
FBS	Fetal Bovine Serum
FGF	Fibroblastic growth factor
FISH	Fluorescence in-situ hybridisation
Flt3-L	Fms-related tyrosine kinase 3 ligand
FT	Flow through
GAGs	Glycosaminoglycans
G-CSF	Granulocyte colony stimulating factor
GFP	Green fluorescent protein
GM-CSF	Granulocyte macrophage colony stimulating factor
GPx	Glutathionne peroxidase
GvHD	Graft verus Host Disease
hESCs	Human embryonic stem cells
HGF	Hepatocyte growth factor
HIV	Acquired immunodeficiency syndrome
HMGB1	High mobility group box -1
HPCs	Hematopoietic progenitor cells
HSCs	Hematopoietic stem cells
Hsp	Heat shock protein
hUC	Human umbilical cord
hWJSC-CL	hWJSC-cell free lysate
hWJSC-CM	hWJSC-conditoned medium
hWJSCs	Human Wharton’s jelly stem cells
ICAM-1	Intracellular adhesion molecule 1
ICD	Immunogenic cell death
ICM	Inner cell mass
iPSCs	Induced pluripotent stem cells
ITS	Insulin-transferin-selenium
LIF	Leukemia inhibitory factor

MCP-1	Monocyte chemoattractant protein 1
M-CSF	Macrophage colony stimulating factor
mPB	Mobilized peripheral blood
MSCs	Mesenchymal stem cells/Mesenchymal stromal cells
MTP	Mitochondria transition pore
MWCO	Molecular weight cut off
NGS	Normal goat serum
PBS	Phosphate buffered saline
PI	Propidium iodide
ROS	Reactive oxygen species
SCF	Stem cell factor
SDF-1	Stromal cell derived factor 1
SEM	Scanning electron microscopy
SEM	Standard error mean
SOD	Superoxide dismutase
TAF	Tumor associated fibroblasts
TE	Trophectoderm
TLR4	Toll-like receptor 4
TPO	Thrombopoietin
TPx	Thioredoxin peroxidase
UCB	Umbilical cord blood

SYMBOLS/UNITS

sec	second
min	minute
h	hour
cm	centrimeter
µm	micrometer
nm	nanometer
^{o}C	Celsius degree
mg	milligram
µg	microgram
ng	nanogram
g	gram
g	Centrifugal *g* force
rpm	revolutions per mol mole
l	litre
ml	millilitre
µl	microlitre
mM	millimolar
µM	micromolar
nM	nanomolar
U	Unit

Chapter 1: Introduction

1.1 Background

1.1.1 Human Umbilical Cord

The human umbilical cord (hUC) that connects the fetus and placenta enables the transport of blood supply and the removal of biological waste from the developing fetus during pregnancy. The fertilization of oocytes and embryonic development up to the early blastocyst stage takes place in the fallopian tubes. The early blastocyst will then descend down into the uterus and the fully expanded blastocyst will implant in the uterine endometrium around day 7 to 9 after fertilization. The migration of cells within the expanded blastocyst results in the formation of two distinct cell layers, a peripheral layer of trophectoderm (TE) which will become the placenta and a cluster of 30-50 cells known as the inner cell mass (ICM). The ICM which protrude from the inner wall of the polar TE will eventually form the entire fetus. In the process of embryonic development, the ICM becomes delineated into the hypoblast and epiblast. The epiblast cells are pluripotent in nature and give rise to the three germ layers which later develop into various organs and extra-embryonic membranes that include the amnion, chorion, placenta and umbilical cord [1]. The umbilical cord which is derived from the extraembryonic mesoderm and/or embryonic mesoderm during day 26 of gestation, weighs approximately 40g, is 30-65 cm long and has a mean diameter of 1.5 cm at birth. The hUC contains three blood vessels (2 arteries and a vein) which are surrounded by a mucous proteoglycan-rich matrix known as Wharton's jelly. Wharton's jelly, first described by Thomas Wharton in 1656, is a primitive connective tissue mainly composed of gelatinous ground substance rich in sulfated proteoglycans, collagenous fibers (collagen types I and III),

glycosaminoglycan and extracellular matrix proteins. It serves to protect the hUC vessels from compression, torsion and strangulation during fetal development.

1.1.2 Human Wharton's Jelly Stem Cells

Ever since the first isolation of fibroblastic-like cells from the Wharton's jelly of hUC in 1991 was first reported [2], many research groups worldwide (including ours) have been trying to isolate, characterize and evaluate the cells within the hUC or Wharton's jelly both *in vitro* and *in vivo* for therapeutic and regenerative use. To date, various mesenchymal stem/stromal cells (MSCs) populations, namely amniotic, subamniotic, perivascular and Wharton's jelly regions, have been identified within the hUC [1]. In our laboratory, we have derived a method to isolate MSCs from the Wharton's jelly directly and it has been referred to as human Wharton's jelly stem cells (hWJSCs). The collected hUC pieces were first cut open, then inverted (Wharton's jelly portion facing down) into an enzymatic solution containing collagenase/hyaluronidase to loosen and detach the Wharton's jelly. The hWJSCs were then separated and collected from the Wharton's jelly by passing the detached Wharton's jelly through a syringe needle [1,3,4]. There are two possible hypotheses on why these hWJSCs reside in the Wharton's jelly during gestation. First, findings in a study on cells collected from fetal bone marrow, yolk sac and aorta-gonadal mesonephros (AGM) of whole aborted human conceptuses postulated that there are two waves of migration of fetal MSCs where they first migrated from the yolk-sac and AGM to the placenta via hUC in the first wave and then reverse-migrated from the placenta back to home in the fetal liver and bone marrow via hUC in the second wave [5]. It was suggested some of the MSCs got trapped and resided in the gelatinous Wharton's jelly during the migration [5,6]. The second hypothesis suggests that MSCs in the Wharton's jelly are primitive MSCs which originate from

mesenchyme that is within the hUC matrix [1]. Though the role of these hWJSCs was probably to secrete (1) various glycoproteins, mucopolysaccharides, glycosaminoglycans and extracellular matrix to maintain the gelatinous nature of Wharton's jelly to prevent strangulation of hUC [1] and (2) secrete several bioactive molecules like interferons, growth factors, interleukins and cell adhesion molecules [7-9] for immunomodulatory and tissue repair mechanism during gestation but the exact role during fetal development remains to be elucidated .

These hWJSCs meet the minimum criteria of MSCs set by the International Society for Cellular Therapy [10]. Similar to adult tissue-derived MSCs, hWJSCs (1) adhere to plastic, (2) express cell surface antigens CD105, CD90, CD73, but not CD34, CD45, CD14, CD11b, CD19 and HLA class II and (3) differentiate along the adipogenic, osteogenic and chondrogenic lineages *in vitro* [3,11-14]. hWJSCs shared the same developmental origins as human bone marrow MSCs (hBMMSCs) and resemble them in terms of morphology, MSC marker expression, absence of hematopoietic surface markers, hypoimmunogenecity and multipotency but both are distinctly different, probably due to the differences in niche microenvironment [1]. As the umbilical cord lies between the embryo and adult organs on the developmental map (Fig. 1), hWJSCs also express different levels of pluripotency markers such as Oct4, Sox2, Nanog and Rex2, embryonic surface marker antigens such as SSEA-4, Tra-1-60 and Tra-1-81 and alkaline phosphatase [15-18]. Given their unique characteristics, hWJSCs appear to have the best attributes (which will be described in details later) for usage clinically as compared to stem cells isolated from the embryo and adults (Table 1). The suitability of these stem cells are also supported by numerous FDA-approved or local regulatory approved human clinical trials using hWJSCs in treating neurological, diabetic, liver, cardiovascular, immune and blood disorders worldwide [19-25] (Table 2).

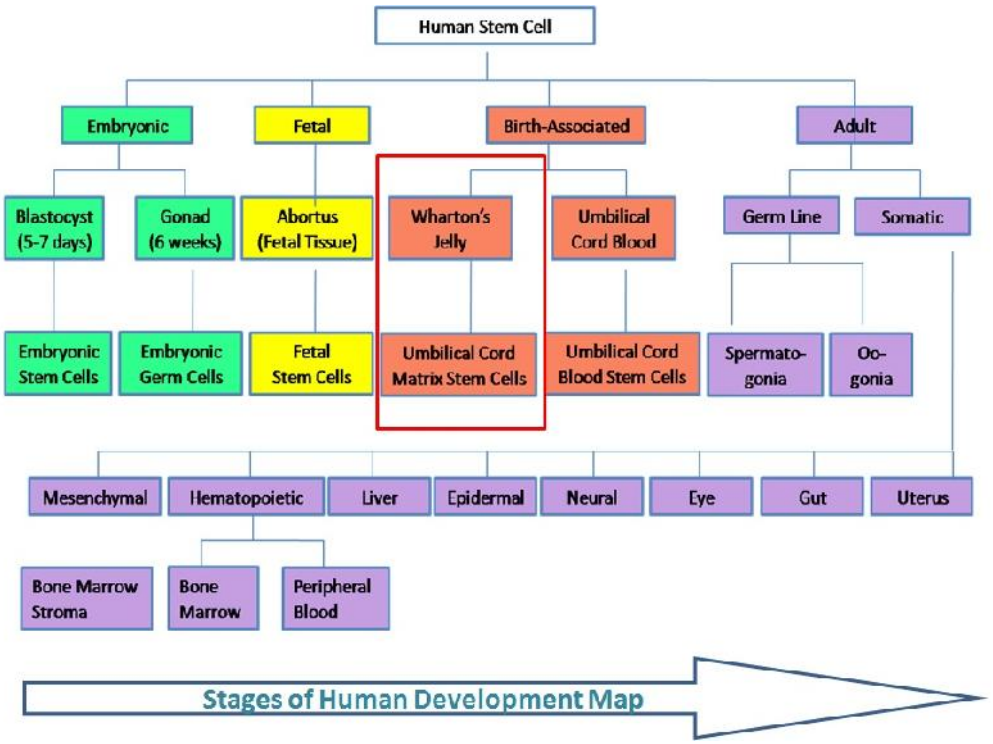

Figure 1 Stages of Human Developmental Map and types of stem cells isolated from each stages. Human Wharton's jelly stem cells also known as umbilical cord matrix stem cells (red box) and are isolated from birth associated tissues lies between the embryo and adult organs.

Table 1. Comparison of hWJSCs with hESCs and adult BM-MSCs

	hESCs	hWJSCs	BM-MSCs
Availability/Harvest	×	√	×
Ethics	×	√	√
Bankable	√	√	×
Numbers	√	√	×
Maintenance	×	√	×
Pluripotent Markers	√	√	×
Hypo-immunogenic	×	√	√
Do not form teratomas	×	√	√
Do not form tumor associated fibroblast	√	√	×

Table 2 List of FDA and Local regulatory approved human clinical trials

FDA/Local Clincal Trials	Disease	References
FDA	Spinocerebellar ataxia/ Multiple system atrophy	Dongmei et al 2011
Local	Severe aplastic anemia	Chao et al 2011
Local	Severe steroid resistant acute GvHD	Wu et al 2011
FDA	Chronic Liver Failure	Zhang et al 2012
Local	Thrombocytopenia	Ma et al 2012
FDA	Autism	Lv et al 2013
FDA	HIV	Zhang et al 2013
Local	Multiple Sclerosis	Hou et al 2013
FDA	Type I Diabetes Mellitus	Hu et al 2013
Local	Leukemia	Wu et al 2013
Local	Leukemia/Severe aplastic anemia/ B-thalassemia major	Wu et al 2013

1.1.3 Characteristics and use of Human Wharton's Jelly Stem Cells in Stem-cell based therapy

1.1.3.1 Plasticity

hWJSCs are multipotent cells. Other than the common adipogenic, chondrogenic and osteogenic classical lineages expected from MSCs, hWJSCs have been shown to differentiate into other cell types including neural, islet-like clusters cells, hepatocyte-like cells, cardiomyoctes, skeletal muscles and endothelial cells *in vitro*. As such, they have immense therapeutic potential in the management of neurological diseases, type 1 diabetes, hepatic, cardiovascular and myogenic diseases. Many studies using hWJSCs in experimental diseased animal models have shown improved functional outcomes [26] (Table 3).

Table 3 List of differentiated cell types of hWJSCs and their potential areas of application.

Types of Cell Differentiated Into	Applications
Adipocytes	Esthetic
Osteoblasts	Orthopedic
Chrondrocytes	Orthopedic
Neurons	Neurological
Islet Cells	Diabetic
Hepatocytes	Hepatic
Skeletal Muscles	Myogenic
Endothelial	Angiogenic
Cardiomyocytes	Cardiovascular

Neuronal lineages

Mitchell and colleagues first demonstrated that hWJSCs could be induced into neuronal lineages [27]. Since then hWJSCs have been successfully differentiated into different neuronal cell types such as dopaminergic neurons [26,28] and Schwann cells [29-31]. Moreover, hWJSCs were also able to produce significant amounts of trophic factors such as glial-derived neurotrophic factor and fibroblastic growth factor (FGF)-20, interleukin-6, FGF2, brain-derived neurotrophic factor [26,32,33]. Ding and colleagues previously transplanted one million hWJSCs into the cortex of stroke rat model and observed improvement in neurological function and cortical neuronal activity with increased local cortical blood flow in the ischemic hemisphere [34]. Other researchers also observed that the experimental rat model transplanted with hWJSCs have reduced injury volume and neurological functional deficits significantly [26]. Transplanted hWJSCs into rat model of spinal cord injury secrete large amounts of human neutrophil-activatin protein-2, NT-3, FGF2, glucocorticoid induced tumor necrosis factors receptor, VEGF receptor 3 in host spinal cord and significant improvements in locomotor function and increased numbers of regenerated axons around the lesion site were observed [35]. In a phase II FDA-approved clinical trial, spinocerebellar ataxia and multiple system atrophy patients were injected with hWJSCs intrathecally once every two weeks. Though the disease continued to progress in some patients, there was significant improvement in the International Cooperative Ataxia Rating Scale, neural function and better quality of life post-treatment [36]. In another FDA-approved trial, hWJSCs were co-transplanted with cord blood mononuclear cells in Autism patients and showed significant reduction in Childhood Autism Rating Scale and Aberrant Behavior Checklist score. There was also marked improvement in Clinical Global Impression Scale, visual

responses, emotional responses, intellectual responses, typical displays and behaviours [37].

Islet-like cell clusters

hWJSCs can differentiate into islet-like cell clusters that contained human C-peptide, and were able to express insulin and pancreatic beta-cell-related genes that are capable of releasing human insulin in response to glucose *in vitro* [38]. Alleviation of hyperglycemia and glucose intolerance were observed after these hWJSC-derived islet-like cell clusters were transplanted into streptozotocin-induced diabetic rat model [38]. In a recently published FDA-approved human clinical trial, 15 patients with type 1 diabetes were transfused with hWJSCs where they showed better glucose control, increased insulin secretion and regeneration of islet cells than the control group. The usage of insulin was progressively reduced in the hWJSCs treated patients and in some patients did not require insulin intervention [20].

Hepatocytes-likes lineages

hWJSCs can differentiate into hepatocytes-like cells after induction with hepatogenic factors [39-42]. hWJSCs exhibited hepatocyte-like morphology, upregulated hepatic markers such as albumin, human alpha-fetoprotein, cytokeratin 18, and also demonstrated glycogen storage, lipoprotein uptake and urea production [40]. Human albumin and human alpha-fetoprotein were observed several weeks after transplantation of undifferentiated hWJSCs into spleen of SCID mice with partial hepatectomy [40]. It was observed that there were significantly lower levels of serum glutamic oxaloacetic transaminase, glutamic pyruvate transaminase, alpha-smooth muscle actin and transforming growth factor beta1 several weeks after transplantation of hWJSCs into livers of carbon tetrachloride-induced liver fibrosis rat model [43]. Though the engrafted hWJSCs

were not shown to differentiate into hepatocyes after transplantation, upregulation in expression of hepatocyte growth factor, hepatic mesenchymal epithelial transition factor-phosphorylated type, tryptophan 2, 3-dioxygenase, human alpha-fetoprotein, cytokeratin-18, fibroblast secretory protein-1 and alpha smooth muscle actin were seen. They also secreted a variety of bioactive factors such as human cutaneous T cell attracting chemokines, leukemia inhibitory factor, prolactin which contributed to attain functional recovery of liver functions probably by degradation of fibrous matrix and stimulation of endogenous parenchymal cells to promote liver regeneration [43]. A FDA-approved trial where hWJSCs were transfused into patients with acute-on-chronic liver failure showed significant improvement in Model for End-stage Liver Disease scores, liver function and survival rates as compared to control [44]. In another human clinical trial, the transfusion of hWJSCs improved liver function as determined by (i) increased serum albumin levels, (ii) decreased total serum bilirubin level, (iii) decreased in the sodium model for end-stage liver disease scores and (iv) significant reduction in the volume of ascites in decompensated liver cirrhosis patients compared to control [45].

1.1.3.2 Immune-modulating properties

Similar to hBM-MSCs, hWJSCs have been shown to possess hypoimmunogenic properties and are capable of immune suppression. They do not express MHC class II (HLDA-DR) or co-stimulatory molecules such as CD80, CD86, CD40 known to activate the adaptive T and B cells responses [46-48]. hWJSCs do express low levels of MHC class I (HLA ABC) [46]; B7-H1,a negative regulator of T-cell activation and pan-HLA-G which contribute to immune tolerance during pregnancy [48,49]. In addition, they secrete large amounts of anti-inflammatory

factors such as interleukin-10, indoleamine 2,3-dioxygenase-mediated tryptophan depletion, TGF-B, LIF, HGF and prostaglandin E2 [47,49].

Concanavalin-induced splenocyte proliferation was inhibited by hWJSCs and there were no stimulation of T cells in either one-way or two way mixed lymphocyte reaction assay [46]. In addition, hWJSCs also inhibited CD4+, CD8+, CD2+ and CD3+ T cells subset proliferation but stimulated the expansion of CD4+CD25+Foxp3+ T-regulatory cells (Treg) in hWJSCs/Treg co-cultures [46]. Furthermore, hWJSCs also prevented CD14+ monocytes differentiation into mature dendritic cells and leading to their arrest as immature dendritic cells [49]. Expression of co-stimulatory ligands were also blocked in hWJSCs/monocytes co-cultures [49]. Given the immuno-modulation properties, Kikuchi-Taura et al. investigated whether hWJSCs help the suppression of Graft verus Host Disease (GvHD) in mice model [50]. Significant reduction in the frequency of GvHD was observed at 6 weeks post-transplantation in C57BL/6 mice that underwent allogeneic bone marrow transplantation with unexpanded hWJSCs at day 0 and day 6. Those mice that received concomitant treatment with hWJSCs also showed better survival at 6 weeks and 25 weeks after transplantation as compared to control. Moreover, in a human clinical trial, no chronic GvHD was observed when hWJSCs were transfused into human patients with severe steroid-resistant acute GvHD [25]. Similarly, there were lesser incidence or lesser side effects of GvHD in other human clinical trials which hWJSCs were co-transplanted with cord blood HSCs or peripheral blood stem cells for the treatment of leukemia and severe aplastic anemia [19,23].

1.1.3.3 Tumoridicial

Numerous independent studies have reported the tumoricidal properties of hWJSCs or its extracts both *in vitro* and *in vivo* on solid tumors like mammary

adenocarcinoma, ovarian carcinoma, osteosarcoma, cholangiocarcinoma, hepatocellular carcinoma, bronchioloalveolar and bladder carcinoma [9,51-61] (Table 4). De Coppi et al. first reported the migration of hWJSCs to metastatic tumor sites in the lungs after intravenous injection into SCID mice with mammary adenocarcinomas which suggested their homing abilities [62]. Ganta et al. in an elegant experiment first documented the direct tumoridicial effect of WJSCs where intravenous or intra-tumoral injection of un-engineered rat WJSCs into rats with mammary carcinomas led to completely abrogation of cancer growth compared to control [53]. Likewise, Ayuzawa et al demonstrated that hWJSCs administered intravenously into human mammary adenocarcinoma xenograft rat model, migrated to metastatic tumor sites in the lungs and attenuated tumor growth [52]. As hWJSCs tended to home into tumor sites, WJSCs were engineered to express cytotoxic cytokines like interferon-B that effectively homed and attenuated the growth of human breast adenocarcinoma and bronchioloalveolar carcinoma cells in xenograft SCID mice [51,54].

The tumoridicial effect of hWJSCs were mediated via cell-to-cell and/or non-cellular contact mechanism. Several modes of action of the inhibitory effects of hWJSCs on cancer cells have been demonstrated. Most groups demonstrated an induction of apoptosis, inhibition of proliferation and cell cycle arrest after treatment with hWJSCs or its extracts. Time lapse imaging study showed that hWJSCs inhibited mammary carcinoma cehlls by an entosis mechanism where the hWJSCs were first engulfed by mammary adenocarcinoma cells, which underwent disintegration due to apoptosis [56]. Another group reported a G2 cell cycle arrest and inhibition of PI3K/Akt signaling pathway when hWJSCs were co-cultured with breast cancer cell lines or primary breast cancer cells [60].

Earlier studies from our group as well as others have also demonstrated the tumoricidal effects of the extracts of hWJSCs like hWJSC-conditioned medium

(hWJSC-CM); its cell-free lysate (hWJSC-CL) or its microvesicles (MVs). The extracts of hWJSCs inhibited the growth of mammary carcinoma, osteosarcoma cells, bladder carcinoma, cholangiocarcinoma both *in vitro* and *in vivo* [9,57,59,61]. The tumoridicial effect of hWJSC extracts (hWJSC-CM and hWJSC-CL) on breast adenocarcinoma, ovarian carcinoma and osteosarcoma cell lines were evident by their inhibition of growth and morphological changes that ranged from cell shrinkage, blebbing to vacuolation with resultant cell death either due to apoptosis or autophagy [9]. Intra-tumor injection of hWJSCs or hWJSC-CM on mammary adenocarcinoma xenograft decreased tumor size [57]. Likewise, Liu et al. also demonstrated that subcutaneous injection of hWJSCs and hWJSC-CM on xenograft model of cholangiocarcinoma decreased tumor size [59]. *In vitro* treatment of cholangiocarcinoma cell lines inhibited cell growth via the inhibition of PI3K/Akt and Wnt/B-catenin signaling pathways [59]. Likewise, Wu et al also demonstrated inhibition of bladder tumor cell line proliferation was mediated through downregulation of Akt phosphorylation, as well as upregulation of p21, p53 and cell cycle arrest at G0/G1 phase. In addition, subcutaneous injection of hWJSCs or its MVs decreased tumor incidence and tumor size in xenograft model of bladder tumor in BALB/c nude mice [61].

Another possible mechanism of hWJSC-mediated inhibition or death of cancer cells is through the modulation of immune response to cancer cells. Ganta et al. observed via immunohistochemistry that T cells formed the majority of infiltrating lymphocytes in rat WJSCs treated rat mammary carcinomas [53]. Rat WJSCs treatment increased CD8+ T cell infiltration throughout the tumor tissues. Moreover, the same group later showed that rat WJSCs attenuated orthotopic Mat B III rat mammary tumor cell growth via the modulation of an endogenous immune response through the secretion of monocyte chemotactic protein-1 (MCP-1) [58]. The attenuation of tumor growth was accompanied by lymphocytes

infiltration and immunohistochemistry analysis indicate that the rat WJSCs increased number of CD3+, CD8+ and CD4+ T cells, natural killer cells throughout tumor tissue while CD68+ monocytes/macrophages and Foxp3+ regulatory T cells were rarely observed compared to control [58].

Table 4 List of publication on the tumoridicidal effects of Wharton's jelly Stem Cells

Tumoricidal effects of Wharton's Jelly Stem Cells				
Author	Type of Cancer and Model Used	Treatment	Results	Possible Mechanism
Rachakatla *et. al.* (2007)	Breast adenocarcinoma (MDA-231) in SCID mice	*IV injection of hWJSC engineered to express human interferon beta*	Tumor size decreased	1.Induction of apoptosis 2.Inhibition of proliferation
Ayuzawa *et al.* (2009)	Pulmonary metastatic xenograft of MDA231 (breast adenocarcinoma) in SCID mice	*IV injection of hWJSCs*	Tumor size decreased	1.G2 arrest 2.Inhibition of proliferation
Ganta *et al.* (2009)	Orthotopic graft of Mat B III (breast cancer) in F344 rats	*IT and IV injection of rat WJSCs*	Tumor abolished and no evidence of metastasis or recurrence 100 days after post injection	1.Induction of apoptosis
Matsuzuka *et al.* (2010)	Orthotopic xenograft of H358 (bronchioloalveolar carcinoma) in SCID mice	*IV injection of hWJSC engineered to express human interferon beta*	Tumor multiplicity and size decreased	1.Inhibition of proliferation 2.Induction of apoptosis
Maurya *et al.* (2010)	Orthotopic graft of LLC (Lewis lung carcinoma) in C57/BL mice	*Intratracheal injection of rat WJSCs*	Tumor multiplicity and size decreased	1.G0/G1 arrest 2.Decrease of cyclin A and CDK2
Chao *et. al.* (2012)	Breast adenocarcinoma (MDA-231) cell line, xenograft of MDA-231 and hepatocellular carcinoma (HCC) in SCID mice	*In vitro co culture with hWJSCs, Local fat pad injection of hWJSCs*	Cancer cell apoptosis *in vitro* *In vivo* bioluminescence signal of MDA-231 decreased	1.Induction of apoptosis 2.Inhibition of proliferation
Gauthaman *et. al.* (2012)	Breast adenocarcinoma (MDA-231), ovarian carcinoma (TOV-112D) and osteosarcoma (MG-63) cell lines	*In vitro treatment with conditioned media and cell lysate*	Inhibition of cell growth Increase in number of apoptotic cells	1.Induction of apoptosis 2.Metaphase arrest 3.Induction of autophagy
Gauthaman *et. al.* (2013)	Osteosarcoma cell lines (MG-63 and SKES-1), subcutaneous xenograft of mammary adenocarcinoma (MDA-231) in SCID mice	*In vitro treatment with conditioned media and cell lysate, IT injection of hWJSCs and conditioned media*	Inhibition of cell growth *in vitro* Tumor size decreased *in vivo*	1. Induction of apoptosis 2.Induction of autophagy
Kawabata *et. al.* (2013)	Orthotopic Mat B III rat mammary tumor grafts in F344 rats	*IT injection of rat WJSCs*	Tumor size decreased	1.Increase of CD8+ and CD4+ T-cell and NK cell infiltration, mediated by MCP-1
Liu *et. al.* (2013)	Cholangiocarcinoma cell line (HCCC-9810) and subcutaneous xenograft of HCCC-9810 in BALB/c nude mice	*In vitro treatment with hWJSC conditioned media, subcutaneous injection of hWJSCs and conditioned media*	Inhibition of cell growth *in vitro* Tumor size decreased *in vivo*	1.Inhibition of PI3K/Akt and the Wnt/b-catenin signaling pathways
Ma et al. (2013)	Breast carcinoma cell lines MDA-231 and MCF-7, primary human breast cancer cells, xenograft of MDA-231 in CB17 SCID mice	*In vitro co culture with hWJSCs and subcutaneous injection of hWJSCs*	Inhibition of cancer stem cell colony formation *in vitro* Tumor size decreased *in vivo*	1.Inhibition of PI3K/Akt signaling pathway 2.G2 arrest
Wu *et. al.* (2013)	Bladder tumor T-24 cell line and subcutaneous xenograft of T-24 in BALB/c nude mice	*In vitro co culture with hWJSCs and subcutaneous injection of hWJSCs and microvesicles secreted by hWJSCs*	Inhibition of cell growth *in vitro* Decreased tumor incidence and tumor size *in vivo*	1.G0/G1 arrest 2.Inhibition of proliferation through down regulated Akt phosphorylation 3.Up regulation of p21 and p-p53

1.1.4 Advantages in using Human Wharton's Jelly Stem Cells in Stem Cell Therapy

1.1.4.1 Source and Isolation

Isolation of hWJSCs poses no ethical issues as compared to human embryonic stem cells (hESCs) and fetal MSCs. hESCs are derived from the inner cell mass of a blastocysts and its isolation will lead to the destruction of fertilized human embryo [63,64]. As there is no consensus whether these embryos are considered as human being at this embryonic state, its destruction is of ethical issues. Similarly, fetal MSCs isolated from aborted fetuses which their uses can be controversial [1]. hWJSCs, derived from commonly discarded umbilical cord pose no such ethical issues in their isolation and subsequent usage in the clinics [1]. In addition, the isolation of hWJSCs from discarded cord poses no discomfort or risk to the patients or donors as compared to isolating MSCs from bone marrow or adipose tissues, which involves an invasive procedures which is painful, posing infection risks and donor site morbidity to both patients and donors [1,65,66]. The ease of derivation and lack of ethical issues concerning the usage of hWJSCs make them a better stem cell choice over hESCs/iPSCs, fetal BM-MSCs and adult BM-MSCs.

1.1.4.2 Cell Numbers and Maintenance

One major drawback of using adult BM-MSCs in the clinics is the limitation in cell number that can be harvested from the donor bone marrow aspirates and thus an *ex vivo* cell expansion is often needed to obtain the required cell numbers. Moreover, BM-MSCs limited proliferation before reaching senescence and variation in relation to donor age is a concern [67]. In addition, the need to expand BM-MSCs *ex vivo* accentuated the risks of having their genotype altered during the process. It is well documented that *in vitro* manipulation of cells like

continuous passaging leads to major and minor chromosomal changes, loss of stemness properties and poses the risk of contaminations *in vitro* [1]. Likewise, both hESCs and human induced pluripotent stem cells (iPSCs) can develop chromosomal deletions or duplications after serial passaging [68] while chromosomal changes could also be induced during the reprogramming stages in generating iPSCs [69]. On the other hand, our laboratory has successfully isolated hWJSCs from discarded cords and could consistently harvest about 5 million fresh hWJSCs per centimetre of umbilical cord before culture [3,4]. As such, we could theoretically harvest 2500 millions of fresh hWJSCs per hUC. In addition, hWJSCs have higher proliferation rates and longer telomere length than adult BM-MSCs because of its young chronological age. We are able to maintain the hWJSCs for at least 20 passages with no changes to their stemness markers and genome [3,4,15,17]. Moreover, hWJSCs adhere well onto tissue culture dishes and hence their derivation and propagation *in vitro* do not need any feeder cells or cell attachment matrices. As such, the high cell number and easy maintenance of hWJSCs make them a better stem cell choice over hESCs/iPSCs and adult BM-MSCs.

1.1.4.3 Non-tumorigenic behaviour

Though hESCs and human iPSCs are pluripotent, their clinical translation has been limited as undifferentiated pluripotent cells have been shown to induce teratomas when injected into normal or immunocompromised mice [70]. Likewise, teratoma formation was also reported when mouse embryonic stem cell derived insulin producing islets or cardiomyocytes were transplanted in immunosuppressed mice [71,72], presumably due to the inherent property of rogue undifferentiated pluripotent cells. The challenges of eliminating all rogue pluripotent stem cells in the derived population have delayed the use in patients.

Though hWJSCs also expressed different levels of pluripotent markers such as Oct4, Sox2, Nanog and Rex2, embryonic surface marker antigens such as SSEA-4, Tra-1-60 and Tra-1-81 and alkaline phosphatase [15-18], they did not to form teratomas when injected via subcutaneous; intramuscular ; intraperitoneal routes even after 20 weeks [73]. Similarly, no tumorigenesis has been reported when hWJSCs or hWJSC-derived tissues were transplanted into primates and humans [26]. In addition, no development of tumors in all injection sites and organs and no stem cell transplantation-related toxicity were observed when hWJSCs were injected intravenously every 2 weeks for 6 weeks in non-human primates-cynomolgus monkeys [74].

The use of adult BM-MSCs in numerous regenerative cell therapies also holds immense clinical potential. Tthough BM-MSCs do not form teratomas when injected into mice, fetal and adult MSCs have been shown to produce tumors [75-77]. In addition, it has been reported that BM-MSCs or adipose derived MSCs favor tumor cell growth *in vivo* [78,79]*.* Moreover, MSCs can form tumor associated fibroblasts (TAF) in tumor microenvironment and played an important role in tumor formation, tumor growth, angiogenesis and metastasis [80-84]. BM-MSCs can also acquire TAF phenotypes after exposure to or systemic recruitment into xenograft models of breast, pancreatic and ovarian cancers [85]. As such, it has been hypothesized that the precursor cells that form TAFs in solid tumors are the hBMMSCs [85-87]. An alternative MSCs, hWJSCs (though they share the same developmental origin as BM-MSCs) failed to transform into TAF phenotype after their growth in the presence of breast and ovarian cancer cell conditioned medium for 30 days [88]. Our group demonstrated that unlike BM-MSCs, hWJSCs did not express TAF markers like fibroblast specific proteins, fibroblast activated proteins, cell aggressive markers, tumor growth factors and angiogenic factors [88]. In addition, unlike BM-MSCs, hWJSCs cultured for 30 days in cancer cell

conditioned medium also failed to stimulate cancer cell growth *in vitro* in the same study [88].

As recent report on a 13-year old child developing multiple brain and spinal cord glioneuronal tumors after receiving fetal stem cells for ataxia telangiectasia [77] highlighted the importance of ensuring the tumourigenic potential of any stem cells are assessed before using them on human patients. Therefore, hWJSCs which has been demonstrated to be non-tumorigenic and did not formed TAF serves as an ideal stem cell source for future clinical applications.

1.1.4.4 Hypoimmunogenicity

Another hurdle that has delayed the translation of stem cells usage in human clinical trials is the concern of immunorejection of stem-cell derived tissues in an allogeneic settings [70]. Like all tissue/organ transplants, in the use of hESCs cell therapy, there is a need to circumvent the host immune system rejection or the need to prevent Graft vs host disease (GvHD) during the treatment. Though the breakthrough in creating patients' specific iPSCs by nuclear reprogramming of patients' somatic cells should be immune-tolerated [1], there are now conflicting reports as to whether these patient specific iPSCs will be immuno-tolerated [89,90]. Zhao et al. reported in 2012 that teratomas of iPSCs generated from B6 mouse embryonic fibroblasts were mostly immune-rejected by B6 mice recipients [89], but Guha et al. on the other hand did not observe an immune response against iPSCs or iPSCs derived cells *in vitro* and after transplantation into syngeneic mouse recipients [90]. It was suggested that the low immunogenicity of hWJSCs protected hWJSCs or hWJSC-derived cells from immune-rejections in immune-competent rats [91]. Swine derived WJSCs multiplied following transplantation into rat brain without activation of host immune response and swine WJSCs could be

recovered 6 weeks after transplantation from the brain of rat that did not receive immune suppression [32,91]. Likewise, human hWJSCs did not trigger host immune response when transplanted into immuno-competent rats [32]. The lack of immuno-rejection or infiltration of host immune cells after hWJSCs or hWJSC-derived cells transplantation in immuno-competent animal model bodes well for its engraftment in an allogeneic transplantation setting. In addition, hWJSCs have more robust immunomodulatory properties than BM-MSCs. Though BM-MSCs inhibited mitogen-, alloantigen- or specific antigen- driven T cell responses [92,93], hWJSCs exhibited a robust suppression as compared to BM-MSCs at a very low dose range [47,94]. Moreover, hWJSCs were able to suppress allogeneically stimulated T cells to a greater extent than BM-MSCs and this regulation is stimuli-independent [47]. The kinetics of pro-inflammatory cytokines secretion profiles of hWJSCs or BM-MSCs co-cultured with PHA-activated lymphocytes indicated that the threshold and kinetics of IL-2 changes only with BM-MSCs but not with hWJSCs [47]. The early activation of negative co-stimulatory ligands on lymphocytes was more evident with hWJSCs [47]. As such, it demonstrated that hWJSCs were less immunogenic than BM-MSCs making them a more ideal choice for allogeneic transplantation.

1.1.5 Stem Cell-based Therapy for the Management of Hematological Malignancies and Blood Disorders.

Currently, hematopoietic stem cells (HSC) transplantation is by far the most widely performed stem cell based therapy in the clinics since its introduction in 1968. Since then, HSC transplantation has been used to treat blood disorders, immunodeficiency disorders, hematopoietic malignancies like leukemia, and lymphoma, as well as in the treatment of diseases like chronic liver failure and acquired immunodeficiency syndrome (AIDS) [95,96]. HSC transplantations *in utero*

were successful in the treatments of fetuses diagnosed with severe combined immunodeficiency disorder [97,98]. Data provided by the Center for International Blood and Marrow Transplant Research shows a rising trend of transplantation performed worldwide over the last decade. Therefore, large numbers of HSCs are needed to support the increasing demand of HSC transplantation.

Despite its success, there are two major limitations to a successful HSCT. They are (i) the identification of tissue-matched HSC sample and (ii) the presence of adequate numbers of HSCs. The current sources of HSCs come from the bone marrow (BM), mobilized peripheral blood (mPB) and umbilical cord blood. Collection of HSCs from the BM or mPB depends mainly on patients' relatives and volunteers. In such instance, identification of suitable tissue-matched HSCs remained a challenge. Even though public cord blood banks have been set up to help in identifying suitable tissue-matched HSCs, they are still unable to meet the overwhelming demand. Additionally, harvesting of HSCs from bone marrow is an invasive procedure and is usually associated with discomfort and risk of infection. Rare incidents of rupture of the spleen and sickle cell damage have occurred and the long term safety of the donors following peripheral blood HSCs collection remains unclear [99-102]. With these safety concerns and discomfort surrounding the donors, the ability to collect HSCs samples from the bone marrow or peripheral blood are mainly restricted to patients'-related donors or volunteers.

Harvesting of HSCs from umbilical cord blood (UCB) has several advantages over that of BM or mPB. The advantages are (i) it is easy to collect and store UCB HSCs in cord blood banks which make them easily available to patients, (ii) UCB HSCs pose less risk of graft versus host disease (GVHD) due to their immune naivety, (iii) there is less stringent requirement needed to find a matching sample between donors' cells and recipients' and (iv) UCB HSCs have higher proliferation rates, and longer telomeres due to their young chronological age [103-

[105]. The UCB HSCs are also associated with delayed neutrophil response, slower platelets recovery and higher incidence of infection-hemorrhage related morbidity and mortality as compared to BM or mPB HSCs [106-108].

Despite having many advantages, the biggest obstacle in using UCB HSCs is the limited number of HSCs that can be isolated from a cord blood unit. The number of UCB HSCs from a single UCB unit that can be harvested typically ranges from 0.4 to 1.0x 10^7 CD34+ cells but a minimum of 2.0 to 2.5x10^7 MNCs/kg CD34+ cells are required for a favorable transplantation outcome [109]. Thus, HSCs collected from each cord unit can only be used for one patient and its use is mainly restricted to children or small sized adults. Most patients therefore succumb to their illness due to the lack of suitable tissue-matched HSCs units and also insufficient HSCs number for a successful treatment.

1.1.6 Human Wharton's Jelly Stem Cells and Hematological Disorder Management

hWJSCs could provide the structural and physiological support for self renewal, expansion and homing of HSCs as reported by several groups [110,111]. This supportive role of hWJSCs was demonstrated through long-term culture initiating cells assays and also when cord blood CD34+ cells that were co-cultured with hWJSCs for a period of up to 5 weeks could still demonstrate methylcellulose colony-forming potential [110,111]. The mechanism of this supportive role was attributed to the high expression and secretion of hematopoietic cytokines and growth factors such as SCF, LIF, VEGF, Flt3-L, TPO, HGF, IL-1a, IL-6, IL-8, IL-11, GM-CSF, G-CSF, M-CSF, and SDF-1 [111,112]. Furthermore, hWJSCs express and secrete high level of adhesion molecules, extracellular matrix components like glycosaminoglycans, osteopontin, MCP-1 and ICAM-1 which are inherent

constituents of the hematopoietic stem cell niche that help regulate the expansion and maintenance of HSCs. Previous studies have indicated that co-transplantation of human MSCs enhanced the engraftment of UCB HSCs in NOD/SCID mice model and also in human patients [113-117]. The hypoimmunogenic properties of MSCs were often cited as the main reason for the improved engraftment which reduced immune-rejection [118]. However, the capacity of MSCs to engraft in the patients' bone marrow is still debatable [119] because most studies indicate a lack of engraftment [120]. Recent research has shown that these MSCs homed to the bone marrow eventually [121,122] especially when the stromal niche was considerably damaged [123]. The myeloablative regime used during pre-transplantation preparation to eliminate malignant cells and/or to immunosuppress the patients prior to HSC transplantation often also damaged the bone marrow microenvironment extensively [124-126] and this influenced the HSCs engraftment kinetics [126]. More recent studies indicate that MSCs could home to the bone marrow microenvironment and help reconstitute and repair the hematopoietic microenvironment *in vitro* and *in vivo* mouse bone marrow-damaged models [119,127,128]. Likewise, co-transplantation of hWJSCs with UCB CD34+ cells could accelerate hematopoietic recovery in NOD/SCID mice even when limited numbers of UCB CD34+ cells were infused [112]. Though results showed presence of human CD105+ cells only in some of the bone marrow of the recipient mice, it is still indicative of engraftment of the transplanted hWJSCs into the recipient mice [112]. Yet, another study observed that hWJSCs could mitigate chemotherapy-associated tissue injury in pre-clinical mouse model [128].

There were a few human clinical trials that involved hWJSCs transplantation for the treatment of leukemia, severe aplastic anemia and thrombocytopenia [19,23,24,129]. In one of these trials, hWJSCs were co-transplanted with cord blood HSCs in patients with high-risk acute lymphoblastic or acute myeloid leukemia [129].

The results indicated that co-transplantation with hWJSCs led to faster engraftment and faster recovery of absolute neutrophil and platelets counts which indicated enhanced hematopoiesis after cord blood transplantation as compared to patients that received cord blood transplantation alone [129]. In addition, higher survival rates were associated with hWJSCs co-transplantation [129]. Similar results were seen in the another trial where patients with acute lymphoblastic or acute myeloid leukemia or severe aplastic anemia and B-thalassemia major were treated with cord blood co-transplanted with hWJSCs [23]. In another clinical trial, hWJSCs were co-transplanted with peripheral blood stem cells in patients with severe aplastic anemia and similarly, accelerated engraftment and higher survival rates were associated with hWJSCs co-transplantation compared to control [19]. hWJSCs were also transplanted into 2 patients with chronic immune thrombocytopenia in a human clinical trial where both patients showed no signs of bleeding and normal peak platelet count after hWJSCs transplantation [24].

1.2 Research hypotheses and aims

The current management of hematological malignancies involved the use of chemotherapeutic agents, irradiation and hematopoietic stem cells (HSCs) transplantation. There are 2 challenges with these methods of treatments. Firstly, the use of aggressive chemotherapeutic agents or radiation-conditioning regimes prior to HSC transplantation often cause damage to the bone marrow microenvironment and have a profound influence on HSC engraftment kinetics and the outcome of patient treatment [126,130-133]. As the bone marrow microenvironment made up of mesenchymal stem cells (MSCs) and extracellular matrix (ECM) serves as an important hematopoietic niche which influences the abilities of hematopoietic stem cells (HSCs) or hematopoietic progenitor cells (HPCs) to home, engraft, self-renew and differentiate via direct cell-cell contact

and secretion of hematopoietic growth factors [119,134,135]. It is therefore important to explore alternative anti-cancer therapies that will inhibit leukemic or lymphoma cell growth while at the same time do not damage the bone marrow microenvironment. Secondly, HSCs from the bone marrow have been traditionally used in the form of bone marrow transplants for the treatment of malignant hematopoietic diseases. However, aspiration of HSCs from the bone marrow is painful and there is the potential risk of infection and morbidity. Additionally, optimal HSC numbers from the bone marrow are not available for successful transplantation in many cases. In order to avoid these disadvantages, HSCs from the human umbilical cord blood (UCB) have been successfully used for the treatment of malignant and non-malignant blood-related diseases in infants and children in both autologous and allogeneic settings [136,137]. However, UCB also has its limitations in that the HSC and HPC yields are low and the cell numbers are usually inadequate for the treatment of blood-related diseases in the adult. Therefore, to overcome these challenges, this thesis hypothesized that the dual anti-tumorigenic and MSCs properties hWJSCs and its extract could be used to manage and improve to the treatment of hematological malignancies and blood disorders.

Hypothesis:

It was hypothesized that the dual anti-tumorigenic and MSCs properties of hWJSCs and/or its extract can be used to manage and improve the treatment of hematological malignancies and blood disorders.

Specific Aims:

The specific aims of the thesis were:

1. To evaluate the use of hWJSCs and its extract as an direct anti-tumorigenic agent for hematological malignancies.

   (i) To evaluate the anticancer effects of hWJSCs, its conditioned medium (hWJSC-CM) and cell-free lysate (hWJSC-CL) on various malignant cell lines of the hematopoietic system.

   (ii) To evaluate the hydrogen peroxide mediated tumoridical effect of hWJSC-CM on malignant cell lines of the hematopoietic system.

   (iii) To evaluate the immunogenic cell death induction of hWJSC-CM on cancer cell lines of the hematopoietic, osteosarcomas and breast cancer system.

2. To evaluate the use of hWJSCs and its extracts for increasing the number cord blood CD34+ cells

   (i) To evaluate the use of hWJSCs and its conditioned medium (hWJSC-CM) as stromal and non-stromal support systems for the *ex vivo* expansion of hematopoietic stem cells (HSCs).

   (ii) To comparatively evaluate the use of hWJSC-CM + DMSO freezing media for the improvement of thaw-survival rates of HSCs so as to maximize cell numbers for treatment of hematopoietic diseases.

Chapter 2: Tumoricidal Effect on Lymphoma Cells

2.1 Introduction

Human or murine bone marrow mesenchymal stem cells (hBMMSCs) are known to home to cancer tissues and have been explored as vehicles for gene or anti-cancer drug delivery to inhibit cancer growth [138,139]. However, their anticancer effects have been controversial as reports shows an inhibitory and proliferative effect on cancer cells [140]. hBMMSCs were demonstrated to have a potent anti-cancer effect in numerous *in vivo* experimental models including Kaposi's sarcoma, colon carcinoma, Lewis lung carcinoma and melanoma [141-143]. However, it has also been reported that when hBMMSCs is in the vicinity of breast, pancreatic and ovarian cancer cells, they could transform to tumor associated fibroblasts (TAFs) which enhance tumor growth in human xenograft animal models [86,144]. Such hBMMSC-derived TAFs also encourages metastasis of the tumors resulting in systemic spread of the solid tumors [80-83,85]. Thus, the use of hBMMSCs as vehicles for the delivery of anti-cancer agents remains a clinical hurdle.

Our laboratory have derived a primitive stromal cell from the Wharton's jelly compartment of the human umbilical cord with high expression of MSC CD markers and low level expression of human embryonic stem cell (hESC) markers. These stem cells have similar CD signatures, differentiation capabilities and share common developmental origins as hBMMSCs [3-5]. There are numerous reports which have confirmed their tumour inhibitory properties both *in vitro* and *in vivo* on solid tumours such as mammary adenocarcinoma, ovarian carcinoma, osteosarcoma, cholangiocarcinoma and bladder carcinoma [9,51-53,55-57,59-61].

Though extensive studies have been carried out on the tumoricidal effects of hWJSCs on solid cancer tissues, no studies have evaluated whether non-solid

tumors such as leukemia and lymphoma cells are susceptible to the tumoricidal effects of hWJSCs. One study suggested that adult hBMMSCs improved the overall survival of disseminated non-Hodgkin's lymphoma [145]. These workers showed massive stromal infiltration of hBMMSCs into tumor masses that resulted in necrosis. In *in vitro* experiments they suggested that the release of pro-angiogenic cytokines by hBMMSCs induced endothelial cell migration and apoptosis thus prevented new blood vessel formation which consequently was the cause of tumor growth inhibition [145]. Umbilical cord MSCs inhibited leukemia cell growth *in vitro* possibly by the release of interleukins such as IL-6 and IL-8 [146]. Since hWJSCs secrete high levels of various factors not observed with hBMMSCs, the aim of this chapter was to evaluate the tumoricidal effects of hWJSCs and its extracts on Burkitt's lymphoma cancer cells and the mechanism involved.

2.2 Material and Methods

2.2.1 Cell Culture

Human Wharton's jelly stem cells (hWJSCs)

The hWJSCs were derived from human umbilical cords after informed patient consent and approval from the Institutional Domain Specific Review Board (DSRB). In all experiments, early passages of hWJSCs (3P to 5P) were used. In some experiments, green fluorescent protein (GFP)-transduced hWJSCs (GFP-hWJSCs) that were generated in our laboratory were used. hWJSCs were maintained in hWJSC medium that comprised of 80% DMEM medium supplemented with 20% fetal bovine serum (FBS) (Biochrom, Berlin, Germany), 1% non-essential amino acids, 2 mM L-glutamine, 0.1 mM β-mercaptoethanol, 1% insulin-transferrin-selenium (ITS), antibiotic/antimycotic mixture [penicillin (50IU), streptomycin (50µg/ml), amphotericin B(0.25µg/ml)] (Invitrogen Life Technologies,

Carlsbad, CA) and 16 ng/ml basic fibroblast growth factor (Millipore Bioscience research agents, Temecula, CA).

Human lymphoma cells (Ramos)

Approval for purchase and use of commercial human Burkitt's lymphoma cell line (Ramos, CRL 1596) (American Type Culture Collection, ATCC, Rockville, MD, USA) was granted by the National University of Singapore Institutional Review Board (NUS-IRB). The cell lines were thawed and cultured in lymphoma medium consisting of RPMI medium (Thermo Scientific) supplemented with 10% heat inactivated FBS (Biochrom) and 1% antibiotic/antimycotic mixture (Invitrogen).

Human skin fibroblasts (CCD1112sk) and bone marrow mesenchymal stem cells (hBMMSCs)

Approval for purchase and use of commercial adult hBMMSCs (Lonza, Allendale, NJ, USA) and human foreskin fibroblasts (CCD-1112sk) (ATCC) (abbreviated as CCD) was granted by the NUS-IRB. The cells were thawed and cultured in medium consisting of DMEM-high glucose (Invitrogen) supplemented with 10% FBS (Biochrom), 1% antibiotic/antimycotic mixture and 2mM L-glutamine (Invitrogen).

2.2.2 Preparation of hWJSC conditioned medium (hWJSC-CM)

The preparation of hWJSC-CM was carried out as previously described [8,9,57]. Briefly, early passages of hWJSCs (3P to 5P) were first cultured in hWJSC medium until 70% confluency. The medium was then replaced with basal RPMI medium (Thermo Scientific) supplemented with 1% antibiotic/antimyotic mixture (Invitrogen). After 48 h, the medium (hWJSC-CM) was collected, filtered through a 0.22 μM filter (Millipore) and stored at -80^{o}C until use.

2.2.3 Preparation of hWJSC lysate (hWJSC-CL)

The preparation of hWJSC-CL was carried out as previously described [9,57]. Early passages of hWJSCs (3P to 6P) were cultured in hWJSC medium until 80% confluency, dissociated with trypsin (TrypLE™ Express, Invitrogen) and centrifuged to obtain a cell pellet. The hWJSC lysate was harvested using a commercial mammalian cell extraction kit supplemented with protease inhibitor cocktail and dithiothreitol (BioVision Inc., Mountain View, CA). Briefly, 100 μl of cell lysis buffer containing the protease inhibitor cocktail and dithiothreitol were added to the hWJSC pellet, mixed and incubated at 4°C for 45 min. The mixture was then centrifuged at 15,000 x g for 15 min and the supernatant separated and stored at -80°C until use. The total protein content of the lysate was measured using a Nanodrop™ spectrophotometer (Nanodrop Technologies, Wilmington, DW). hWJSC-CL containing 15 μg/mL protein was used for all experiments.

2.2.4 Experimental Design

Co-Culture

Lymphoma (Ramos), skin fibroblasts (CCD) and hBMMSCs were first stained with CellTracker™ Red (CTR) (Invitrogen) according to the manufacturer's instructions. Briefly, the cells were incubated with 10 μM of Cell Tracker™ Red in growth medium for 30 min at 37°C in a 5% CO_2 at room temperature and pressure. The media were then discarded and cells washed with PBS before incubation for another 30 min with growth media. The cells were then passaged and equal numbers of GFP-hWJSCs and CTR-lymphoma cells cocultured in a Lab-Tek(R) Chambered #1.0 Borosilicate coverglass system (Thermo Scientific).

Time lapse imaging and fluorescence in-situ hybridisation (FISH) for Y-chromosomes

To find out whether the CTR-lymphoma cells were actually engulfed by the GFP-hWJSCs as whole cells or in parts or that there was no engulfment, the interaction of the two cell types was monitored under time lapse imaging and after 24h of cell interaction z-stack images of cell-to-cell interaction and cell death was taken using an Olympus FluoView FV1000 laser scanning confocal microscope (Olympus, Japan).

Since the two cell types were of opposite sex, the Y chromosomes of the lymphoma cells were probed using FISH to further confirm whether whole lymphoma cells or their remnants were taken up by the GFP-hWJSCs. GFP-hWJSCs were not used in this experiment as their green signals which are closer in color to yellow FISH-Y chromosome signals would interfere with interpretation. We therefore first stained hWJSCs with Cell Tracker^{TM} Red (CTR) as described above before co-culturing with unstained lymphoma (Ramos) cells on coverslips in 24-well plates (Thermo Fisher Scientific, Rochester, NY) for 24h. The cells were then fixed in cold methanol: acetic acid (3:1) overnight and stored at -80^{o}C until use. The X-spectrum Orange/ Y-spectrum Green DNA probe (Vysis Ltd, London, UK) (5mL of 2:3 dilution) was added to the fixed cells and placed in a hybridization block for 7 min at 71^{o}C and subsequently for 4h at 37^{o}C in a humidified chamber. The cells were then washed with 0.4X salted sodium citrate (SSC) for 2 min at 71^{o}C followed by further washing with 2X SSC for 2 min at room temperature. After air-dying, the cells were then stained with DAPI and mounted with Fluoroshield^{TM} (Sigma, St. Louis, MO). The cells were observed and Y chromosome FISH signals photographed with an Olympus FluoView FV1000 laser scanning confocal microscope.

Exposure of lymphoma cells to hWJSCs, hWJSC-CM and hWJSC-CL

Lymphoma (Ramos) cells (0.5 to 10 x 10^4 cells) were separately exposed to hWJSCs (0.5 to10 x10^4 cells in lymphoma medium), hWJSC-CM (supplemented

with 10% heat inactivated FBS (Biochrom) and 1% antibiotic/antimycotic mixture; 0.5 to 2 ml) and hWJSC-CL (15 μg/mL in lymphoma medium; 0.5 to 2 ml) for 48h in 24-well plates or T25 culture flasks at 37^0C in a 5% CO_2 atmosphere. The lymphoma cells were then evaluated for morphology (phase contrast inverted optics), viability and proliferation rate (MTT, BrdU and Ki67), cell survival (Annexin V-FITC and live/dead analysis) and cell cycle analysis.

Exposure of hWJSC-CM and hWJSC-CL to hBMMSCs

To evaluate whether hWJSCs or its extracts would harm the bone marrow, hBMMSCs were exposed to the chemotherapeutic agents VP-16 (100 μM) (control), hWJSC-CM (100%) and hWJSC-CL (15 μg/mL) for 6 days with change of respective medium after 72 h. The cells were then evaluated for cell morphology, cell viability (MTT) and cell survival (percentage of PI+ cells).

2.2.5 Experimental Analysis Test

Cell viability (MTT assay)

The lymphoma (Ramos) cells were collected, washed once with PBS (-), centrifuged at 300 x g and then re-suspended in 100 μL growth media. 10 μl [3-(4, 5-dimethylthiazolyl-2)-2, 5-diphenyltetrazolium bromide] (MTT, 0.5 mg/ml) (Duchefa Biochemie B.V., Haarlem, Netherlands) was added to the medium for each sample and the tubes were incubated overnight at 37^oC in 5% CO_2. The cell suspension was then centrifuged at 1,500 x g for 5 min, medium decanted and 100 μl of DMSO reagent (Sinopharm Chemical Reagent Co.Ltd) added to the cell pellet. The cells were dispensed into 96-well assay plates (NUNC, Rochester, NY) and incubated in the dark at 37^oC for 10 min. Absorbance at 570 nm against a reference wavelength of 630 nm was measured using a spectrophotometer microplate reader (mQuant; BioTek, Winooski, VT, USA).

Cell proliferation assay

BrdU assay

The bromodeoxyuridine (BrdU) assay was carried out on the lymphoma cells using a commercial kit according to the manufacturer's instructions (Cell Signaling Technology, Danvers, MA). Briefly, the lymphoma cells were first separately exposed to hWJSCs, hWJSC-CM and hWJSC-CL for 48 h in medium containing 1X BrdU. The cell suspension was collected, washed once with PBS (-) before resuspending the cell pellet in 100 μL of the fixation/denaturing solution for 30 min at room temperature and centrifuged at 300 x g. After removing the solution, 100 μL of 1X BrdU detection antibody solution was added and incubated at room temperature for 1h. The cells were then washed with 1X wash buffer before the addition of 100 μL of 1X HRP-conjugated secondary antibody solution for 30 min at room temperature. The cells were washed again with 1X wash buffer before addition of 100 μL of TMB substrate for 30 min at room temperature. Finally, 100 μL of STOP solution was added to the cells and BrdU levels measured using a spectrophotometer microplate reader (mQuant; BioTek) at 450nm wavelength.

Ki67+ analysis

The lymphoma cells were collected, washed once with PBS (-), centrifuged at 300 x g for 5 min and then fixed in cold 70% ethanol at -20^{o}C overnight. The cells were then washed and blocked with 10% normal goat serum (NGS) (Invitrogen) for 10 min at room temperature. The cells were incubated with primary anti-human Ki67 antibodies (1:100) (Biolegends, San Diego, USA) for 30 min at room temperature. The cells were then incubated with anti-mouse IgG (H+L) Alexa Fluor® 488 secondary antibody (1:750) (Invitrogen) for 30 min at room temperature in the dark. The cells were centrifuged, cell pellet resuspended in 10%

NGS and filtered using a 40 μm nylon strainer to remove any cell clumps before analysis using CyAn ADP Analyser (Beckman Coulter).

Cell Death Analysis

Morphology

Changes in cell morphology of the lymphoma cells were monitored using inverted phase contrast optics (Nikon Instruments, Tokyo, Japan).

Annexin V/PI assay

The lymphoma cells were collected, washed once with PBS (-), centrifuged and then resuspended with 500 μL of 1X Annexin V binding buffer (BioVision, Inc., Mountain View, CA). The cells were then stained with 1 μL of Annexin V- FITC (BioVision) and counterstained with 1 μL of propidium iodide (PI, Invitrogen), at room temperature for 15 min, filtered with a 40 μm nylon strainer and analyzed using a CyAn^{TM} ADP analyzer (Beckman Coulter, Fullerton, CA, USA).

Live/Dead cell assay

The live/dead cell assay was performed on the lymphoma cells using the Live/Dead® Viability/Cytotoxicity Kit for mammalian cells (Invitrogen). A working solution of component A (included in the kit) was first made by adding 1 μl of component A into 79 μl of DMSO (Sinopharm Chemical Reagent Co.Ltd). 1 μL of component A working solution and 2 μL of component B (supplied in the kit) were added to 500 μl of PBS (-) to make the staining solution.

The cells were later collected, washed once with PBS (-), centrifuged and resuspended in 500 μl of staining solution and then incubated for 15 min in the dark. The cell suspension was filtered with a 40 μm nylon strainer and analyzed using a CyAn^{TM} ADP analyzer (Beckman).

Cell cycle analysis

The lymphoma cells were collected, washed once with PBS (-), then fixed in cold 70% ethanol at -20^{o}C overnight. The cells were later washed with PBS (-) once before adding 20 μg/mL PI, 100 μg/mL RNase A (AppliChem GmbH, Garmstadt, Germany) to each sample and then incubated for 15 min at 37^{o}C in 5% CO_2. The cell suspension was then filtered using a 40 μm nylon strainer to remove any cell clumps before analysis using a CyAn^{TM} ADP analyser (Beckman).

2.2.6 Statistical Analysis

All results were expressed as mean ± SEM and statistical significance between the groups was calculated using the two-tailed Student's t-test (SPSS Statistic v 17.0 software package) (SPSS, Inc, IL). The p-value of <0.05 was considered as statistically significant.

2.3 Results

2.3.1 Co-culture of hWJSCs with lymphoma cells

In the beginining of the co-culture, both GFP-hWJSCs and red-labelled lymphoma cells were separated [Fig. 2A (i)]. Sections of Z-stack images of the Lab-Tek$^{(R)}$ Chambered #1.0 Borosilicate coverglass co-culture system after 24 h of cell seeding showed that the red-labelled lymphoma cells were engulfed by the green-labelled GFP-hWJSCs and were located in the cytoplasm [Fig. 2A (ii)] compared to red-labelled CCD cells (controls) that were not engulfed by GFP-hWJSCs (Fig. 2B). When sections of Z-stack images of female red-labelled hWJSCs were examined after FISH, green Y-chromosome signals of male lymphoma nuclei were observed in

the hWJSC cytoplasm (Fig. 2C).

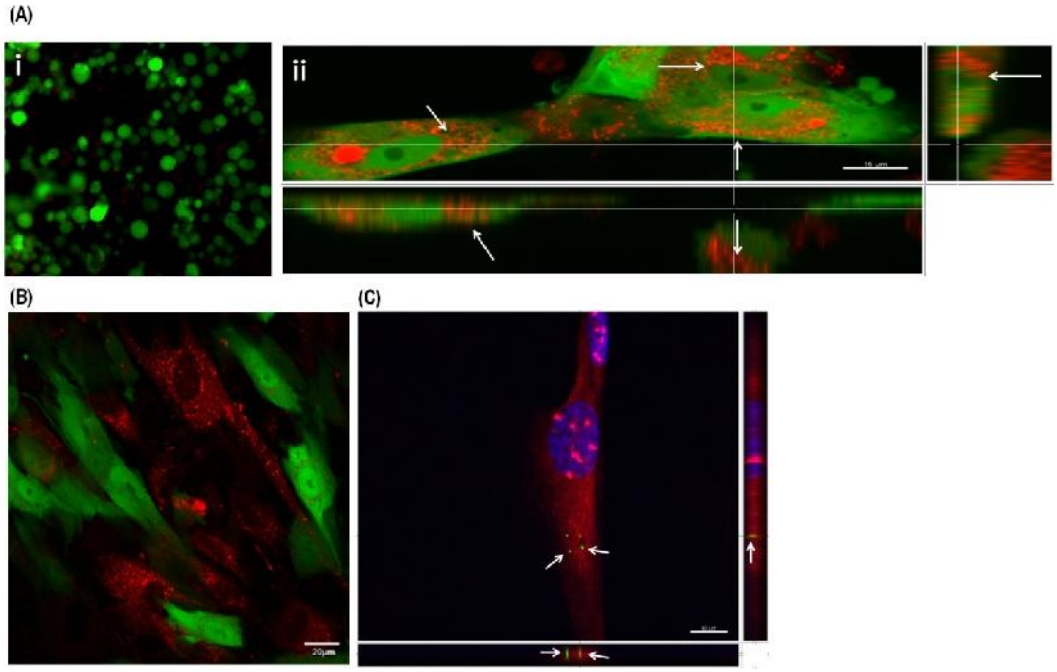

Figure 2 Confocal images of hWJSCs co-cultured with Ramos cells

(A) (i) Image of GFP-tagged hWJSC and CellTracker™ Red-labelled Ramos at zero time point. **(ii)** Z-stack confocal images of GFP-hWJSCs co-cultured with CellTracker™ Red-labelled Ramos lymphoma cells. In horizontal and cross-sectional images. Note that parts of lymphoma cells were localized within the cytoplasm of GFP-hWJSCs after 48h (white arrows) (Magnification: 600X; Scale Bar: 15 μM). **(B)** Confocal image of GFP-hWJSCs cocultured with CellTracker™ Red-labelled skin fibroblasts. Note that both GFP-hWJSCs and skin fibroblasts grow side by side (Magnification: 200X; Scale Bar: 20 μM). **(C)** Horizontal and cross-sectional z-stack confocal images of female CellTracker™ Red-labelled hWJSCs showing Y-chromosome FISH signals (arrows) of male lymphoma cells in hWJSC cytoplasm (Magnification: 1200X; Scale Bar: 10 μM).

2.3.2 Cell Viability and Proliferation

Lymphoma cells showed significant decreases in cell viability after 48h exposure to hWJSCs, hWJSC-CM and hWJSC-CL compared to controls. The cell viability rates reduced to 0.91 ± 0.01, 0.65 ± 0.02 and 0.68 ± 0.04 for the hWJSCs, hWJSC-CM and hWJSC-CL respectively (Fig. 3A). Lymphoma cells showed significant decreases in cell proliferation after 48h exposure to hWJSCs, hWJSC-CM (not significant) and hWJSC-CL compared to controls. The cell proliferation rate using the BrdU assay decreased to 2.74 ± 0.07, 2.47 ± 0.09 and 2.48 ± 0.12 for the hWJSC, hWJSC-CM and hWJSC-CL respectively (Fig. 3B). The cell

proliferation rate using the Ki67+ assay showed significant decreases in Ki67+ cells when exposed to hWJSC-CM or hWJSC-CL for 48h. The percentage of Ki67+ cells were 71.28 ± 3.51% and 83.91 ± 2.3% for the hWJSC-CM and hWJSC-CL arms respectively (Fig. 3C).

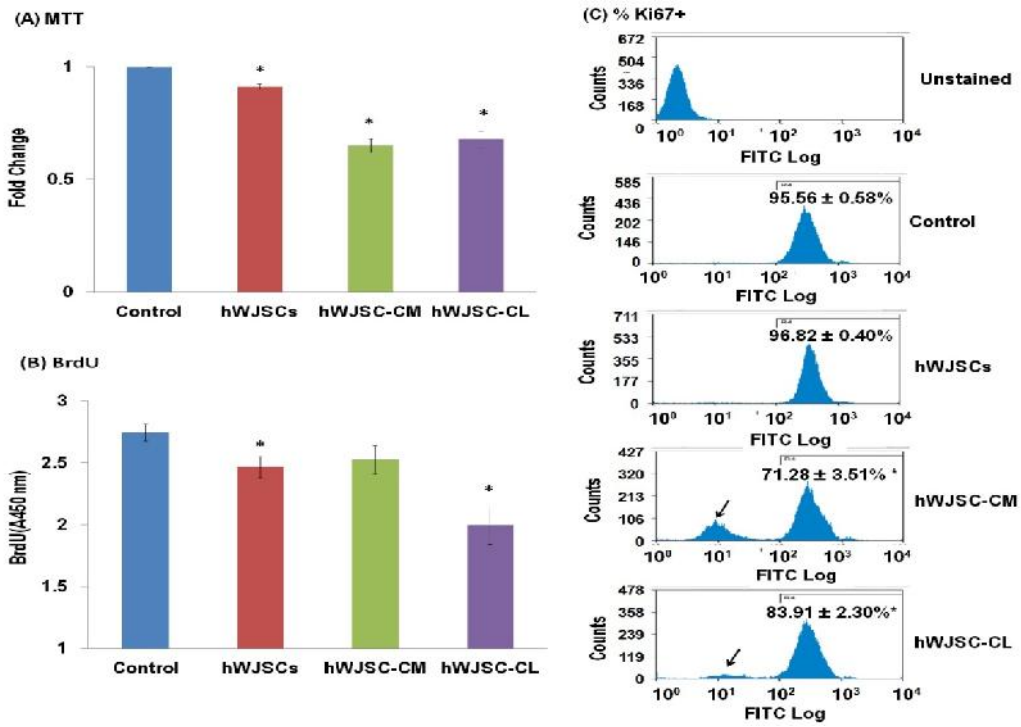

Figure 3 Cell viability and cell proliferation assay of Ramos lymphoma cells

(A) Cell viability (MTT assay) of Ramos lymphoma cells exposed to hWJSCs, hWJSC-CM and hWJSC-CL. Note significant decrease in cell viability (normalized to control) when lymphoma cells were exposed to hWJSCs, hWJSC-CM and hWJSC-CL for 48h. **(B)** Cell proliferation (BrdU assay) of lymphoma cells exposed to hWJSCs, hWJSC-CM and hWJSC-CL. Note significant decrease in cell proliferation when lymphoma cells were exposed to hWJSCs and hWJSC-CL for 48h. **(C)** Cell proliferation (Ki67 assay) of lymphoma cells exposed to hWJSCs, hWJSC-CM and hWJSC-CL. Note significant decrease in the percentages of Ki67+ lymphoma cells when exposed to hWJSC-CM and hWJSC-CL for 48h. All values in (**A-C)** are expressed as mean ± SEM of 3 different experiments. Asterisk (*) indicates statistical significance of $p<0.05$.

2.3.3 Cell Death Analysis

The lymphoma cells after 48h exposure to hWJSCs, hWJSC-CM or hWJSC-CL showed morphological changes like degeneration and shrinkage indicating cell death (Fig. 4A).

The Annexin V/PI assay of lymphoma cells exposed to hWJSCs showed no significant differences in the percentage of late apoptotic cells (AV+PI+ cells) but there were significant increases in the percentages of AV+PI+ lymphoma cells when exposed to hWJSC-CM or hWJSCs-CL for 48 h. The percentage of late apoptotic cells after 48 h of treatment were 4.8 ± 0.30%, 7.31 ± 0.02% and 13.8 ± 1.76% for the hWJSCs, hWJSC-CM and hWJSC-CL arms respectively (Fig. 4B).

The live/dead assay of lymphoma cells exposed to hWJSCs showed no significant differences in the percentage of dead cells but significant increases in the percentages of dead lymphoma cells were observed when they were exposed to hWJSC-CM or hWJSCs-CL for 48h. The percentages of dead cells after treatment were 5.6 ± 0.28% and 8.4 ± 1.18% for hWJSC-CM and hWJSC-CL respectively (Fig. 4C).

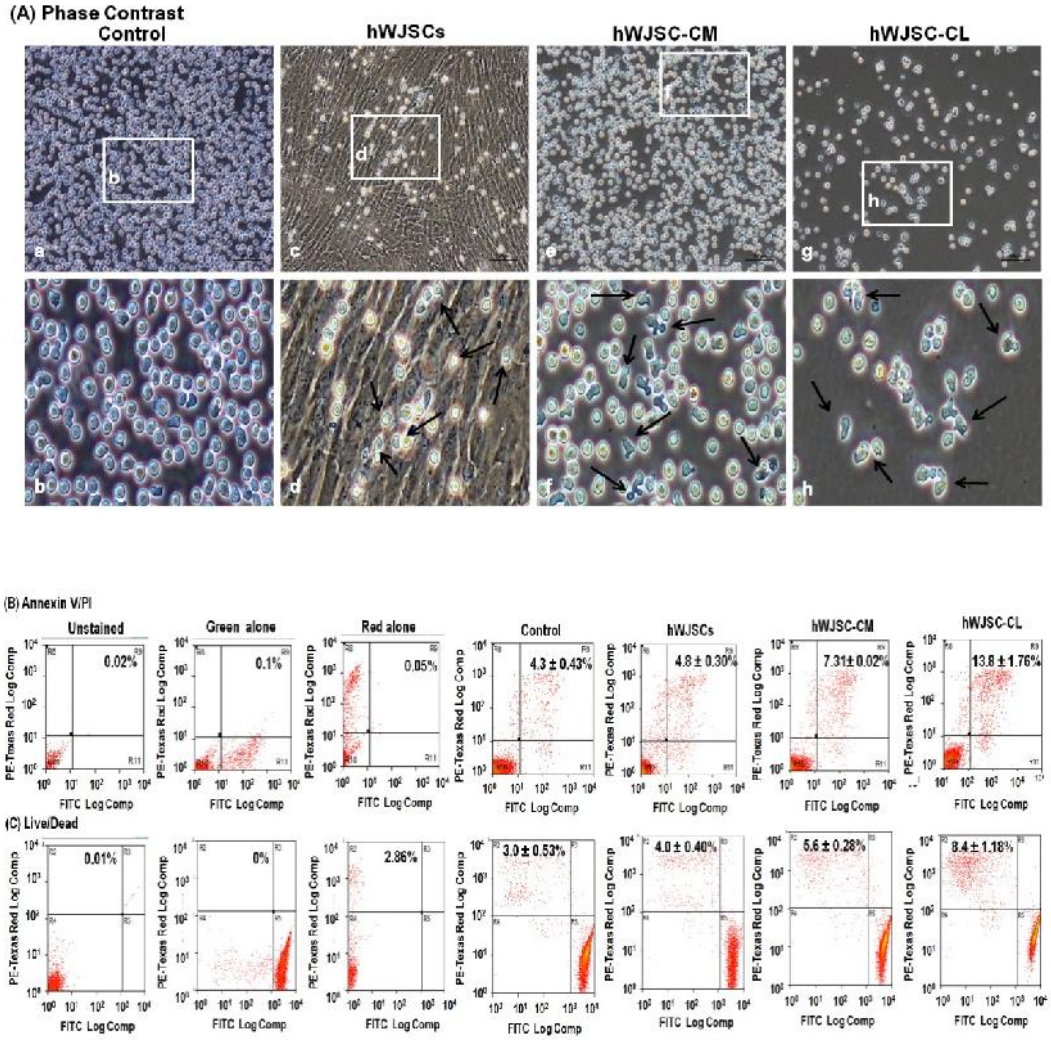

Figure 4 Cell death assays of Ramos lymphoma cells

(A) Phase contrast images of Ramos lymphoma cells exposed to hWJSCs, hWJSC-CM and hWJSC-CL. **(a) Low magnification and (b) Inset enlarged:** Lymphoma cells show typical spherical morphology in controls. **(c, e, g) Low magnification and (d, f, h) Inset enlarged:** Increased cell death (black arrows) were observed when lymphoma cells were exposed hWJSCs, hWJSC-CM and hWJSC-CL for 48h (Magnification 100X; Scale Bar: 100µM) **(B)** Annexin V/PI assay of lymphoma cells exposed to hWJSCs, hWJSC-CM and hWJSC-CL**.** No significant differences in percentages of late apoptotic AV+PI+ lymphoma cells were observed between hWJSC and control arms. However, significant increases in AV+PI+ lymphoma cells were observed when exposed to hWJSC-CM and hWJSC-CL. **(C)** Viability (Live/Dead assay) of lymphoma cells exposed to hWJSCs, hWJSC-CM and hWJSC-CL. No significant differences in the percentages of dead cells between hWJSC and control arms were observed but significant increases in the percentages of dead cells were observed in lymphoma cells exposed to hWJSC-CM and hWJSC-CL for 48h. All values in **(B-C)** are expressed as mean ± SEM of 3 different experiments. Asterisk (*) indicates statistical significance of $p<0.05$.

2.3.4 Cell Cycle Analysis

Evaluation of the cell cycle of lymphoma cells showed increases in the sub-G1 and S phases when exposed to hWJSCs, hWJSC-CM or hWJSC-CL. The rates of increase in sub-G1 cells compared to controls were hWJSCs: 1.41 ± 0.24, hWJSC-CM: 4.77 ± 0.77 and hWJSC-CL: 6.87 ± 1.45. However, only the increase observed for the hWJSC-CM arm was statistically significant (Fig. 5A). The rates of increase in S phase cells compared to controls were hWJSCs: 1.10 ± 0.04, hWJSC-CM: 1.19 ± 0.02 and hWJSC-CL: 1.14 ± 0.01. The increases observed with hWJSC-CM and hWJSC-CL were statistically significant (Fig. 5B).

There was also a significant decrease in G2/M phase lymphoma cells when exposed to hWJSCs, hWJSC-CM or hWJSC-CL. The rates of decrease in G2/M phase cells compared to controls were hWJSCs: 0.73 ± 0.07, hWJSC-CM: 0.61 ± 0.03 and hWJSC-CL: 0.57 ± 0.04 (Fig. 5C).

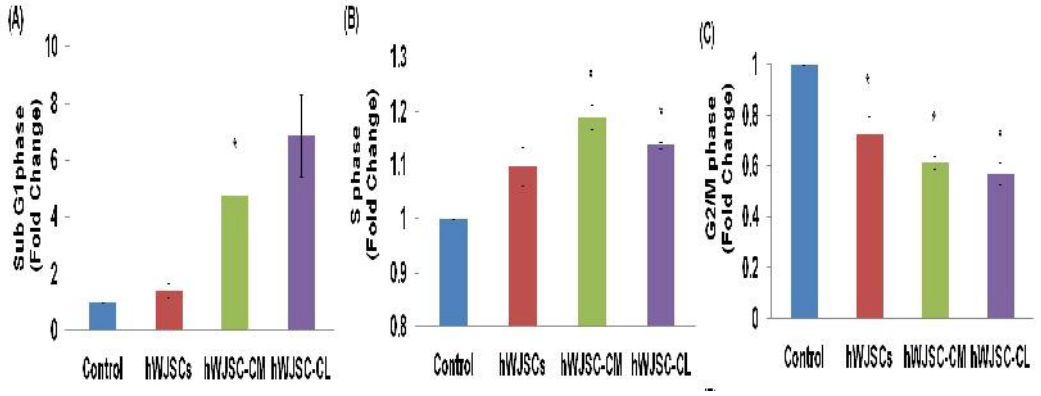

Figure 5 Cell cycle analysis of Ramos lymphoma cells

(A-C) Cell Cycle analysis of Ramos lymphoma cells exposed to hWJSCs, hWJSC-CM and hWJSC-CL. Increased percentages (normalized to control) of lymphoma cells were observed at Sub-G1 **(A)** and S phases **(B)** when they were exposed to hWJSCs, hWJSC-CM and hWJSC-CL. Lower percentages of lymphoma cells were observed in G2/M phase **(C)** when they were exposed to hWJSCs, hWJSC-CM and hWJSC-CL. All values are expressed as mean ± SEM of 3 different experiments. Asterisk (*) indicates statistical significance of $p<0.05$.

2.3.5 Effect on adult BMMSCs

When green GFP-hWJSCs were co-cultured with red CTR-stained hBMMSCs no engulfment or inhibition of the hBMMSCs by hWJSCs were observed. The GFP-hWJSCs and CTR-stained hBMMSCs were seen to grow side by side in the tissue culture plates when observed under fluorescent confocal microscopy (Fig. 6A). Additionally, treatment of hBMMSCs for 6 days with hWJSC-CM and hWJSC-CL showed no cell death unlike the exposure to the chemotherapeutic agent etoposide (VP-16) (Fig. 6B). The MTT assay on the hBMMSCs showed significant decreases in cell viability after 6 days when exposed to hWJSC-CL (15 μg/mL) and VP-16. However, cell viability was not significantly decreased in hBMMSCs exposed to hWJSC-CM (Fig. 6C). hBMMSCs showed significantly increased percentages of PI+ cells after 6 days of culture in VP-16 compared to hWJSC-CM and hWJSC-CL. The percentages of PI+ cells were 2.76 ± 0.15, 21.74 ± 0.24, 4.44 ± 0.41 and 4.33 ± 0.13 for controls, VP-16, hWJSC-CM and hWJSC-CL respectively (Fig. 6D).

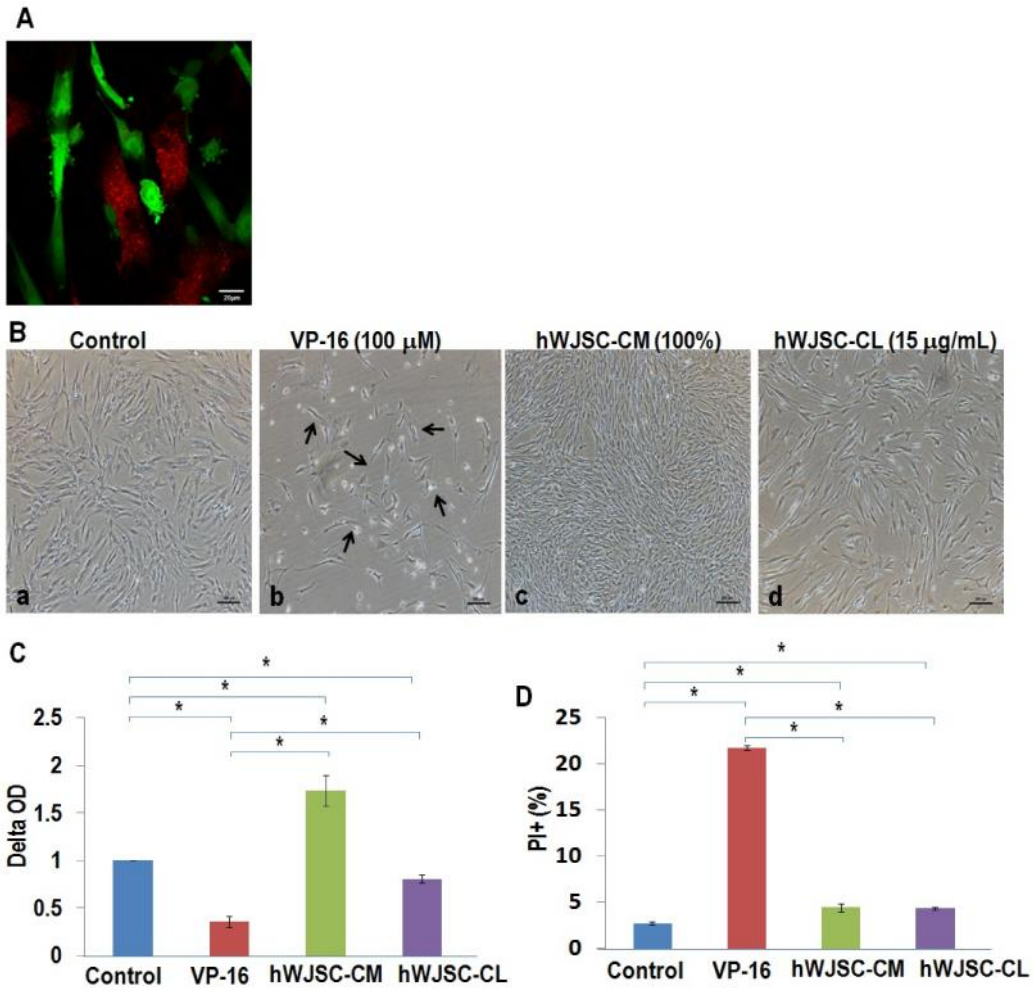

Figure 6 Effects of hWJSCs and its extract on adult BM-MSCs

(A) Confocal images of GFP-hWJSCs cocultured with CellTracker^{TM} Red-labelled human bone marrow MSCs (hBMMSCs). Both GFP-hWJSCs and red labeled hBMMSCs grew side by side with no inhibition or engulfment of either cell type (Magnification: 200X; Scale Bar: 20 μm). **(B)** Phase contrast images of hBMMSCs exposed to VP-16, hWJSC-CM and hWJSC-CL for 6 days. No hBMMSC cell death was observed in **(a)** controls, **(c)** hWJSC-CM and **(d)** hWJSC-CL dishes but increased cell death was observed in **(b)** VP-16 positive controls (black arrows) (Magnification: 400X; Scale Bar: 200 μm) **(C)** Cell viability (MTT assay) of hBMMSCs exposed to VP-16, hWJSC-CM and hWJSC-CL. Significantly high cell viability (normalized to controls) measured in delta OD (differences in absorbance reading at 570 nm with reference wavelength 630 nm) were observed when lymphoma cells were exposed to hWJSC-CM or hWJSC-CL compared to VP-16 exposure. **(D)** Cell death analysis (PI) of hBMMSCs exposed to VP-16, hWJSC-CM and hWJSC-CL for 6 days. Significant decreases in the percentages of dead PI+ hBMMSCs were observed when exposed to hWJSC-CM or hWJSC-CL as compared to VP-16 exposure. All values in **(C-D)** are expressed as mean ± SEM of 3 different experiments. Asterisk (*) indicates statistical significance of $p<0.05$.

2.4 Discussion

Human Wharton jelly stem cells (hWJSCs) are a homogeneous population of primitive mesenchymal-like stem cells that have been trapped in the gelatinous connective tissue matrix of the Wharton's jelly following their migration to and from the placenta during early embryogenesis [5]. However, the actual role of these hWJSCs during embryonic and foetal development is not clear. Yang and Chao [147] recently postulated that their paradoxical tumoricidal properties suggested that they are a natural defence mechanism against the migration of metastasizing cancer cells from the mother via the umbilical cord since the incidence of malignant cancer cells in the fetus was significantly low in pregnant mothers suffering from ovarian carcinoma, mammary carcinoma, sacromas or chorocarcinomas of the placenta [147-152].

The results of this chapter confirmed that hWJSCs have tumoricidal effects not only on solid tumours but also on hematological malignancies. The mechanisms whereby the hWJSCs attenuate the growth of the lymphoma cells appeared to be both by direct cell-to-cell engulfment and apoptosis as well as by non-cellular contact via secretions from the hWJSCs because the hWJSC extracts (conditioned medium and lysate) were also able to inhibit lymphoma cell growth. The former engulfing mechanism observed under time lapse imaging appears to be different from an engulfing mechanism reported recently by another group where they reported that mammary carcinoma cells engulfed hWJSCs via an entosis mechanism and then undergo disintegration [56]. These inconsistencies may be related to the differences in size of lymphoma and mammary carcinoma cells. Lymphoma cells being small (about 5-12 µm) would be unable to engulf the larger hWJSCs (about 15-20 µm). In addition, this engulfment-like mechansim do mimic that of macrophages and it have been shown that macrophages phagocytosed tumor cells and later act as a antigen presenting cells to bridge the

innate and adaptive immune response [153,154]. It would be interesting to see whether hWJSCs could also act as a antigen presenting cells after engulfment lymphoma to stimulate host immune system too. With respect to the latter non-contact mechanism the higher percentages of cells in the sub-G1 and lower percentages in G2/M phases in the cell cycle analysis suggested that certain components released by hWJSCs arrest cell division of lymphoma cells in the S phase.

Most chemotherapy or radiation treatment regimens administered to lymphoma patients often result in damage to the bone marrow, gastrointestinal tract, heart, brain and kidney [128,155-157]. The bone marrow microenvironment made up of mesenchymal stem cells (MSCs) and extracellular matrix (ECM) served as an important hematopoietic niche which influenced the abilities of hematopoietic stem cells (HSCs) or hematopoietic progenitor cells (HPCs) to home, engraft, self-renew and differentiate via direct cell-cell contact and secretion of hematopoietic growth factors [119,127,134,135]. The use of aggressive chemotherapeutic agents or radiation-conditioning regimes prior to HSC transplantation often cause damage to the bone marrow microenvironment and have a profound influence on HSC engraftment kinetics and the outcome of patient treatment [126,130-133]. The non-specific inhibition of growth of normal cells by conventional regimes is an unwanted side effect. Also, previous studies indicated that aggressive chemotherapeutic or radiation conditioning regimens prior to HSC transplantation often caused irreversible damage to the stromal cells in the hematopoietic microenvironment ultimately affecting HSC engraftment and reconstitution after transplantation [127,158-161]. Co-transplantation of HSCs together with hBMMSCs or MSCs from other sources which repaired or reconstituted the bone marrow microenvironment often improved the functional outcome of transplantation both in animal models and human clinical trials [23,112,117,129,162]. The

results of the present study showed that hWJSCs, hWJSC-CM inhibited lymphoma cells but not hBMMSCs. Therefore, they would be safe options for not only targeting cancerous cells but also reconstitution of the bone marrow hematopoietic niche during co-transplantaion with HSCs in patients with hematological malignancies.

Chapter 3: H_2O_2 mediated Tumoricidal Effects on Lymphoma Cells

3.1 Introduction

Human Wharton jelly stem cells (hWJSCs) which share the same developmental origin as adult bone marrow MSCs get trapped in the gelatinous connective tissue matrix of the WJ during migration to and from the placenta during early embryogenesis [5]. It has been reported that hWJSC extracts inhibited the growth of mammary carcinoma, osteosarcoma, cholangiocarcinoma and bladder cancer *in vitro* or *in vivo* [9,57-59,61]. These studies have suggested that the tumoricidal effects of hWJSCs or its extracts may be mediated by a variety of mechanisms with probably each cancer cell type being inhibited by a separate mechanism. Kawabata et al. [58] reported that rat WJSCs secreted monocyte chemotactic protein-1 (MCP-1) that modulated the endogenous immune response to attenuate mammary carcinoma growth. It was reported that hWJSC-CM or its microvesicles attenuated cholangiocarcinoma or bladder cancer growth via the inhibition of phosphoinositide 3-kinase, Akt and Wnt/ B-catenin signalling pathways [59,61].

Increasing evidence has suggested that the concentration of intracellular H_2O_2 plays a crucial dual role in cancer cell development [163,164]. At low concentrations, H_2O_2 played a physiological role in cell signaling, and a constitutive increase in H_2O_2 has been associated with malignant transformation by exerting increased proliferation [165], DNA damage [166], genetic instability [167], apoptosis resistance [168], angiogenesis [169] and metastasis in cancer cells [165]. There is also compelling evidence that high H_2O_2 concentration could efficiently and specifically induce cancer cell death after treatment with H_2O_2-generating drugs [164,170,171]. As the cellular level of H_2O_2 in animal cells are carefully regulated by key antioxidant enzymes such as Mn^{+2}- dependent superoxide dismutase (SOD), glutathione peroxidase (GPx), catalase and thioredoxin peroxidase (TPx), new cancer

therapies targeting these H_2O_2-regulating enzymes to increase intracellular H_2O_2 level selectively in cancer cells will be an attractive clinical approach. We recently postulated that hWJSC-CM modulated changes in key oxidative stress enzyme activities involved in maintaining hydrogen peroxide (H_2O_2) levels as a mechanism to attenuate Burkitt lymphoma growth [172].

As such, the aim of this chapter is to investigate the tumoricidal effect of a 3kDa MWCO concentrate of hWJSC-CM on two B-cell lymphoma cell lines (Ramos and Toledo) for cell viability, cell death, mitochondria health, apoptosis, oxidative stress enzyme and reactive oxidative species (ROS) levels to explore whether the tumoricidal effects are H_2O_2 mediated.

3.2 Material and Methods

3.2.1 Cell Culture

Human Wharton's jelly stem cells (hWJSCs)

After informed patient consent and approval from the Institutional Domain Specific Review Board (DSRB), hWJSC lines were derived from human umbilical cords. hWJSCs were cultured in hWJSC medium comprising of 80% DMEM, 20% fetal bovine serum (FBS) (Biochrom, Berlin, Germany), 1% non-essential amino acids, 2 mM L-glutamine, 0.1 mM β-mercaptoethanol, 1% insulin-transferrin-selenium, antibiotic/antimycotic mixture (Invitrogen Life Technologies, Carlsbad, CA) and 16 ng/ml basic fibroblast growth factor (Millipore Bioscience, Temecula, CA).

Human lymphoma cells (Ramos and Toledo)

Approval for purchase and use of commercial human Burkitt's lymphoma cell lines (Ramos, CRL 1596) and diffuse large B cell lines (Toledo, CRL-2631) (American Type Culture Collection, ATCC, Rockville, MD, USA) was granted by

the National University of Singapore Institutional Review Board (NUS-IRB). The cell lines were thawed and initially cultured in lymphoma medium consisting of RPMI medium (Thermo Scientific) supplemented with 10% heat inactivated FBS (Biochrom) and 1% antibiotic/antimycotic mixture (Invitrogen).

Bone marrow mesenchymal stem cells (hBMMSCs)

Approval for purchase and use of commercial adult hBMMSCs (Lonza, Allendale, NJ, USA) was granted by the NUS-IRB. The cells were thawed and cultured in medium consisting of DMEM-high glucose (Invitrogen) supplemented with 10% FBS (Biochrom), 1% antibiotic/antimycotic mixture and 2 mM L-glutamine (Invitrogen).

3.2.2 Preparation of hWJSC conditioned medium (hWJSC-CM)

The preparation of hWJSC-CM was carried out as previously described [8,9,57,172]. Briefly, early passages of hWJSCs (3P to 5P) were first cultured in hWJSC medium until 70% confluency. The medium was then replaced with basal RPMI medium (Thermo Scientific) supplemented with 1% antibiotic/antimyotic mixture (Invitrogen). After 48 h, the medium (hWJSC-CM) was collected, filtered through a 0.22 μM filter (Millipore) and stored at -80^{o}C until use.

3.2.3 Preparation of hWJSC-CM concentrate

Twenty ml aliquots of the 48h hWJSC-CM were concentrated by centrifuged by placing them in 100kDa, 50kDa, 30kDa, 10kDa, 5kDa and 3kDa MWCO Vivaspin 20 tubes (Sartorius, Goettingen, Germany) and centrifugation at 3,000 x g for 1-2 h. The concentrates which were retained at the collection column were collected and stored at -20^{o}C. The protein concentration of concentrated hWJSC-CM was estimated using the Bradford assay (Biorad, USA).

3.2.4 Exposure of Ramos and cells to 3kDa to 100kDa hWJSC-CM concentrates

Ramos cells (1 x 10^5) were exposed to different hWJSC-CM MWCO concentrates (equal volumes) supplemented with 10% heat inactivated FBS, 1% antibiotic/antimycotic mixture and 20 mM L-glutamine (Invitrogen) for 48 h in 12-well plates at 37^0C in a 5% CO_2. The cells were then evaluated for cell viability (MTT).

3.2.5 Exposure of Ramos cells to 3kDa MWCO hWJSC-CM concentrate and flow-through fractions

Ramos cells (1 x 10^5) were exposed to equal volume of 3kDa MWCO concentrate and flow-through supplemented with 10% heat inactivated FBS, 1% antibiotic/antimycotic mixture and 20mM L-glutamine for 48 h in 12-well plates at 37^0C in a 5% CO_2. The cells were then evaluated for cell viability (MTT).

3.2.6 Exposure of Ramos and cells to 3kDa hWJSC-CM concentrate and heat-inactivated 3kDa hWJSC-CM concentrate

Equal volume of 3kDa concentrates were heat inactivated at 56^oC and 80^oC for 30 mins. Ramos cells (1 x 10^5) were then exposed to equal volume of 3kDa concentrates, 3kDa concentrates that were heat-inactivated at 56^oC (HI-56) and 3kDa concentrates that were heat-inactivated at 80^oC (HI-80) supplemented with 10% heat inactivated FBS, 1% antibiotic/antimycotic mixture and 20mM L-glutamine for 48 h in 12-well plates at 37^0C in a 5% CO_2. The cells were then evaluated for cell viability (MTT).

3.2.7 Experimental Design

Exposure of Ramos, Toledo and hBMMSCs to 3kDa MWCO hWJSC-CM concentrates

Ramos and Toledo cells, (1 x 10^5 each) were exposed to 3kDa MWCO hWJSC-CM concentrates (3kDa hWJSC-CM concentrates, 500 μg/mL) for 48h at 37^0C in a 5% CO_2. The lymphoma cells were then evaluated for viability (MTT assay), cell death analysis (PI+ and mitochondrial membrane potential), apoptosis (caspases 3, 8, 9), functional activity of key oxidative stress enzymes [superoxide dismutase, glutathione peroxidase, catalase and thioredoxin peroxidase], intracellular and extracellular hydrogen peroxide levels and oxidative stress analysis (mitochondrial superoxides, hydroxyl/peroxynitrile radicals, lipid peroxidation). Similar experiments were also carried out with hBMMSCs.

3.2.8 Experimental Analysis Test

Cell viability (MTT assay)

For cell viability, the treated Ramos, Toledo, hBMMSC cells and controls were collected and then re-suspended in 100 μL lymphoma media with 10 μl [3-(4, 5-dimethylthiazolyl-2)-2, 5-diphenyltetrazolium bromide] (MTT, 0.5 mg/ml) (Duchefa Biochemie B.V., Haarlem, Netherlands) and incubated for at least 4h at 37^oC in a 5% CO_2. The cell suspension was then centrifuged at 1,500 x g for 5 min and cell pellet resuspended in 100 μl of DMSO reagent (Sinopharm Chemical Reagent Co.Ltd) and dispensed into 96-well plates (NUNC, Rochester, NY). The plates were incubated in the dark at 37^oC for 10 min. Absorbance at 570 nm against a reference wavelength of 630 nm was measured using a spectrophotometer microplate reader (mQuant; BioTek, Winooski, VT, USA).

Cell Death Analysis

Propidium Iodide (PI+ Assay)

The treated and control cells were analyzed for PI positive cells using the propidium iodide molecular probe (Invitrogen). Briefly, the cells were collected and then resuspended with 500 μL of culture medium containing 1 μL of PI (1.0 mg /mL, Invitrogen) at 37°C for 30 min. The cells were filtered with a 40 μm strainer and analyzed with CyAn™ ADP analyzer (Beckman Coulter, Fullerton, CA, USA).

*Mitochondrial membrane potential assay (*a ⋅ *)*

The mitochondrial membrane potential ($\Delta\psi$) of the treated and control cells were analyzed using MitoTracker(R) Red CMXRos (Invitrogen). Briefly, the cells were collected and then incubated with 500 μL of culture medium containing 1 μL of 1 mM MitoTracker(R) Red CMXRos stock solution (Invitrogen) at 37°C for 30 min. The cells were filtered with a 40 μm strainer and analyzed with CyAn™ ADP analyzer (Beckman Coulter).

Apoptosis analysis

The treated and control cells were analyzed for caspase 3, 8, 9 activities using the CellEvent™ Caspase-3/7 Green Detection Reagent (Invitrogen), Vybrant(R) FAM Caspase-8 Assay Kit (Invitrogen) and Caspase 9 (active) FITC Staining Kit (Abcam, Cambridge, UK). Briefly, for caspase 3, the cells were collected and then incubated with 500 μL of culture medium with 0.125 μL of the 2.0 mM CellEvent™ Caspase-3/7 Green Detection Reagent at 37°C for 30 min. For caspase 8, the cells were collected and then resuspended with 300 μL of culture medium with 10 μL of 30X FLICA at 37°C for 60 min. For caspase 9, cells were collected and then incubated with 300 μL of culture medium with 1 μL of 30X FITC-LEHD-FMK at 37°C for 60 min. The cells were then washed, filtered with a 40 μm strainer and analyzed with a CyAn™ ADP analyzer (Beckman Coulter).

Oxidative stress enzyme analysis

The treated and control cells were collected and lysed using a mammalian cell extraction kit without protease cocktail and dithiothreitol (BioVision). Briefly, the cell pellet was incubated with 1000 μL of cell lysis buffer at 4^{o}C for 45 min. The mixture was then centrifuged at 15, 000 x g for 15 min. The supernatant was collected and stored at -80^{o}C until further analysis. Protein concentration of cell lysates were estimated using the conventional Bradford protein assay (Biorad). These cellular lysates were used for the analysis of superoxide dismutase, glutathione peroxidase (Sigma), catalase (Invitrogen) and thioredoxin peroxidase (Redoxica) activites using commercial kits.

Superoxide dismutase (SOD)

Briefly, for the SOD assay, 80 μL of the cell lysate was added to 200 μL of WST and 20 μL of enzyme working solutions and incubated at 37^{o}C for 30 min. Cell lysis buffer was used as a blank reference. Absorbance at 450 nm was measured using a micro plate ELISA reader (mQuant, BioTek).

Glutathione peroxidase (GPx)

Briefly for the GPx assay, 50 μL of the cell lysate was mixed with 890 μL of GPx assay buffer, 50 μL NADPH assay reagents and 10 μL t-Bu-OOH in 24-well plates and changes in absorbance at 340 nm were measured spectrophotometrically using a kinetic program (interval of 50 seconds, 6 readings) using a microplate ELISA reader (mQuant, BioTek). Cell lysis buffer was used as a blank reference.

Catalase

Briefly for catalase activity assay, 25 μl of cellular lysate was mixed with 25 μl of 40 μM H_2O_2 in 96-well microreader plates and incubated at room temperature for 30 min. 50 μl of HRP/Amplex Red reaction mixture reagent was then added into each sample and incubated at 37^{o}C for 30 min or longer. Cell lysis buffer was used as a blank reference. Absorbance at 560 nm was measured using a microplate ELISA reader (mQuant, BioTek).

Thioredoxin peroxidase (TPx)

Briefly, TPx activity was analyzed using the 2-Cys-Peroxiredoxin Activity Assay Kit (Redoxica, Arkansas, USA). The treated and control cells were collected and sonicated with a microtip sonicator on ice for 1 min with 10-15 seconds pulse in the supplied assay buffer. The samples were then centrifuged at 12,000 x g at 4^{0}C for 20 min. The cell lysates (supernatant) were collected, quantified using the Bradford assay and stored at -80^{o}C. Briefly, for peroxiredoxin activity assay, 25 μL of the cell lysate was mixed with 91 μL of reaction buffer, 5 μL of thioredoxin, 25 μL NADPH, 2 μL thioredoxin reductase and 2 μL of substrate in 96-well plates and changes in absorbance at 340 nm were measured spectrophotometrically using a kinetic program (interval of 50 seconds, 6 readings) using a microplate ELISA reader (mQuant, BioTek). Similar plates without the addition of thioredoxin were used as reaction blanks. The 2-Cys-peroxiredoxin activity was then calculated using the formula dA (Total-Reaction Blank)/0.0062 where dA=change in absorbance (Reaction-Reaction Blank).

Hydrogen peroxide assay

The culture media from the treated and control arms were collected and stored at -80^{o}C. The treated and control cells were then collected and lysed as described above.

Briefly, for hydrogen peroxide assay, 50 μl of cell lysate or 50 μl of supernatant was mixed with 50 μl of HRP/Amplex Red reaction (Invitrogen) in a 96-well plate and incubated at 37°C for 30 min or longer. Fluorescence readings using excitation 560 nm and emission detection at 590 nm were measured using a Tecan Infinite M1000 microplate reader (Tecan Group Ltd, Mannedorf, Switzerland).

Oxidative Stress assay

Mitochondrial superoxide assay

The treated and control cells were analyzed for mitochondrial superoxide using the MitoSOX™ Red mitochondrial superoxide indicator (Invitrogen). Briefly, the cells were collected and incubated with 100 μL of culture medium containing 0.1 μL of 5mM MitoSOX™ working solution at 37°C for 30 min. The cells were then washed, filtered with a 40 μm strainer and analyzed with CyAn™ ADP analyzer (Beckman Coulter).

Hydroxyl radical and peroxynitrile anion

The treated and control cells were analyzed for highly reactive oxygen species (hydroxyl radical and peroxynitrile anions) using 3'-(p-hydroxyphenyl) fluorescein (HPF, Invitrogen). Briefly, the cells were collected and incubated with 100 μL of culture medium containing 0.2 μL of 5 mM HPF at 37°C for 30 min. The cells were then washed, filtered with a 40 μm strainer and analyzed with CyAn™ ADP analyzer (Beckman Coulter).

Lipid peroxidation

The treated and control cells were collected and stained using the Image-iT(R) Lipid Peroxidation Kit based on the manufacturer's instructions (Invitrogen). Briefly, the cells were collected and incubated with 100 μL of culture medium containing 1 μL of 10 mM Image-iT(R) Lipid Peroxidation Sensor (Component A) for 30 min at 37°C. The cells were then washed, filtered with a 40 μm strainer

before analysis using BD LSRFortessa™ (BD Bioscience, Heideberg, Germany) with excitation/emission 581/591 nm and 488/510 nm.

3.2.9 Statistical Analysis

All results were expressed as mean (fold change) ± SEM and statistical significance between the groups was calculated using the one way ANOVA or two-tailed Student's t-test (SPSS Statistic v 17.0 software package) (SPSS, Inc, IL). The *p*-value of <0.05 was considered as statistically significant.

3.3 Results

3.3.1 Evaluation of the best MWCO of hWJSC-CM that inhibit lymphoma cell growth

The results showed that there were significant reductions in cell viability of Ramos cells after 48 h across all MWCO concentrates compared to controls. Additionally, the 3kDa MWCO concentrate had the greatest inhibition of cell viability. The fold changes for cell viability normalized to controls were 0.86 ± 0.001, 0.84 ± 0.016, 0.71 ± 0.005, 0.82 ± 0.014, 0.67 ± 0.018, 0.58 ± 0.019 for 100kDa, 50kDa, 30kDa, 10kDa, 5kDa and 3kDa concentrates respectively (Fig. 7).

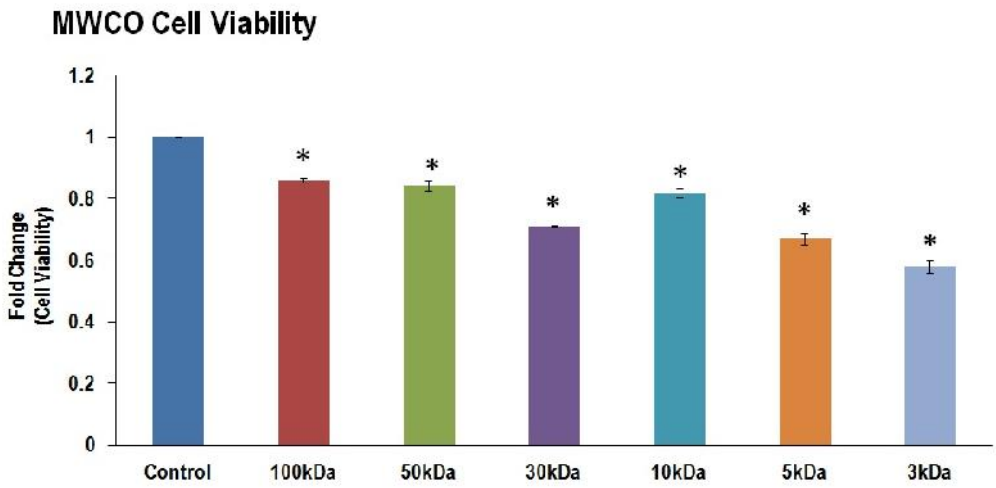

Figure 7 MWCO Cell viability of Ramos lymphoma cells

Cell viability (MTT assay) of Ramos lymphoma cells exposed to different MWCOs' concentrates of hWJSC-CM for 48 h. Note significant decreases fold changes of cell viability (normalized to control) in the Ramos cells exposed to the different MWCO concentrates. Values are expressed as mean ± SEM of 3 different experiments. Asterisk (*) indicates statistical significance of $p<0.05$.

3.3.2 Evaluation of 3kDa hWJSC-CM concentrate and flow-through factions on lymphoma cells

The concentrated hWJSC-CM fraction and flow-through (FT) fractions were collected as shown in Fig. 8A (Fig. 8A). There was significant decreases cell viability after 48h exposure to 3kDa hWJSC-CM concentrates compared to the FT fractions and controls. The cell viability rates for the concentrated hWJSC-CM were 0.60 ± 0.05, compared to 1.14 ± 0.02 for FT and controls (Fig. 8B).

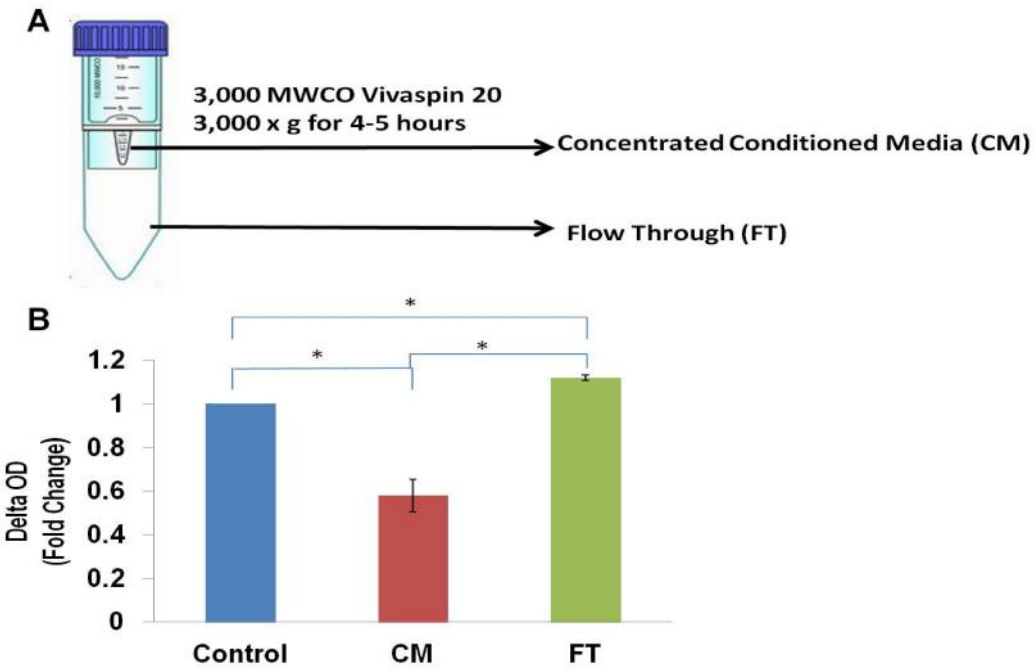

Figure 8 Cell viability of Ramos lymphoma cells exposed to CM and FT

(A) Schematic diagram showing VIVASPIN centrifugation of hWJSC-CM to separate concentrated (CM) and flow-through (FT) fractions. **(B)** Cell viability (MTT assay) of Ramos lymphoma cells exposed to CM and FT fractions for 48h. Significant decreases in cell viability of lymphoma cells when exposed to CM compared to FT and controls. The values are expressed as mean ± SEM of 3 different experiments. Asterisk (*) indicates statistical significance of $p<0.05$.

3.3.3 Evaluation of 3kDa hWJSC-CM concentrate and heat-inactivated 3kDa hWJSC-CM concentrate on lymphoma cells

The 3kDa concentrated hWJSC-CM fraction were heat-inactivated at 56^{o}C (HI-56) and 80^{o}C (HI-80). The lymphoma cells had significant decreased in cell viability after 48h exposure to concentrated hWJSC-CM (hWJSC-CM) and heat-inactivated 3kDa hWJSC-CM concentrates (HI-56/HI-80) compared to control. There were no significant difference in cell viability between the concentrated hWJSC-CM and 3kDa hWJSC-CM concentrates heat-activated at both 56^{o}C (HI-56) and 80^{o}C (HI-80). The fold change in cell viability rates normalised to control for hWJSC-CM, HI-56 and HI-80 were 0.86 ± 0.009), 0.90 ± 0.01 and 0.84 ± 0.02 respectively (Fig. 9).

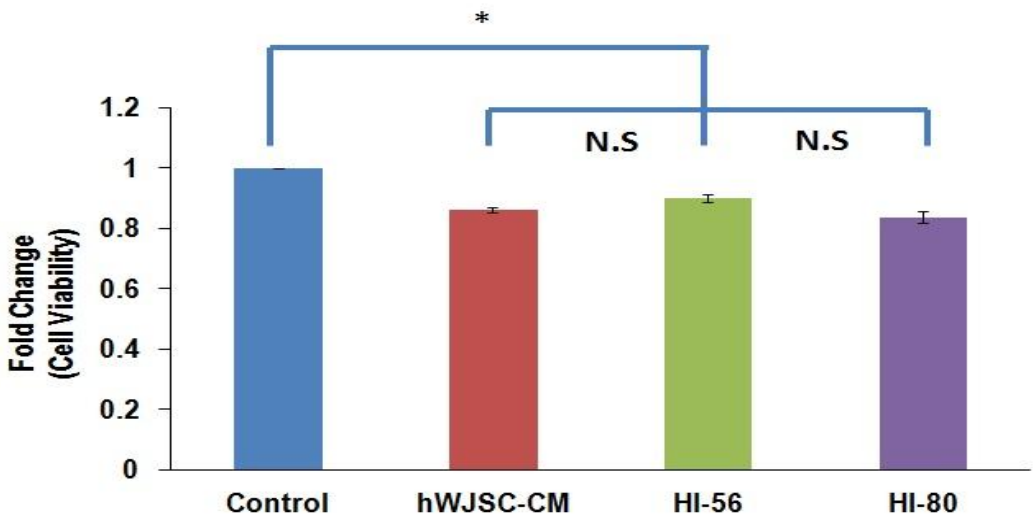

Figure 9 Cell viability of Ramos lymphoma cells exposed to heat-inactivated 3kDa hWJSC-CM concentrates

Cell viability (MTT assay) of Ramos lymphoma cells exposed to heat-inactivated 3kDa concentrates of hWJSC-CM for 48 h. No significant decreases fold changes of cell viability (normalized to control) in the Ramos cells exposed to hWJSC-CM concentrates and heat-inactivated hWJSC-CM concentrates. Note no significant difference (N.S) in cell viability between hWJSC-CM concentrates compared to heat-inactivated hWJSC-CM concetrates Values are expressed as mean ± SEM of 3 different experiments. Asterisk (*) indicates statistical significance of $p<0.05$.

3.3.4 Evaluation of 3kDa hWJSC-CM concentrate on cell viability, mitochondrial membrane potential and cell death in lymphoma cells

Both Ramos and Toledo lymphoma cells had significant reductions in cell viability, significant increases in the percentage of cells positive for PI and significant reductions in mitochondrial membrane potential but there were no significant changes to hBMMSCs.

The fold changes for cell viability normalized to their respective controls were Ramos cells (0.70 ± 0.05), Toledo cells (0.84 ± 0.03) and hBMMSCs (1.0 ± 0.03) (Fig. 10A).

The fold changes for the percentages of PI+ cells normalized to their respective controls were Ramos (1.50 ± 0.11), Toledo (1.76 ± 0.03) and hBMMSCs (1.07 ± 0.04) (Fig. 10B).

The fold changes for $\Delta\psi$ normalized to their respective controls were Ramos (0.86 ± 0.015), Toledo (0.95 ± 0.003) and hBMMSCs (1.00 ± 0.002) (Fig. 10C).

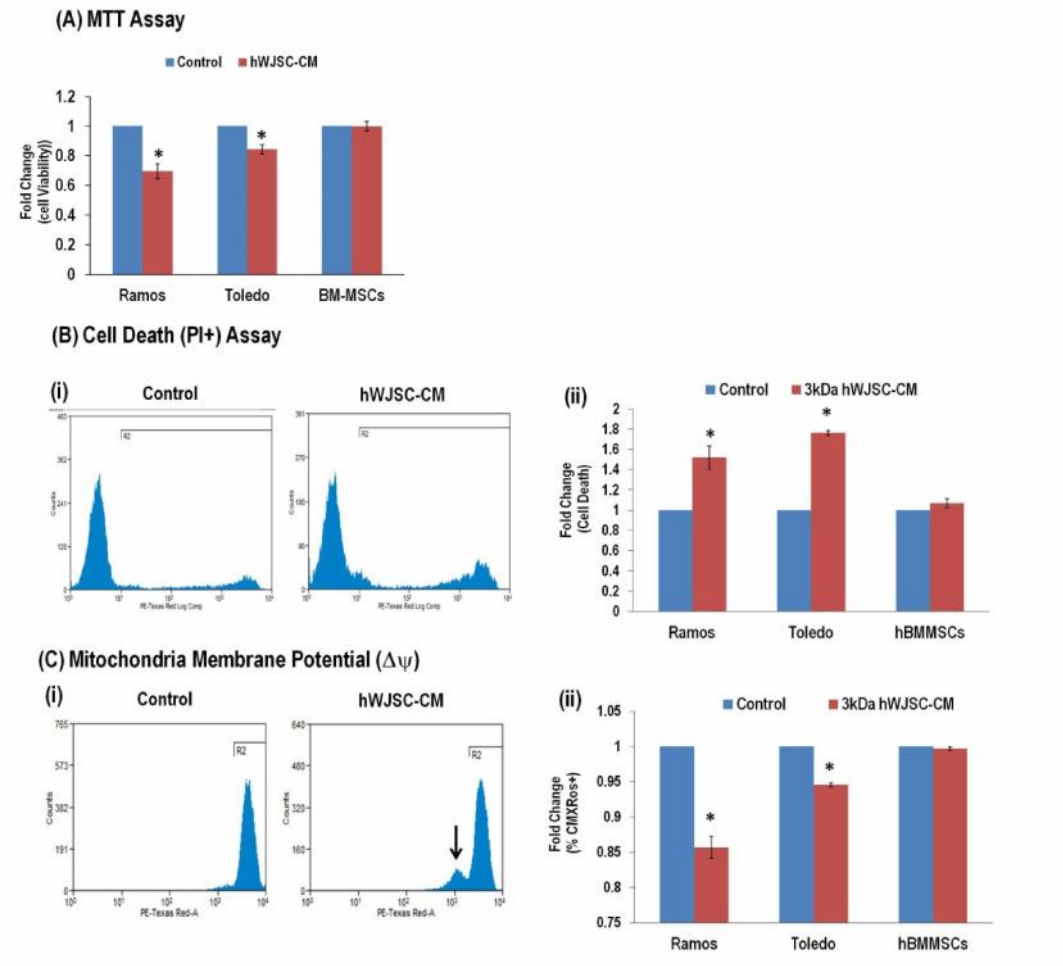

Figure 10 Cell viability, cell death and mitochondria membrane potential of Ramos, Toledo and hBM-MSCs

(A) Cell viability fold changes (MTT assay) of Ramos, Toledo and hBMMSCs exposed to 500 µg/ml of the 3kDa MWCO concentrate for 48 h. Note significant decreases in cell viability (normalized to control) when Ramos and Toledo cells were exposed to the 3kDa MWCO concentrate with no significant changes in hBMMSCs. **(B) (i)** Representative flow cytometry histogram for cell death analysis. **(ii)** Cell death (PI+ assay) fold changes of Ramos, Toledo and BMMSCs exposed to 500 µg/ml of the 3kDa MWCO concentrate for 48 h**.** Note significant increases in cell death (normalized to control) of Ramos and Toledo cells exposed to the 3kDa MWCO concentrate with no significant changes in hBMMSCs. **(C) (i)** Representative flow cytometry histogram for mitochondria membrane potential analysis. **(ii)** Mitochondrial membrane potential fold changes of Ramos, Toledo and hBMMSCs exposed to 500 µg/ml of the 3kDa MWCO concentrate for 48 h. Note significant decreases in mitochondrial membrane potential (normalized to control) in the Ramos and Toledo cells exposed to the 3kDa MWCO concentrate with no significant changes in hBMMSCs. All values in (**A-C)** are expressed as mean ± SEM of 3 different experiments. Asterisk (*) indicates statistical significance of $p<0.05$.

3.3.5 Evaluation of 3kDa hWJSC-CM concentrate on apoptosis in lymphoma cells

Both Ramos and Toledo cells had significant increases in activated caspase 3, caspase 8 and caspase 9 after 48 h of exposure to the 3kDa MWCO concentrate but there were no significant changes to the hBMMSCs. The fold changes in activated caspase 3 normalized to their respective controls were Ramos (1.70 ± 0.01), Toledo (1.53 ± 0.12) and hBMMSCs (0.98 ± 0.10) (Fig. 11A). The fold changes in activated caspase 8 normalized to their respective controls were Ramos (1.80 ± 0.02), Toledo (1.50 ± 0.09) and hBMMSCs (0.77 ± 0.2) (Fig. 11B).The fold changes in activated caspase 9 normalized to their respective controls were Ramos (3.00 ± 0.15), Toledo (1.62 ± 0.08) and hBMMSCs (1.25 ± 0.05) (Fig. 11C).

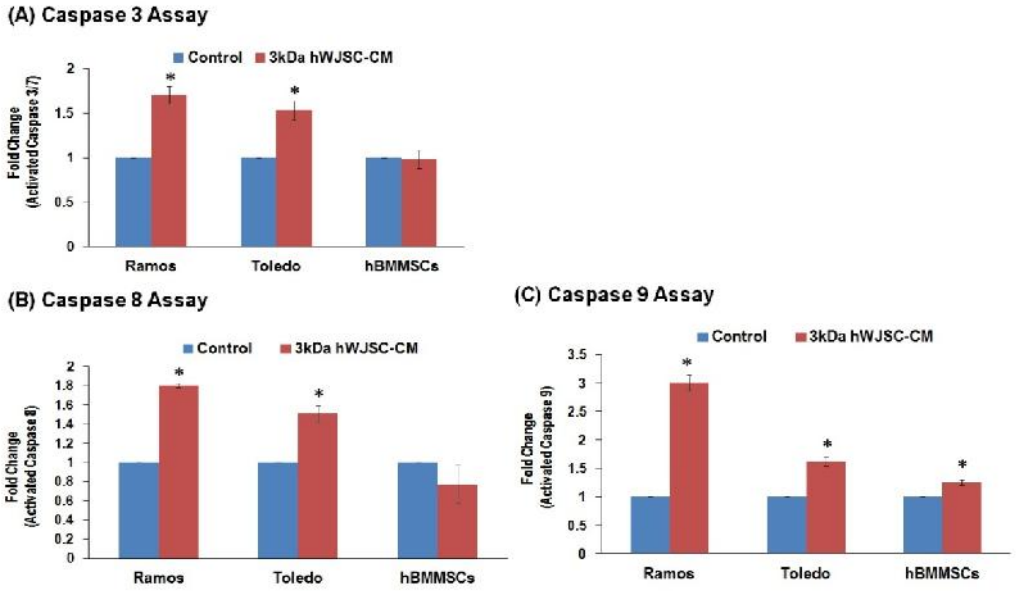

Figure 11 Apoptotic analysis of Ramos, Toledo and hBM-MSCs

(A-C) Apoptosis analysis fold changes of Ramos, Toledo and hBMMSC cells exposed to 500 µg/ml of the 3kDa MWCO concentrate for 48 h. Note significant increases (normalized to control) in activated caspase 3 **(A)** and activated caspase 8 **(B)** when Ramos and Toledo cells were exposed to the 3kDa MWCO concentrate with no significant changes in hBMMSCs. Note significant increases (normalized to control) of activated caspase 9 **(C)** in Ramos, Toledo and hBMMSCs. All values in (**A-C)** are expressed as mean ± SEM of 3 different experiments. Asterisk (*) indicates statistical significance of $p<0.05$.

3.3.6 Evaluation of 3kDa hWJSC-CM concentrate on oxidative stress enzyme in lymphoma cells

The Ramos, Toledo and hBMMSC cells had significant increases in SOD functional activity after 48 h of exposure to 500 μg/ml of the 3kDa MWCO concentrate. The fold changes in SOD functional activity normalized to its respective controls were Ramos (1.43 ± 0.04), Toledo (1.28 ± 0.05) and hBMMSCs (1.19 ± 0.02) (Fig. 12A).

The Ramos, Toledo and hBMMSC cells had significant decreases in GPx and catalase functional activity after 48 h exposure to the 3kDa MWCO concentrate. The fold changes in GPx functional activity normalized to its respective controls were for Ramos (0.68 ± 0.06), Toledo (0.88 ± 0.01) and hBMMSCs (0.95 ± 0.02) (Fig. 12B).

The fold changes in catalase functional activity normalized to their respective controls were Ramos (0.61 ± 0.06), Toledo (0.98 ± 0.003) and hBMMSCs (0.48 ± 0.03) (Fig. 12C).

Both Ramos and Toledo cells had decreased (not significant for Toledo) TPx functional activity after 48 h of exposure to 500 μg/ml of the 3kDa MWCO concentrate with no significant changes to hBMMSC TPx functional activity. The fold changes in TPx functional activity normalized to their respective controls were Ramos (0.78 ± 0.07), Toledo (0.87 ± 0.003) and hBMMSCs (1.03 ± 0.10) (Fig. 12D).

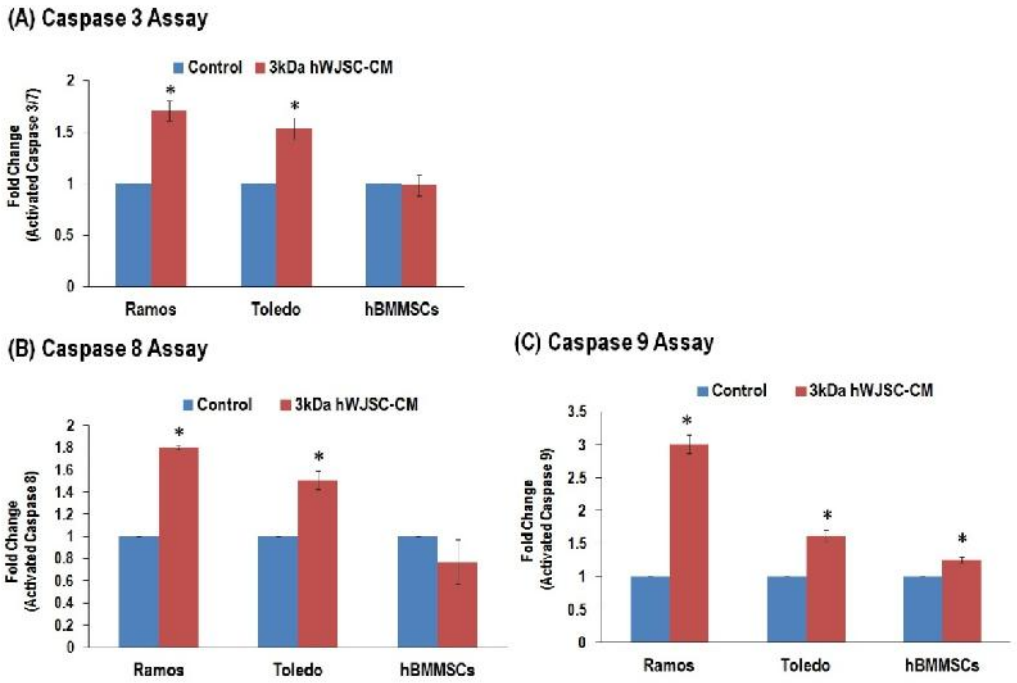

Figure 12 Oxidative stress enzymes functional activities analysis

(A) SOD functional activity fold changes of Ramos, Toledo and hBMMSC cells exposed to 500 µg/ml of the 3kDa MWCO concentrate for 48h. Note significantly greater SOD functional activity (normalized to control) was observed in Ramos, Toledo and hBMMSCs when exposed to the 3kDa MWCO concentrate **(B)** GPx functional activity fold changes of Ramos, Toledo and hBMMSC cells exposed to 500 µg/ml of the 3kDa MWCO concentrate for 48h. Note significantly lower GPx activity (normalized to control) was observed in the Ramos, Toledo and hBMMSC cells exposed to the 3kDa MWCO concentrate **(C)** Catalase functional activity fold changes of Ramos, Toledo and hBMMSCs exposed to 500 µg/ml of the 3kDa MWCO concentrate for 48h. Note significantly lower catalase activity (normalized to control) was observed in the Ramos, Toledo and hBMMSC cells exposed to the 3kDa MWCO concentrate. **(D)** TPx functional activity fold changes of Ramos, Toledo and hBMMSC cells exposed to 500 µg/ml of the 3kDa MWCO concentrate for 48h. Note significantly lower TPx activity (normalized to control) was observed in the Ramos and Toledo cells exposed to the 3kDa MWCO concentrate with no significant changes in hBMMSCs. All values are expressed as mean ± SEM of 3 different experiments. Asterisk (*) indicates statistical significance of $p<0.05$.

3.3.7 Evaluation of 3kDa hWJSC-CM concentrate on hydrogen peroxide levels in lymphoma cells

The Ramos, Toledo and hBMMSC cells had increased (not significant for Toledo and hBMMSCs) intracellular and significant increased in extracellular H_2O_2 after 48 h exposure to 500 µg/ml of the 3kDa MWCO concentrate. The fold changes of intracellular H_2O_2 normalized to their respective controls were Ramos (1.21 ± 0.03), Toledo (1.07 ± 0.03) and hBMMSCs (1.33 ± 0.06) (Fig. 13A). The fold

changes of extracellular H_2O_2 normalized to their respective controls were Ramos (3.42 ± 0.34), Toledo (1.57 ± 0.19) and hBMMSCs (1.23 ± 0.02) (Fig. 13B).

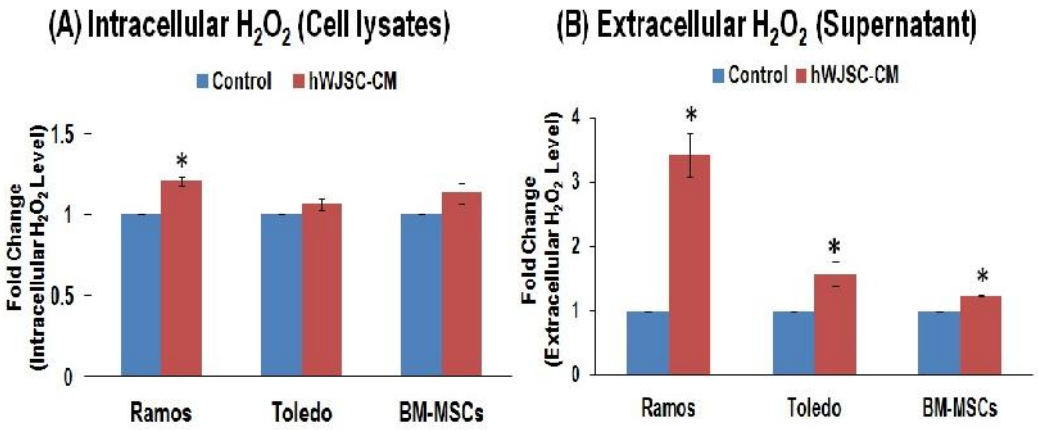

Figure 13 Hydrogen peroxide analysis of Ramos, Toledo and hBM-MSCs

(A) Hydrogen peroxide fold changes in Ramos, Toledo and hBMMSC cells exposed to 500 µg/ml of the 3kDa MWCO concentrate for 48 h. There were significantly higher intracellular hydrogen peroxide levels (normalized to control) in cell lysates **(A)** and supernatants **(B)** of Ramos cells exposed to the 3kDa MWCO concentrate. All values are expressed as mean ± SEM of 3 different experiments. Asterisk (*) indicates statistical significance of $p<0.05$.

3.3.8 Evaluation of 3kDa hWJSC-CM concentrate on mitochondrial superoxide, hydroxyl radical/peroxynitrile anion and lipid peroxidation levels in lymphoma cells

The Ramos, Toledo and hBMMSCs had increases (not significant for Toledo) in mitochondrial superoxide ($^{\cdot}O_2^-$) after 48 h exposure to 500 µg/ml of the 3kDa MWCO concentrate with no significant changes to the hBMMSCs. The fold changes of mitochondrial superoxide ($^{\cdot}O_2^-$) normalized to their respective controls were Ramos (4.30 ± 0.17), Toledo (1.28 ± 0.05) and hBMMSCs (1.08 ± 0.16) (Fig. 14A).

Both Ramos and Toledo cells had significant increases in hydroxyl radical/peroxynitrile anion ($^{\cdot}OH^-/^{\cdot}OONO^-$) after 48 h exposure to the 3kDa MWCO concentrate with no significant changes to the hBMMSCs. The fold changes of $^{\cdot}OH^-/^{\cdot}OONO^-$ (normalized to their respective controls were Ramos (4.64 ± 0.57), Toledo (1.77 ± 0.13) and hBMMSCs (1.05 ± 0.03) (Fig. 14B).

Ramos, Toledo and hBMMSC cells had significant increases in lipid peroxidation after 48 h exposure to the 3kDa MWCO concentrate. The fold changes of lipid peroxidation normalized to their respective controls were Ramos (2.07 ± 0.12), Toledo (1.45 ± 0.12) and hBMMSCs (1.10 ± 0.03) (Fig. 14C).

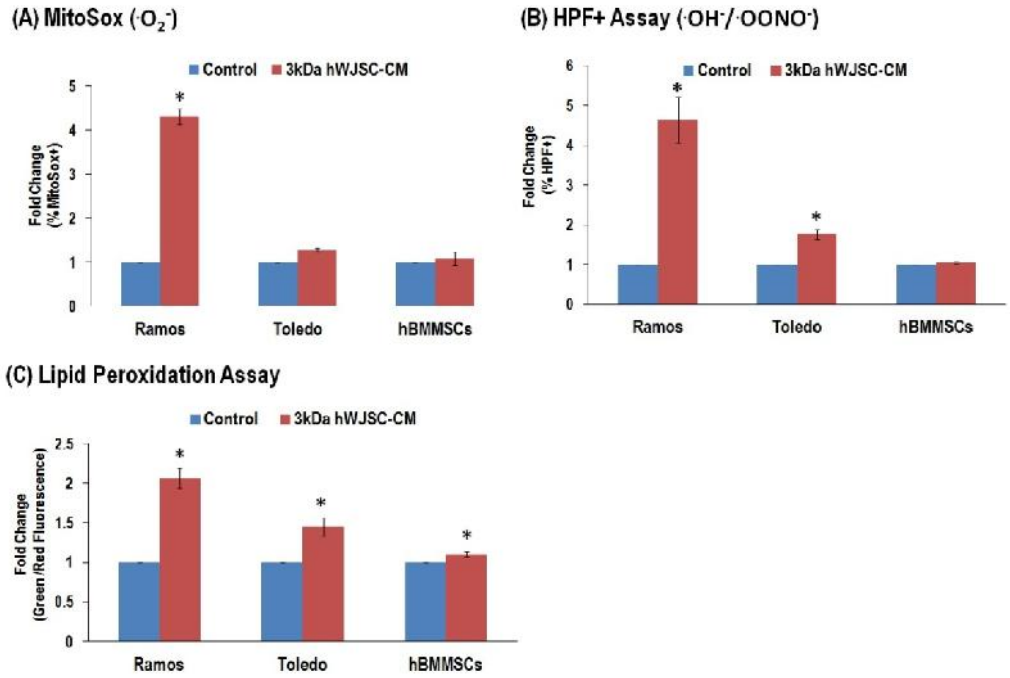

Figure 14 Oxidative stress analysis of Ramos, Toledo and hBM-MSCs

(A) Mitochondria superoxide fold changes in Ramos, Toledo and hBMMSC cells exposed to 500 µg/ml of the 3kDa MWCO concentrate for 48 h. Note significant increases in mitochondria superoxide levels (normalized to control) when Ramos cells were exposed to the 3kDa MWCO concentrate with no significant changes in Toledo and hBMMSC cells. **(B)** Hydroxyl radical and peroxynitrile anion fold changes (HPF assay) of Ramos, Toledo and hBMMSCs exposed to 500 µg/ml of the 3kDa MWCO concentrate for 48 h**.** Significant increases in hydroxyl radical and peroxynitrile anions (normalized to control) in Ramos and Toledo cells exposed to the 3kDa MWCO concentrate with no significant changes in hBMMSCs. **(C)** Lipid peroxidation fold changes of Ramos, Toledo and hBMMSC cells exposed to 500 µg/ml of the 3kDa MWCO concentrate for 48 h. Note significant increases in lipid peroxidation levels (normalized to control) when Ramos, Toledo and hBMMSC cells were exposed to the 3kDa MWCO concentrate. All values in (**A-C)** are expressed as mean ± SEM of 3 different experiments. Asterisk (*) indicates statistical significance of $p<0.05$.

3.4 Discussion

In this study we first reported that exposing lymphoma cells to a 3kDa molecular weight cut-off (MWCO) concentrate of hWJSC-CM induced the cell death in the cancer cells compared to other molecular weight cut-offs. Further analysis suggested that the bioactive molecules were larger than 3kDa as lymphoma cell

viability significant decreases with the 3kDa hWJSC-CM concentrates fraction and not with the flow through (FT) fraction. Subsequent experiments using the 3kDa MWCO concentrate showed greater reductions in cell viability, disruption of mitochondrial membrane potential and increased caspase 3, 8 and 9 apoptosis and cell death in both types of B cell lymphomas but not in adult bone marrow MSCs. Current anti-cancer chemotherapy and radiation treatments in lymphoma patients frequently induce non-specific damage to the bone marrow, stromal cells, gastrointestional tract, heart, brain and kidney that impede survival outcome [128,155,156,159-161]. Since the adult hBMMSCs in the present study were minimally affected by the 3kDa MWCO concentrate, the use of hWJSC-CM as a potential therapy for lymphoma patients may be a safe option in the future as the hematopoietic niche may not be affected. It was observed in the present study increased functional activity of H_2O_2-generating SOD enzymes and concomitant decreases in functional activity of all three H_2O_2-catabolic antioxidative enzymes (GPx, catalase and TPx) in both lymphoma cell types, the mechanism of the tumoricidal effects of hWJSC-CM may be via disruption of these pathways. Under normal physiological conditions, cells remove reactive oxidative stress by converting reactive oxygen species to H_2O_2 via SOD enzymes and the presence of efficient enzymes such as GPx, catalase and TPx kept H_2O_2 levels low in the cells by further breaking them down into water [163]. Many types of cancer cells, including hematological malignancies, were shown to keep H_2O_2 levels low by having lowered SOD, GPx and catalase activities [173-175]. Numerous previous studies aimed at manipulating these specific enzymes have all shown promising results in inhibition of cancer cell growth. For example, extracts of the Creosote bush (*Larrea divaricate*) activated Mn^{2+}-SOD and decreased glutathione peroxidase activity subsequently suppressed lymphoma proliferation and induced apoptosis [164]. Likewise, overexpression of Mn^{2+}-SOD in other cancer cell types such as human melanoma, fibrosarcoma, human glioma, breast cancer cells, oral

squamous carcinoma, prostatic carcinoma have resulted in inhibition of their proliferation *in vitro* or *in vivo* [173,176,177]. Moreover, since these anticancer effects were abolished by overexpression of H_2O_2-removing enzymes (catalase and peroxidase) it suggested that the anticancer effect may be mediated by the increased H_2O_2 [177,178].

We also observed increases in H_2O_2 levels in both lymphoma cell lines after treatment with the 3kDa MWCO concentrate confirming that the level of H_2O_2 plays a decisive role in deciding whether cancer cells proliferate or undergoes apoptosis. Numerous studies have suggested that the high level of intracellular H_2O_2 induces cancer cell death [164,170,171]. However, direct administration of H_2O_2 to cancer patients has been controversial over the years as evidence on both safety and effectiveness were yet to be confirmed [179-181]. As such, direct treatment with H_2O_2 was never seen as an appropriate therapeutic strategy [181]. On the other hand, more and more convincing evidence now suggests that increasing cellular H_2O_2 using a H_2O_2-generating system is an efficient way of inducing cancer cell death [164]. In fact, many current chemotherapeutic agents such as paclitaxel, cisplatin, arsenic trioxide, etoposide and doxorubicin exert their anti-cancer effects by increasing the level of H_2O_2 in the cancer cells [164]. Likewise, Chen et al [182] observed that treatment with pharmacologic ascorbic acid selectively induced cell death in several cancer cell lines by increasing H_2O_2 levels. Their data indicates that the induction of cancer cell death is dependent on ascorbate radical intermediate-mediated extracellular H_2O_2 formation. The increased extracellular H_2O_2 then target cancer cell membrane lipids or diffuse across the membranes to target intracellular DNA, DNA repair proteins or the mitochondria, resulting in oxidative stress. Moreover, recent data using high-dose intravenous vitamin C therapy in patients generated high H_2O_2 that were shown to kill cancer cells [182,183]. On the other hand, reports have shown that intercellular H_2O_2-generating drugs when used together with certain chemotherapeutic agents

such as dexamethasone enhanced cancer cell sensitivity to chemotherapy [184,185]. Consequently, the increase in cellular H_2O_2 level favors the formation of other reactive oxygen species like the superoxides, hydroxyl radical and peroxynitrile anions which leads to higher oxidative stress and lipid peroxidation [164,186] that drive cancer cell death which is consistent with the findings in our present study. However, it is still relatively unclear as to what levels of H_2O_2 exert chemopreventive, carcinogenic and chemotherapeutic effects and more studies are required in this area. A delicate balance in the cell's redox system and H_2O_2 level is paramount to effectively regulate its chemopreventive and chemotherapeutic effects and yet avoid carcinogenic effects when using H_2O_2-generating systems as anti-cancer therapeutics.

The specific active agents present in hWJSC-CM that are responsible for its tumoricidal effects are still not known. Our previous comparative microarray transcriptome profile studies of hWJSCs showed upregulation of several pro-apoptotic and tumor-suppressor genes such as TGF beta-R2, ATM and PTEN in these cells compared to hBMMSCs and embryonic stem cells [15]. Also, our unpublished data on miRNA-profiling indicated that hWJSCs expressed high levels of various tumor suppressor miRNAs such as miRNA-146a and miRNA-126 compared to normal adult hBMMSCs and skin fibroblasts. Furthermore, previous proteomic cytokine arrays indicated that hWJSC-CM contains various cytokines expressed at high levels such as MCP-1, IL-6, IL-8 and IL-12 which are known to regulate cancer cell growth and death [8,58]. It would be interesting to test the tumoricidal effects of these specific molecules in the 3kDa MWCO concentrate by knocking, blocking or neutralizing the mRNA, miRNA or proteins in future studies.

Chapter 4: Immunogenic Cancer Cell Death induced by hWJSC-CM

4.1 Introduction

In recent years, there are growing evidence indicating that the patient's immune competence is crucial in determining the efficacy in chemotherapeutic and radio-therapeutic treatment [187]. However, in many cases, the tumors have already developed some immune tolerance and therefore the patients' undergoing treatment have an immunosuppressive tumor microenvironment and affects the efficacy of chemotherapy and radiotherapy [187].

Recent discoveries of chemotherapeutic and radiothereuptic treatment strategies that induce immunogenic cell death in tumors have resulted in many long-term successful therapeutic options for tumor eradication [188,189]. Immunogenic cell death (ICD), both directly or indirectly, has resulted in the emission of specific signals that render the dying cells visible to the immune system that reinitiate a very potent antitumor immunity response [188,190].

The molecular hallmark of ICD relies on at least 3 independent events: (1) the early surface exposure of calreticulin (ecto-CRT) on dying cells, (2) secretion of ATP and (3) release of high mobility group box-1 (HMGB1) and heat shock proteins (HSPs) by dying cancer cells [187]. These sequences of events presented the "eat-me", 'find-me" signals to facilitate recruitment, phagocytosis, antigen cross-presentation and polarization of immune cells (antigen-presenting cells-dendritic cells), cytotoxic natural killer and T cells in re-activating the immune system for launching a potent anti-tumor immunity response [189]. However, promising as it seems, there are only a few tumor-specific chemotherapeutic drugs that induce ICD in cancer cells available in the market. Hence it is

important to explore for novel agents that can elicit ICD response which can be used alone or as part of an combinational therapy [188].

In chapter 2 and 3, we have previously isolated a primitive population of MSCs from the Wharton's jelly of discarded umbilical cord. These hWJSCs have been shown to exhibit anti-tumorigenic properties on many cancer cell types both *in vitro* and *in vivo* animal models. As earlier studies reported that hWJSCs secrete large varieties of cytokines and factors like IL-6, IL-8, MCP-1 [8] that have been known to play a role in releasing DAMPs and modulating the innate immune response [58]. In addition, treatment of mammary carcinoma xenograft rat model with rat WJSCs increases CD8+ T cell infiltration in the tumor tissue [53]. However, there are currently no studies evaluating whether these hWJSCs and or its extract could induce ICD and release signals indicating of immunogenic cell death.

It has previously been shown that hWJSCs do not induce tumorigenesis in laboratory animals, primates and in humans [22,23,73,74] and unlike adult BM-MScs, they do not transform to tumor-associated fibroblasts (TAFs) [88]. Additionally, there have been no reports of any toxicity or side effects when hWJSCs were injected into laboratory animals [26], non-human primates [74] and in human clinical trials for the treatment of aplastic anemia [19], leukemia [23], type 1 diabetes mellitus [20], heart failure [22] and neurological disorders [21]. All these studies point to the safety of using hWJSCs or hWJSC-derived products as future cancer therapeutics. Therefore, the aim of this chapter is to evaluate the immunogenic cell death effects of 3kDa MWCO hWJSC-CM *in vitro* assays.

4.2 Material and Methods

4.2.1 Cell Culture

Human Wharton's jelly stem cells (hWJSCs)

After informed patient consent and approval from the Institutional Domain Specific Review Board (DSRB), hWJSC lines were developed from human umbilical cords. hWJSCs were cultured in hWJSC medium comprising of 80% DMEM, 20% fetal bovine serum (FBS) (Biochrom, Berlin, Germany), 1% non-essential amino acids, 2 mM L-glutamine, 0.1 mM β-mercaptoethanol, 1% insulin-transferrin-selenium, antibiotic/antimycotic mixture (Invitrogen Life Technologies, Carlsbad, CA) and 16 ng/ml basic fibroblast growth factor (Millipore Bioscience, Temecula, CA).

Human lymphoma cells (Ramos)

Then approval for purchase and use of commercial human Burkitt's lymphoma cell lines (Ramos, CRL 1596, ATCC) was granted by the National University of Singapore Institutional Review Board (NUS-IRB). The cell lines were thawed and initially cultured in lymphoma medium consisting of RPMI medium (Thermo Scientific) supplemented with 10% heat inactivated FBS (Thermo Scientific Hyclone) and 1% antibiotic/antimycotic mixture (Invitrogen).

Human Osteosarcoma (MG63)

The approval for purchase and use of commercial human osteosarcoma cell lines (MG63, CRL-1427, ATCC) was granted by the NUS-IRB. The cells were thawed and cultured in medium consisting of RPMI (Biowest, Nuaille, France) supplemented with 10% FBS (Thermo Scientific Hyclone), 1% antibiotic/antimycotic mixture and 2 mM L-glutamine (Invitrogen Life Technologies).

Human Mammary Adenocarcinoma (MDA-MB-231)

The approval for purchase and use of commercial human mammary adenocarcinoma (MDA-MB-231, ATCC HTB-26) was granted by the NUS-IRB. The cells were thawed and cultured in medium consisting of RPMI (Biowest, Nuaille, France) supplemented with 10% FBS (Thermo Scientific Hyclone), 1% antibiotic/antimycotic mixture and 2 mM L-glutamine (Invitrogen Life Technologies).

4.2.2 Preparation of hWJSC conditioned medium (hWJSC-CM)

The preparation of hWJSC-CM was carried out as previously described [8,9,57,172]. Briefly, early passages of hWJSCs (3P to 5P) were first cultured in hWJSC medium until 70% confluency. The medium was then replaced with basal RPMI medium (Biowest) supplemented with 1% antibiotic/antimyotic mixture (Invitrogen). After 48h, the medium (hWJSC-CM) was collected, filtered through a 0.22μM filter (Millipore) and stored at -80^{o}C until use.

4.2.3 Preparation of 3kDa MWCO hWJSC-CM concentrate

Twenty ml aliquots of the 48h hWJSC-CM was concentrated by centrifugation by placing them in 3kDa MWCO Vivaspin 20 tubes (Sartorius, Goettingen, Germany) and centrifuged at 3,000 x g for 1-2h. The concentrates which were retained at the collection column were collected and stored at -20^{o}C. The protein concentration of concentrated hWJSC-CM was estimated using the Nanodrop^{TM} spectrophotometer (Nanodrop Technologies, Wilmington, DW).

4.2.4 Experimental Design

Exposure of Ramos, MG63 and MDA-MB-231 to 3kDa MWCO hWJSC-CM concentrates

Ramos (1 x 10^5 cells), MG63 (5 x 10^4 cells) and MDA-MB-231(5 x 10^4 cells), were exposed to 3kDa MWCO hWJSC-CM concentrates (hWJSC-CM, 500 μg/mL) in their respective growth media for 48h at 37^{0}C in a 5% CO_2. The cells were then evaluated for cell morphology, viability (MTT assay), cell death analysis, apoptosis, autophagy, mitochondria stress, endoplasmic reticulcum stress and danger-associated molecular patterns (DAMPs).

4.2.5 Experimental Analysis Test

Cell Morphology

Changes in cell morphology of the cancer cells were monitored using inverted phase contrast optics (Nikon Instruments, Tokyo, Japan).

Cell viability (MTT assay)

To determine cell viability, the treated Ramos, MG63 and MDA-MB 231 cells and controls were collected and then re-suspended in 100 μL growth media with 10 μl [3-(4, 5-dimethylthiazolyl-2)-2, 5-diphenyltetrazolium bromide] (MTT, 0.5 mg/ml) (Duchefa Biochemie B.V., Haarlem, Netherlands) added and incubated for at least 4h at 37^{o}C in a 5% CO_2. The cell suspension was then centrifuged at 1,500 x g for 5 min and cell pellet resuspended in 100 μl of DMSO reagent (Sinopharm Chemical Reagent Co.Ltd) and dispensed into 96-well plates (NUNC, Rochester, NY). The plates were incubated in the dark at 37^{o}C for 10 min. Absorbance at 570 nm against a reference wavelength of 630 nm was measured using a spectrophotometer microplate reader (mQuant; BioTek, Winooski, VT, USA).

Propidium Iodide (PI+ Assay)

The treated and control cells were analyzed for PI positive cells using the propidium iodide molecular probe (Invitrogen). Briefly, the cells were collected and then resuspended with 500 μL of culture medium containing 1 μL of PI (1.0 mg /mL, Invitrogen) at 37°C for 30 min. The cells were filtered with a 40 μm strainer and analyzed with CyAn™ ADP analyzer (Beckman Coulter, Fullerton, CA, USA).

Apoptosis analysis

The treated and control cells were analyzed for caspase 3 using the CellEvent™ Caspase-3/7 Green Detection Reagent (Invitrogen Life Technologies). Briefly, for caspase 3, the cells were collected and then incubated with 500 μL of culture medium with 0.125 μL of the 2.0 mM CellEvent™ Caspase-3/7 Green Detection Reagent at 37°C for 30 min. The cells were then washed, filtered with a 40 μm strainer and analyzed with a CyAn™ ADP analyzer (Beckman Coulter).

Autophagy analysis

The treated and control cells were analyzed for autophagy using the Autophagy Detection Kit (Abcam). Briefly, the cells were collected and then incubated in 250 μL of indicator free growth media with 250 μL of diluted Green stain solution (1 μL Green Detection Reagent to 1000 μL indicator free growth medium) at 37°C for 30 min. The cells were then washed, filtered with a 40 μm strainer and analyzed with a CyAn™ ADP analyzer (Beckman Coulter).

Mitochondria Stress

*Mitochondrial membrane potential assay (*a · *)*

The mitochondrial membrane potential ($\Delta\psi$) of the treated and control cells were analyzed using MitoTracker$^{(R)}$ Red CMXRos (Invitrogen). Briefly, the cells were collected and then incubated with 500 μL of culture medium containing 1 μL of 1 mM MitoTracker$^{(R)}$ Red CMXRos stock solution (Invitrogen) at 37^{o}C for 30 min. The cells were filtered with a 40 μm strainer and analyzed with CyAn^{TM} ADP analyzer (Beckman Coulter).

Mitochondria transition pore (MTP) Assay

The mitochondrial transition pore assay (MTP) of the treated and control cells were analyzed using MitoProbe^{TM} Transition Pore Assay Kit (Invitrogen Life Technologies). Briefly, the cells were collected and then incubated with 500 μL of culture medium containing 1 μL of 1 mM calcein and 80 mM $CoCL_2$ working solution at 37^{o}C for 30 min. The cells were filtered with a 40 μm strainer and analyzed with CyAn^{TM} ADP analyzer (Beckman Coulter).

Endoplasmic Reticulcum (ER) Stress

Immunocytochemistry for ER stress marker eIF2a and XBP-1

For non-adherent Ramos lymphoma cells, the control and treated cells in culture were collected, washed once with PBS (-) and fixed in 4% paraformaldehyde for 10 min, permeabilized with 0.1% Triton-X100 for 10 min and then washed with PBS. Non-specific blocking were done with 10% normal goat serum for 10 min. The cells were then incubated with primary antibodies against phosphorylated eIF2a (Cell Signaling Technologies, Danvers, MA, USA) XBP-1 (Abcam, Cambridge, UK) overnight at 4^{o}C. The cells were then incubated with by secondary goat anti-mouse IgG (H+L) Alexa Fluor 568 antibodies (1:500)

(Invitrogen Life Technologies) for 30 min on ice in the dark. The cells were subsequently washed and mounted with Fluoroshield™ (Sigma, St. Louis, MO), observed and imaged photographed with an Olympus FluoView FV1000 laser scanning confocal microscope (Olympus). For adherent cancer cell lines, MG63 and MDA-MB-231, the cells were grown in Lab-Tek(R) Chambered #1.0 Borosilicate coverglass system (Thermo Scientific), treated with hWJSC-CM and subsequently stained and imaged for ER stress as described above.

Oxidative Stress assay

Mitochondrial superoxide assay

The treated and control cells were analyzed for mitochondrial superoxide using the MitoSOX™ Red mitochondrial superoxide indicator (Invitrogen). Briefly, the cells were collected and incubated with 100 μL of culture medium containing 0.1 μL of 5mM MitoSOX™ working solution at 37°C for 30 min. The cells were then washed, filtered with a 40 μm strainer and analyzed with CyAn™ ADP analyzer (Beckman Coulter).

Hydrogen peroxide assay

The culture media from the treated and control arms were collected and stored at -80°C. Briefly, for hydrogen peroxide assay, 50 μl of cell lysate or 50 μl of supernatant was mixed with 50 μl of HRP/Amplex Red reaction (Invitrogen) in a 96-well plate and incubated at 37°C for 30 min or longer. Fluorescence readings using excitation 560 nm and emission detection at 590 nm were measured using a Tecan Infinite M1000 microplate reader (Tecan Group Ltd, Mannedorf, Switzerland).

Hydroxyl radical and peroxynitrile anion

The treated and control cells were analyzed for highly reactive oxygen species (hydroxyl radical and peroxynitrile anions) using 3'-(p-hydroxyphenyl) fluorescein (HPF, Invitrogen). Briefly, the cells were collected and incubated with 100 μL of culture medium containing 0.2 μL of 5 mM HPF at 37^{o}C for 30 min. The cells were then washed, filtered with a 40 μm strainer and analyzed with CyAn^{TM} ADP analyzer (Beckman Coulter).

Lipid peroxidation

The treated and control cells were collected and stained using the Image-iT$^{(R)}$ Lipid Peroxidation Kit based on the manufacturer's instructions (Invitrogen). Briefly, the cells were stained with 10 mM Image-iT$^{(R)}$ Lipid Peroxidation Sensor (Component A) for 30 min at 37^{o}C. The cells were then washed, filtered with a 40 μm strainer before analysis using BD LSRFortessa^{TM} (BD Bioscience, Heideberg, Germany) with excitation/emission 581/591 nm and 488/510 nm.

Danger associated molecular patterns (DAMPs)

Surface exposed CRT (ecto-CRT)

For FACS analysis of ecto-CRT, the treated and control cells were collected, blocked with 10% NGS on ice for 10 min. The cells were then incubated with primary anti human CRT antibodies (1:500) (Abcam) for 30 min on ice followed by secondary goat anti-mouse IgG (H+L) Alexa Fluor 488 antibodies (1:500) (Invitrogen Life Technologies) for 30 min on ice in the dark. The cells were washed with PBS, resuspended in cold 10% NGS, filtered with a 40 μm strainer and analyzed with CyAn^{TM} ADP analyzer (Beckman Coulter, Fullerton, CA, USA). To visualise the ecto-CRT, the treated and control cells were collected, fixed in cold 4% paraformaldehyde for 10 min, blocked with cold 10% NGS for 10 min

and then incubated with primary anti human CRT antibodies (1:500) (Abcam) overnight in 4^{o}C. The cells were then incubated with by secondary goat anti-mouse IgG (H+L) Alexa Fluor 488 antibodies (1:500) (Invitrogen Life Technologies) for 30 min on ice in the dark. The cells were subsequently with mounted with Fluoroshield^{TM} (Sigma, St. Louis, MO), observed and imaged with an Olympus FluoView FV1000 laser scanning confocal microscope (Olympus).

Surface exposed Hsp90 (ecto-Hsp90)

For FACS analysis of ecto-Hsp90, the treated and control cells were collected, fixed in 0.25% paraformaldehyde for 5 min, washed with cold PBS and then incubated with primary anti human Hsp90 antibodies (1:500) (Abcam) for 30 min on ice in blocking buffer followed by secondary goat anti-rabbit IgG (H+L) Alexa Fluor 568 antibodies (1:500) (Invitrogen Life Technologies) for 30 min on ice in the dark. The cells were washed with PBS, resuspended in cold 10% NGS, filtered with a 40 μm strainer and analyzed with BD LSRFortessa^{TM} (BD Bioscience).

To visualise ecto-Hsp90, the treated and control cells were collected, fixed in cold 4% paraformaldehyde for 10 min, blocked with cold 10% NGS for 10 min and then incubated with primary anti-human Hsp90 antibodies (1:500) (Abcam) overnight in 4^{o}C. The cells were then incubated with by secondary goat anti-mouse IgG (H+L) Alexa Fluor 568 antibodies (1:500) (Invitrogen Life Technologies) for 30 min on ice in the dark. The cells were subsequently mounted with Fluoroshield^{TM} (Sigma, St. Louis, MO), observed and imaged with an Olympus FluoView FV1000 laser scanning confocal microscope (Olympus).

Extracellular ATP concentration

The culture media from the treated and control arms were collected and stored at -80^{o}C. The extracellular ATP concentration were determined using an ATP assay

kit (Abcam) based on manufacturer's instructions. Briefly, 50 μl of supernatant from the control or treated arms were added with 50 μl of ATP reaction mix containing 45.8 μl ATP Assay Buffer, 0.2 μl ATP Probe, 2 μl ATP Converter and 2 μl Developer Mix. The mixtures were incubated at room temperature for 30 min in the dark. Fluorescence readings using excitation 535 nm and emission detection at 587 nm were then measured using a Tecan Infinite M1000 microplate reader (Tecan Group Ltd).

Extracellular HMGB1 concentration

The culture media from the treated and control arms were collected and stored at -80^{o}C. The extracellular HMGB1 concentration were determined using an ELISA assay kit (Uscn Life Science Inc., Wuhan, China) based on manufacturer's instructions. Briefly, 100 μL of supernatant from the control or treated arms, diluted standard and blank were added into the pre-coated 96 well strip plate for 2h at 37^{o}C. After removal of the liquid, 100 μL of Detection Reagent A was added into each well and incubated for 1 h at 37^{o}C. The wells were then washed with 350 μL of 1x Wash Solution 3 times and blotted dry on absorbent paper. 100 μL of Detection Reagent B was then added and incubated 30 min at 37^{o}C. The wells were then washed with 350 μL of 1x Wash Solution 5 times and blotted dry on absorbent paper. 90 μL of Substrate Solution was then added and incubated 20 min at 37^{o}C in the dark. Lastly, 50 μL of Stop Solution was added into each well and HMBG1 level were measured at 450 nm using a spectrophotometer microplate reader (mQuant; BioTek, Winooski, VT, USA).

4.2.5 Statistical Analysis

All results were expressed as mean (fold change) ± SEM and statistical significance between the groups was calculated using two-tailed Student's t-test

(SPSS Statistic v 17.0 software package) (SPSS, Inc, IL). The *p*-value of <0.05 was considered as statistically significant.

4.3 Results

4.3.1 Cell Morphology of Cancer cells after 3kDa MWCO hWJSC-CM concentrate treatment

Phase contrast inverted optics of Ramos cells after 48h exposure to 3kDa MWCO hWJSC-CM concentrates showed morphologically an increased in the number of dead cells. These morphological changes included degeneration and shrinkage (Fig. 15A-B). The morphology of MG63 changes from epithelial-like (in control) to fibroblastic-like cells after treatment with hWJSC-CM. Lesser number of MG63 cells were observed after 48h treatment of hWJSC-CM as compared to the control (Fig. 15C-D). However, there is no distinct morphological change observed in MDA-231 cells after 48h of treatment with hWJSC-CM concentrate as compared to control (Fig. 15E-F).

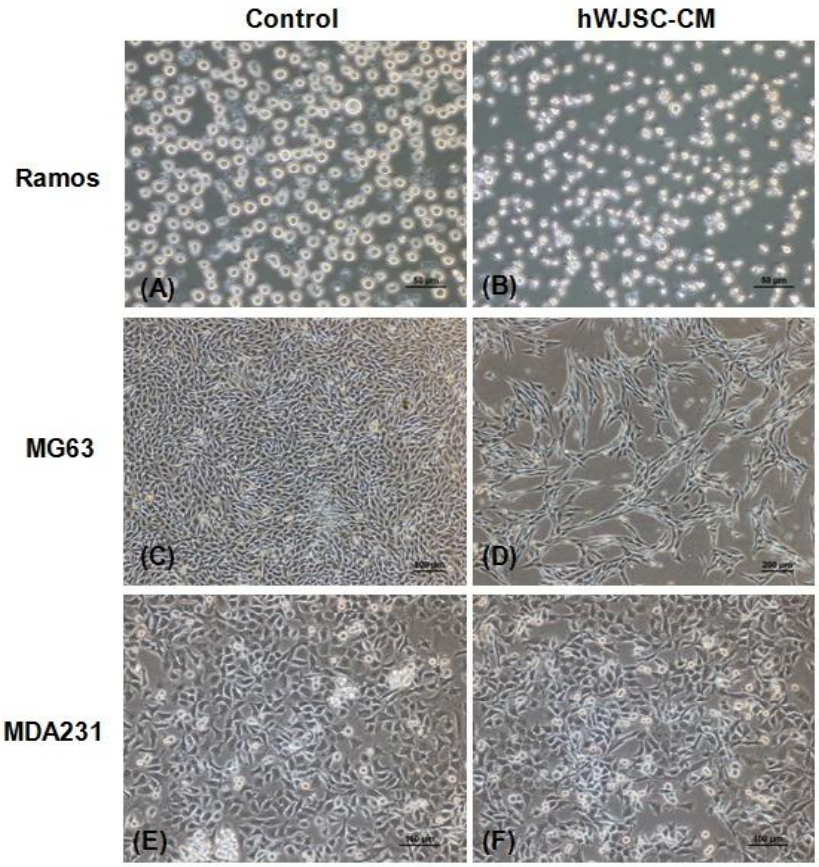

Figure 15 Phase contrast images of Ramos, MG63 and MDA231

Phase contrast images of Ramos, MG63, and MDA231 after exposure to 3kDa hWJSC-CM concentrate. **(A)** Ramos cells show typical spherical morphology in controls. **(B)** Increased cell death was observed when Ramos cells were exposed hWJSC-CM concentrate for 48h (Magnification 100X; Scale Bar: 50µM). **(C)** MG63 cells show typical epithelial-like morphology in controls. **(D)** MG63 cells show a more fibroblastic-like morphology when MG63 cells were exposed to hWJWC-CM concentrate for 48h (Magnification 40X; Scale Bar: 200µM). **(E-F)** No distinct morphological changes observed for MDA231 cells in control and hWJSC-CM concentrate treatment arms (Magnification 40X; Scale Bar: 200µM).

4.3.2 Evaluation of 3kDa MWCO hWJSC-CM concentrate on cell viability, and cell death in Ramos, MG63 and MDA-MB-231 cancer cells

Ramos, MG63 and MDA-MB-231 cancer cells showed significant reductions in cell viability and significant increases in percentage of cells stained positive for cell death marker PI after 3kDa MWCO hWJSC-CM concentrates treatment. The fold changes for cell viability normalized to their respective controls were Ramos

cells (0.82 ± 0.04), MG63 cells (0.66 ± 0.01) and MDA-MB-231 (0.76 ± 0.01) (Fig. 16A). The fold changes for the percentages of PI+ cells normalized to their respective controls were Ramos (3.37 ± 0.36), MG63 (5.12 ± 0.31) and MDA-MB-231 (2.34 ± 0.24) (Fig. 16B).

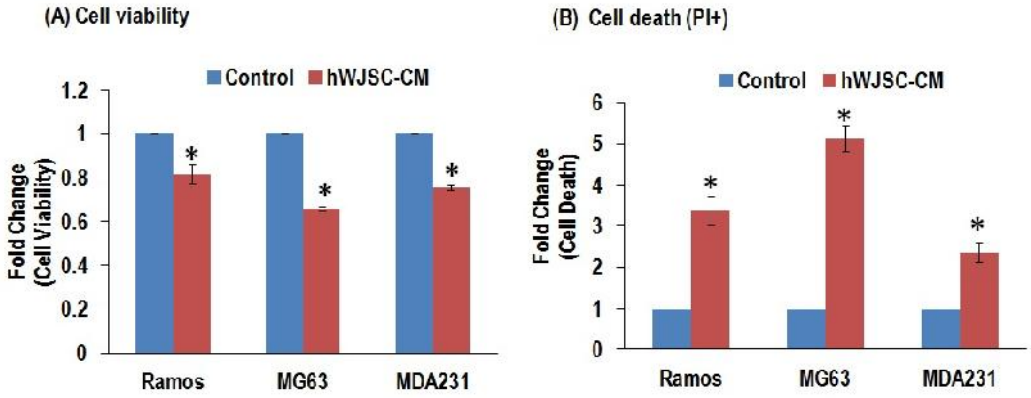

Figure 16 Cell viability and cell death analysis

(A) Cell viability fold changes (MTT assay) of Ramos, MG63 and MDA231 exposed to 500 µg/ml of the 3kDa MWCO concentrate for 48 h. Note significant decreases in cell viability (normalized to control) when Ramos , MG63, MDA231 were exposed to the 3kDa MWCO concentrate. **(B)** Cell death (PI+ assay) fold changes of Ramos, MG63 and MDA231 exposed to 500 µg/ml of the 3kDa MWCO concentrate for 48 h**.** Note significant increases in cell death (normalized to control) of Ramos, MG63 and MDA231 cells exposed to the 3kDa MWCO concentrate. All values are expressed as mean ± SEM of 3 different experiments. Asterisk (*) indicates statistical significance of $p<0.05$.

4.3.3 Evaluation of 3kDa MWCO hWJSC-CM concentrate on apoptosis, and autophagy in Ramos, MG63 and MDA-MB-231 cancer cells

Ramos, MG63 and MDA-MB-231 cancer cells showed a significant increases in cell apoptosis after 3kDa MWCO hWJSC-CM concentrates treatment. The fold changes for activated caspase 3 activities normalized to their respective controls were Ramos cells (2.11 ± 0.12), MG63 cells (4.07 ± 0.31) and MDA-MB-231 (2.41 ± 0.23) (Fig. 17A). Only MG63 and MDA-MB-231 cancer cells showed a significant increase in cell autophagy. The fold changes for the autophagic cells normalized to their respective controls were Ramos (1.02 ± 0.02), MG63 (1.38 ± 0.01) and MDA-MB-231 (1.5 ± 0.04) (Fig. 17B).

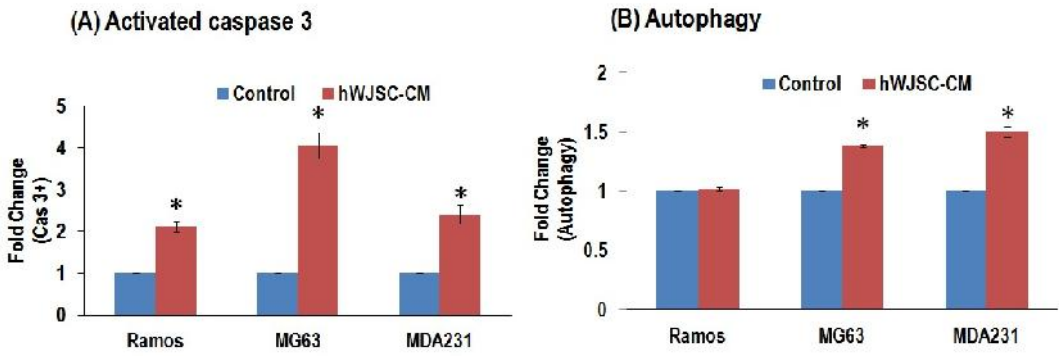

Figure 17 Apoptosis and autophagy analysis

(A) Apoptosis fold changes (activated caspase 3) of Ramos, MG63 and MDA231 exposed to 500 µg/ml of the 3kDa MWCO concentrate for 48 h. Note significant increases in cell apoptosis (normalized to control) when Ramos , MG63, MDA231 were exposed to the 3kDa MWCO concentrate. **(B)** Cell autophagy fold changes of Ramos, MG63 and MDA231 exposed to 500 µg/ml of the 3kDa MWCO concentrate for 48 h**.** Note significant increases in cell autophagy (normalized to control) of MG63 and MDA231 cells exposed to the 3kDa MWCO concentrate. All values in are expressed as mean ± SEM of 3 different experiments. Asterisk (*) indicates statistical significance of $p<0.05$.

4.3.4 Evaluation of 3kDa MWCO hWJSC-CM concentrate on mitochondria stress in Ramos, MG63 and MDA-MB-231 cancer cells

Ramos cells showed a significant reduction in mitochondria membrane potential while Ramos, MG63 and MDA-MB231 all showed significant increases in mitochondria porosity after 3kDa MWCO hWJSC-CM concentrates treatment. The fold changes for mitochondria membrane potential normalized to their respective controls were Ramos cells (0.63 ± 0.05), MG63 cells (0.97 ± 0.01) and MDA-MB-231 (0.97 ± 0.01) (Fig. 18A). The fold changes for increased mitochondria porosity in cells normalized to their respective controls were Ramos (3.87 ± 0.75), MG63 (1.95 ± 0.41) and MDA-MB-231 (2.81 ± 0.4) (Fig. 18B).

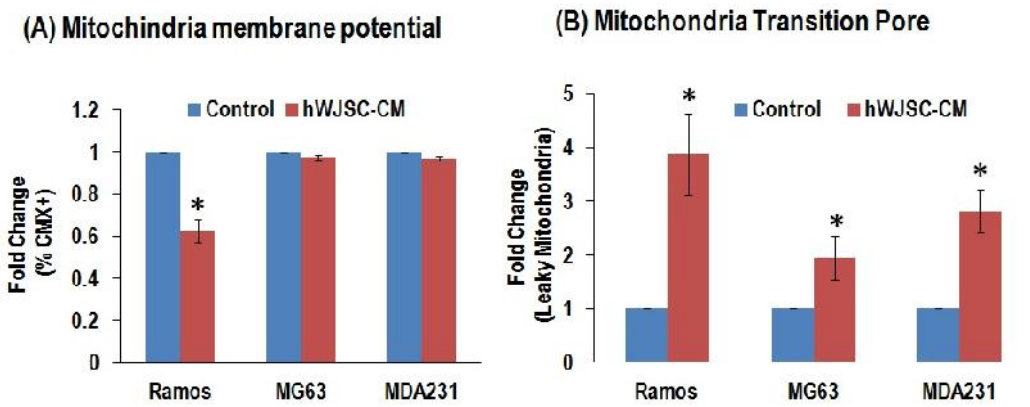

Figure 18 Mitochondria stress analysis

(A) Cell mitochindria membrane potential fold changes (CMXRos) of Ramos, MG63 and MDA231 exposed to 500 µg/ml of the 3kDa MWCO concentrate for 48 h. Note decrease in cell mitochondria membrane potential (normalized to control) when Ramos (significant) , MG63, MDA231 were exposed to the 3kDa MWCO concentrate. **(B)** Cell mitochondria porosity (mitochondria transition pore) fold changes of Ramos, MG63 and MDA231 exposed to 500 µg/ml of the 3kDa MWCO concentrate for 48 h**.** Note significant increases in cell mitochondria porosity (normalized to control) of Ramos, MG63 and MDA231 cells exposed to the 3kDa MWCO concentrate. All values in are expressed as mean ± SEM of 3 different experiments. Asterisk (*) indicates statistical significance of $p<0.05$.

4.3.5 Evaluation of 3kDa MWCO hWJSC-CM concentrate on endoplasmic reticulum (ER) stress in Ramos, MG63 and MDA-MB-231 cancer cells

The cancer cells were evaluated for ER stress marker after 48 h 3kDa MWCO hWJSC-CM concentrates treatment using immunocytochemistry and viewed under confocal microscopy. All 3 cancer cell lines were stained positive for ER stress markers- eLF2a and XBP-1 after hWJSC-CM treatment. These markers were not stained positive in untreated control cancer cell lines (Fig. 19).

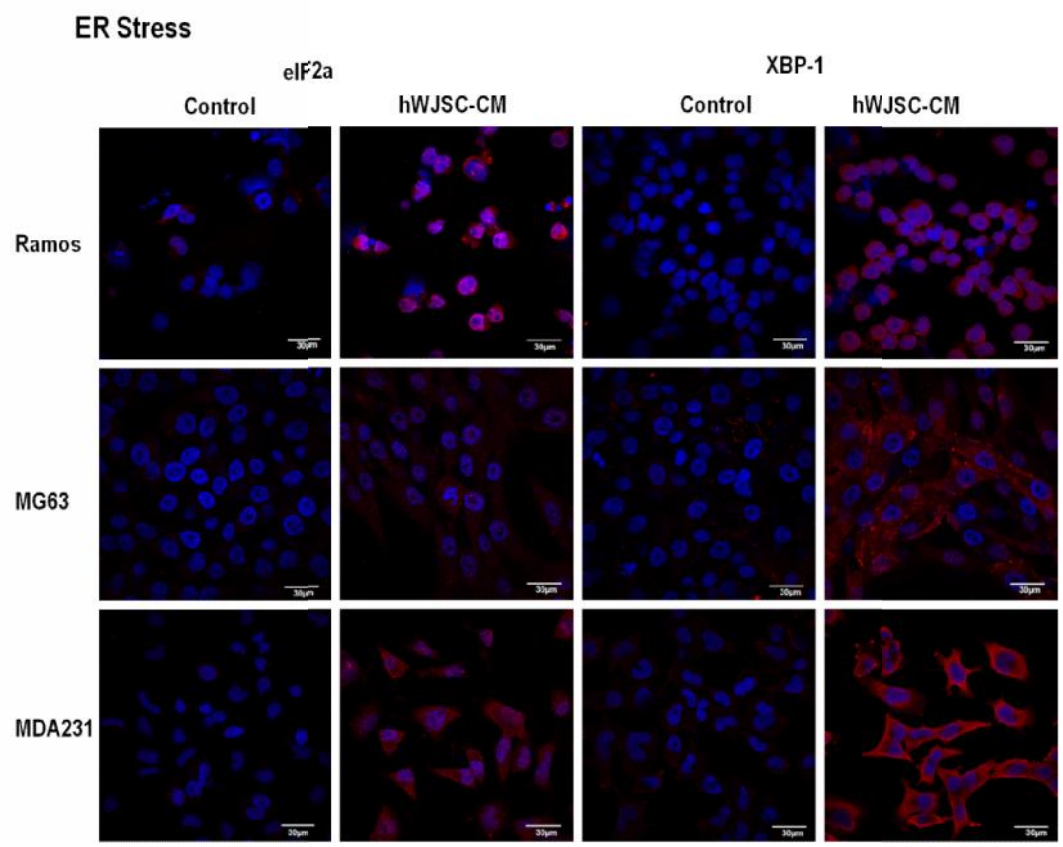

Figure 19 ER stress marker analysis

Immunocytochemistry analysis for ER stress markers. All 3 cancer cell lines were stained postive for ER stress markers eLF2a and XBP-1 after 48 h exposure to 500 µg/ml of the 3kDa MWCO concentrate. Magnification 600X ; Scale Bar: 30µM

4.3.6 Evaluation of 3kDa MWCO hWJSC-CM concentrate on oxidative stress in Ramos, MG63 and MDA-MB-231 cancer cells

Ramos, MG63 and MDA-MB-231 all showed significant increases in mitochondria superoxide level after 3kDa MWCO hWJSC-CM concentrates treatment. The fold changes for percentage of cells positive for mitochondria superoxide level normalized to their respective controls were Ramos cells (0.49 ± 0.4), MG63 cells (1.94 ± 0.4) and MDA-MB-231 (1.35 ± 0.07) (Fig .20A).

All 3 cancer cell lines showed significant increases in hydroxyl radical and peroxynitrile anions levels after 3kDa MWCO hWJSC-CM concentrates treatment. The fold changes in percentage of cells with HPF normalized to their respective

controls were Ramos (1.22 ± 0.02), MG63 (1.28 ± 0.06) and MDA-MB-231 (1.1 ± 0.01) (Fig. 20B).

Ramos, MG63 and MDA-MB-231 all showed an increased (only significant for Ramos) in extracellular hydrogen peroxide and lipid peroxidation level after 3kDa MWCO hWJSC-CM concentrates treatment. The fold changes in hydrogen peroxide level normalized to their respective controls were Ramos (1.35 ± 0.04), MG63 (2.32 ± 0.52) and MDA-MB-231 (1.51 ± 0.19) (Fig.20C). The fold changes in lipid peroxidation normalized to their respective controls were Ramos (1.1 ± 0.01), MG63 (1.19 ± 0.1) and MDA-MB-231 (1.28 ± 0.08) (Fig. 20D).

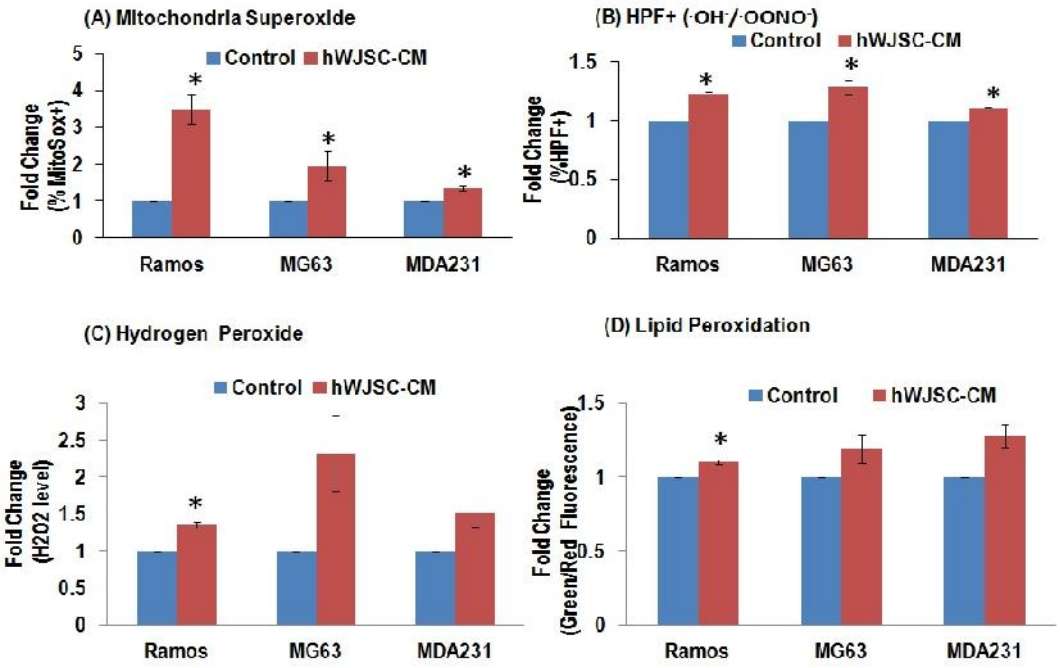

Figure 20 Oxidative stress analysis

(A) Cell mitochondria superoxide fold changes (MitoSox) of Ramos, MG63 and MDA231 exposed to 500 µg/ml of the 3kDa MWCO concentrate for 48 h. Note significant increases in cell mitochondria superoxde level (normalized to control) when Ramos , MG63, MDA231 were exposed to the 3kDa MWCO concentrate. **(B)** Cell hydroxyl radical/peroxynitrile anion fold changes of Ramos, MG63 and MDA231 exposed to 500 µg/ml of the 3kDa MWCO concentrate for 48 h**.** Note significant increases in cell hydroxyl radical/peroxynitrile anion level (normalized to control) of Ramos, MG63 and MDA231 cells exposed to the 3kDa MWCO concentrate. **(C)** Extracellular hydrogen peroxide level fold changes of Ramos, MG63 and MDA231 exposed to 500 µg/ml of the 3kDa MWCO concentrate for 48 h**.** Note increases in hydrogen peroxide level (normalized to control) of Ramos (significant), MG63 and MDA231 cells exposed to the 3kDa MWCO concentrate. **(D)** Lipid peroxidation level fold changes of Ramos, MG63 and MDA231 exposed to 500 µg/ml of the 3kDa MWCO concentrate for 48 h**.** Note increases in lipid peroxidation level (normalized to control) of Ramos (significant), MG63 and MDA231 cells exposed to the 3kDa MWCO concentrate. All values in are expressed as mean ± SEM of 3 different experiments. Asterisk (*) indicates statistical significance of $p<0.05$.

4.3.7 Evaluation of 3kDa MWCO hWJSC-CM concentrate on surface bound CRT (ecto-CRT) and Hsp90 (ecto-Hsp90) in Ramos, MG63 and MDA-MB-231 cancer cells

Ramos, MG63 and MDA-MB-231 all showed significant increases in cells with ecto-CRT after 3kDa MWCO hWJSC-CM concentrates treatment. The fold changes in median fluorescence level for ecto-CRT normalized to their respective controls were Ramos (1.21 ± 0.0004), MG63 (2.02 ± 0.24) and MDA-MB-231 (1.29 ± 0.09) (Fig. 21A). Confocal images of the cancer cells after 48 h hWJSC-CM treatment indicated more CRT staining on the cells plasma membrane as compared to control (Fig. 21B).

Ramos, MG63 and MDA-MB-231 all showed significant increases in cells with ecto-Hsp90 after 3kDa MWCO hWJSC-CM concentrates treatment. The fold changes in median fluorescence level for ecto-Hsp90 normalized to their respective controls were Ramos (1.54 ± 0.15), MG63 (26 ± 4.84) and MDA-MB-231 (16.6 ± 0.06) (Fig. 22A). Confocal images of the cancer cells after 48 h hWJSC-CM treatment indicated more Hsp90 and plasma membrane co-localization compared to control (Fig. 22B).

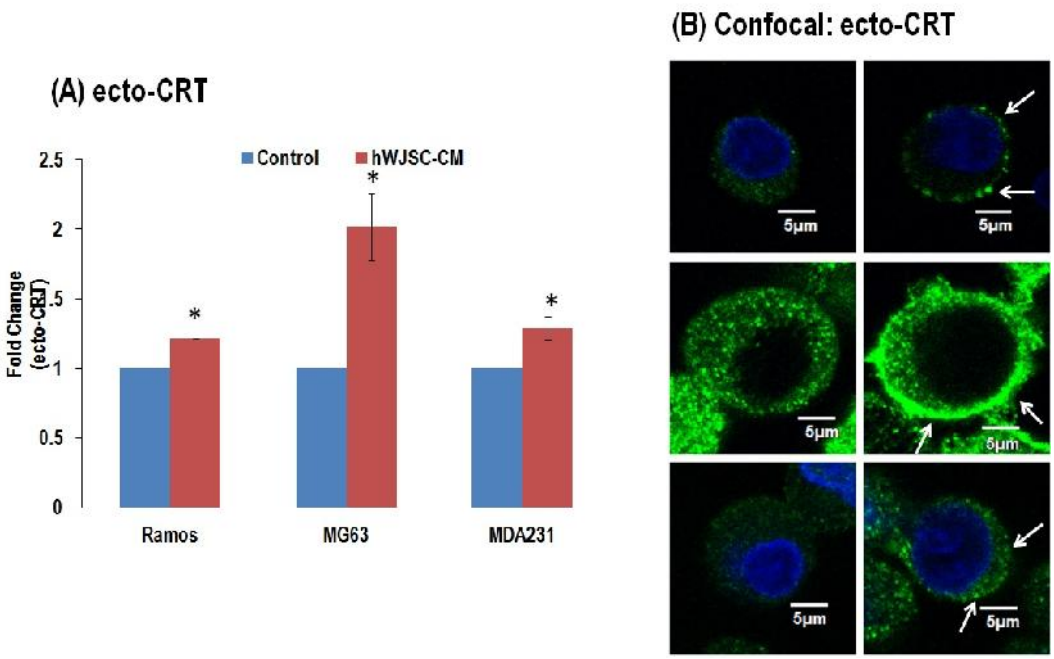

Figure 21 Ecto-CRT analysis

(A) ecto-CRT fold changes of Ramos, MG63 and MDA231 exposed to 500 μg/ml of the 3kDa MWCO concentrate for 48 h. Note significant increases in cell ecto-CRT level (normalized to control) when Ramos , MG63, MDA231 were exposed to the 3kDa MWCO concentrate. **(B)** CRT localization confocal images of Ramos, MG63 and MDA231 exposed to 500 μg/ml of the 3kDa MWCO concentrate for 48 h**.** Note higher level of ecto-CRT in Ramos, MG63 and MDA231 cells (white arrows) exposed to the 3kDa MWCO concentrate. Scale bar: 5μm. All values in are expressed as mean ± SEM of 3 different experiments. Asterisk (*) indicates statistical significance of $p<0.05$.

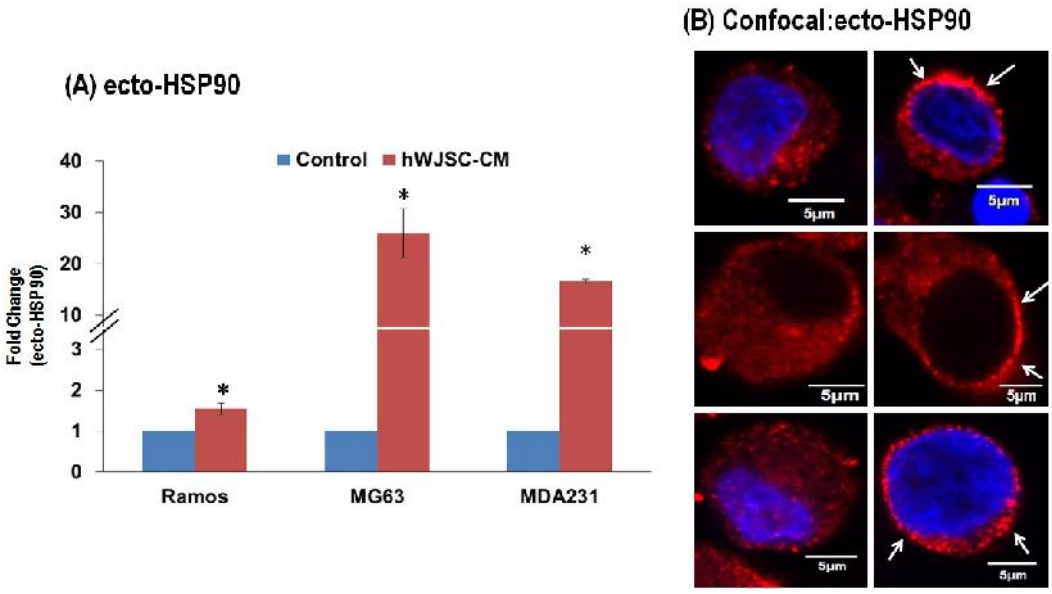

Figure 22 ecto-Hsp90 analysis

(A) ecto-Hsp90 fold changes of Ramos, MG63 and MDA231 exposed to 500 μg/ml of the 3kDa MWCO concentrate for 48h**.** Note significant increases in ecto-Hsp90 level (normalized to control) of Ramos, MG63 and MDA231 cells exposed to the 3kDa MWCO concentrate. **(B)** Hsp90 localization confocal images of Ramos, MG63 and MDA231 exposed to 500 μg/ml of the 3kDa MWCO concentrate for 48h**.** Note higher level of ecto-Hsp90 in Ramos, MG63 and MDA231 cells (white arrows) exposed to the 3kDa MWCO concentrate. Scale bar: 5μm. All values in are expressed as mean ± SEM of 3 different experiments. Asterisk (*) indicates statistical significance of $p<0.05$.

4.3.8 Evaluation of 3kDa MWCO hWJSC-CM concentrate on extracellular ATP and HMGB1 concentration in Ramos, MG63 and MDA-MB-231 cancer cells

Ramos, MG63 and MDA-MB-231 all showed significant increases in extracellular ATP level after 3kDa MWCO hWJSC-CM concentrates treatment. The fold changes in extracelluar ATP level normalized to their respective controls were Ramos (4.25 ± 0.35), MG63 (4.97 ± 0.73) and MDA-MB-231 (4.23 ± 0.59) (Fig. 23A). Ramos, MG63 and MDA-MB-231 all showed significant increases in ATP level in their respective medium after hWJSC-CM treatment. The ATP level measured spectrophotofluorometrically before treatment and after treatment for Ramos, MG63, MDA-MB-231 were 2990 ± 153, 11575 ± 671, 15783 ± 1054 and 15295 ± 601 respectively [Fig. 23(B-D)].

Ramos, MG63 and MDA-MB-231 all showed significant increases in extracellular HMGB1 level after hWJSC-CM treatment. The fold changes in extracelluar HMGB1 level normalized to their respective controls were Ramos (1.12 ± 0.01), MG63 (1.33 ± 0.003) and MDA-MB-231 (1.1 ± 0.03) (Fig. 24A). Ramos, MG63 and MDA-MB-231 all showed significant increases in HMGB1 level in their respective medium after hWJSC-CM treatment. The HMGB1 level measured spectrophotometrically before treatment and after treatment for Ramos, MG63, MDA-MB-231 were 0.103 ± 0.003, 0.124 ± 0.004, 0.169 ± 0.008 and 0.149 ± 0.009 respectively [Fig. 24(B-D)].

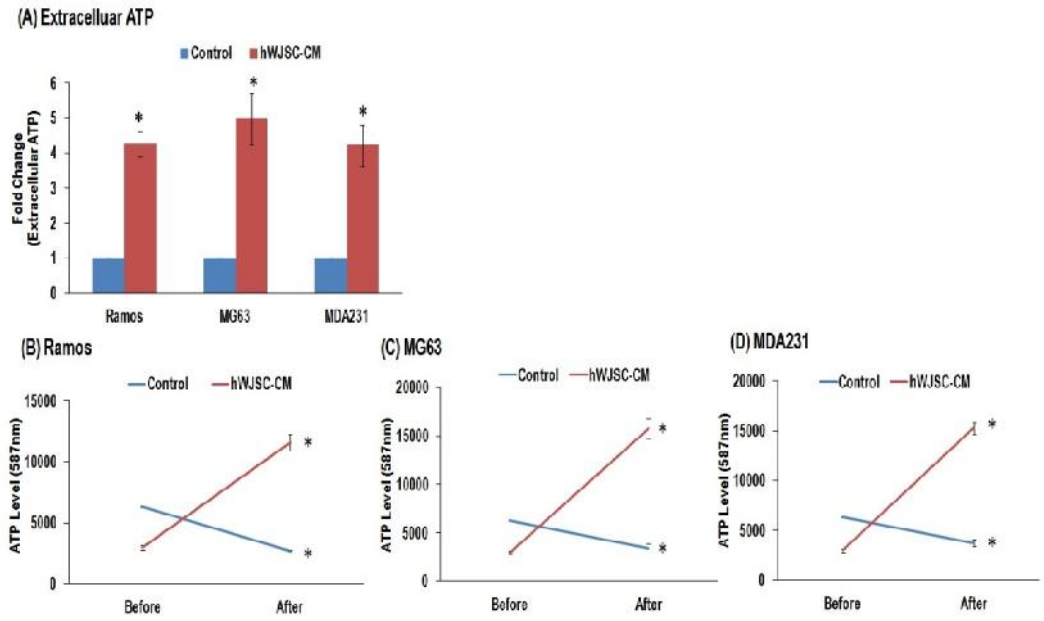

Figure 23 Extracellular ATP analysis

(A) Extracellular ATP level fold changes of Ramos, MG63 and MDA231 exposed to 500 µg/ml of the 3kDa MWCO concentrate for 48 h. Note significant increases in extracellular ATP level (normalized to control) when Ramos , MG63, MDA231 were exposed to the 3kDa MWCO concentrate. **(B-D)** ATP level in respective medium before and after exposure to 500 µg/ml of the 3kDa MWCO concentrate for 48 h. Note significant increases in ATP level in medium when Ramos **(B)**, MG63 **(C)** and MDA231 **(D)** when exposed to 3kDa MWCO concentrate. All values in are expressed as mean ± SEM of 3 different experiments. Asterisk (*) indicates statistical significance of $p<0.05$.

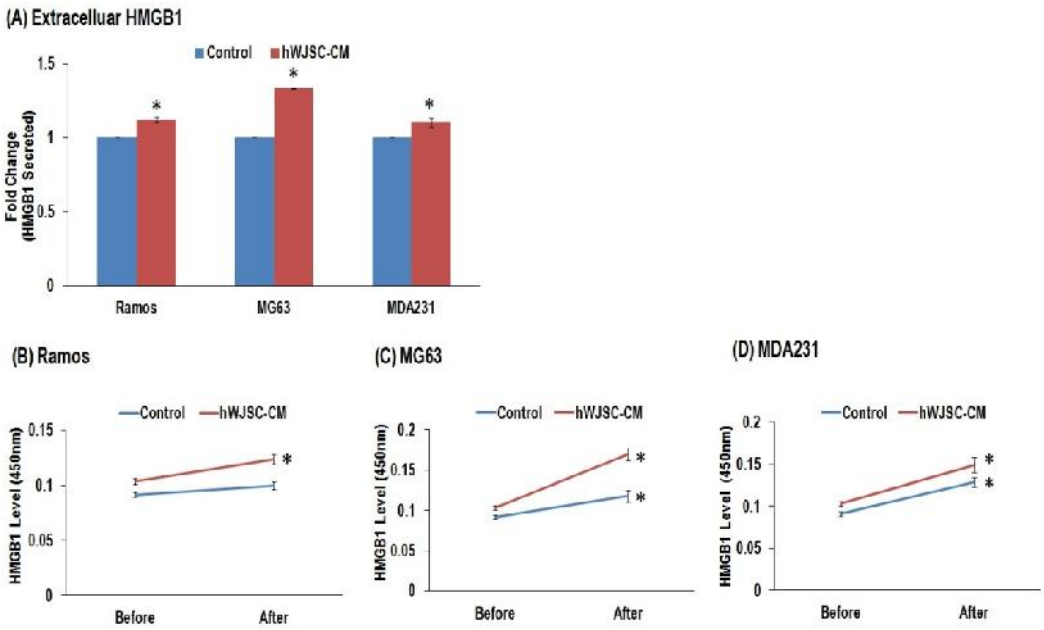

Figure 24 Extracellular HMGB1 ELISA analysis

(A) Extracellular HMGB1 fold changes of Ramos, MG63 and MDA231 exposed to 500 µg/ml of the 3kDa MWCO concentrate for 48 h**.** Note significant increases in extracellular HMGB1 (normalized to control) of Ramos, MG63 and MDA231 cells exposed to the 3kDa MWCO concentrate. **(B-D)** HMGB1 level in respective medium before and after exposure to 500 µg/ml of the 3kDa MWCO concentrate for 48 h. Note significant increases in HMGB1 level in medium when Ramos **(B)**, MG63 **(C)** and MDA231 **(D)** when exposed to 3kDa MWCO concentrate. All values in are expressed as mean ± SEM of 3 different experiments. Asterisk (*) indicates statistical significance of $p<0.05$.

4.4 Discussion

The current standard anti-cancer management is generally assumed to act through the selective killing of tumor cells or induction of their senescence [187]. However, increasing evidence has led to the hypothesis of the possible contribution of the host immune system in the therapeutic process of chemotherapy and radiotherapy. Several studies have indicated that several chemotherapeutic drugs were more efficient in eliminating tumors implanted in immunocompetent than immunocompromised hosts [191]. In addition, immune competence is crucially required for chemotherapy efficacy [187] and improved survival outcome in cancer patients have been consistently observed to be correlated to the presence of tumor infiltrating lymphoctye [192-195], However, current standard of chemoradiotherapy used in cancer management is generally

thought to be immunosuppressive and the systemic immunity in patients is often severely impaired after chemoradiotherapy [196]. Most chemoradiotherapeutic regimes mediate their cytotoxic effects by apoptosis which is generally noninflammatory and nonimmunogenic [197,198]. As such, the aim of this study is to evaluate whether the treatment of cancer cells with 3kDa hWJSC-CM concentrate could elicit an immunogenic cell death (ICD) response.

ICD is characterize by a series of molecular hallmarks that are released by dying tumor cells and are recognized by antigen presenting cells which ultimately re-initiate a tumor-specific adaptive immunity response [190]. Both Burkitt lymphoma (Ramos) and osteosarcomas (MG63) showed distinct morphological changes after 48 hours exposure to 3kDa hWJSC-CM concentrate. Nevertheless, all 3 cancer cell lines of Ramos, MG63 and breast adenocarcinomas (MDA-231) showed a significant decreased in cell viability and significant increased in cell death after 3kDa hWJSC-CM concentrate exposure. Similarly, all 3 cancer cells lines showed significant increase in apoptosis after exposure to hWJSC-CM concentrate while both MG63 and MDA231 showed a significant increased in autophagy after hWJSC-CM treatment.

Tumor cells undergoing ICD start to express and secrete several immunogenic factors, namely the danger associated molecular patterns (DAMPs). DAMPs are the markers of ICD which were recently identified as indispensable in activating the immune response. They includes the pre-apoptotic exposure of calreticulin (ecto-CRT) and heat shock protein 90 (Hsp90), the release of ATP from dying cells and the postmortem release of high-mobility group box 1 (HMBG1) into the extracellular space [187,190]. Ecto-CRT, ATP and HMGB1 secretion are indispensable for ICD and absence of any of these DAMPs abolishes the efficacy of anthracycline- or OXA-induced immunogenicity in mouse models [189,199]. The expression of ecto-CRT stimulate the engulfment of dying tumor cells by DCs [200-

[202] while both ATP and HMGB1 regulate DC-mediated tumor antigen cross-presentation and T-cell polarization [187].

The results in this study demonstrated a significant increased in mitochondria stress (reduced mitochondria membrane potential and increased mitochondria porosity), ER stress markers- eIF2a and XBP-1 and ROS stress (increased in mitochondria superoxide, hydroxyl radical/peroxynitrile anions, hydrogen peroxide and lipid peroxidation) in all three cancer cell lines after exposure to 3kDa hWJSC-CM concentrate. The ability of anti-cancer agents to induce ICD was initially demonstrated using agent capable in inducing ER stress and reactive oxygen species (ROS) stress [188,190]. ER homeostasis ensures the accuracy of protein folding and secretion while oxidative modification of protein and lipids represents an important pathway in efficient presentation of DAMPs [190]. Silenced ER stress induced by ICD inducers showed a reduction of DAMPs like ecto-CRT or ATP secretion in the dying cancer cells and reduces their *in vivo* immunogenicity [190]. This suggests that robust ER stress response accompanied or induced by ROS is essential for the activation of ICD [190].

The induction of ecto-CRT or ecto-Hsp90 depends on the properties of mitochondria stress, ER stress and reactive oxygen species production [188] that were significantly upregulated in this study. All 3 cancer cell lines expressed significantly more ecto-CRT and ecto-Hsp90 after treatment with hWJSC-CM concentrate. Ecto-CRT is an important DAMPs that serves as an 'eat-me' signal which promotes the phagotocytosis of dying cancer cells by antigen-presenting cells such as dendritic cells (DCs). Consequently this facilitates their tumor antigen presentation and induces tumor-associated antigen specific cytotoxic T cells [188,200,203]. Previous studies in both rodent and human patients models have indicated that ecto-CRT can predict the ability of the dying cancer cells to mount a protective anti-tumorigenic immune response [203-205]. During the initiation of ICD,

the dying cells will translocate CRT and Hsp90 from the endoplasmic reticulum (ER) to the cell surface [206]. Depletion or blockage of CRT was shown to abolish the immunogenicity of anthracycline-induced cancer cell death [200,206]. Likewise, previous studies showed that using bortezomib enhances the expression of Hsp90 of myeloma cells and was crucial for the activation of both human and murine DCs [206-208]. In addition, the fact that the immunogenicity of myeloma cells was abolished after specific blockage of Hsp90 suggest that cell surface expression of Hsp90 critical for ICD [207]. Other studies showed that treatment with 5-fluorouracils and doxorubicin upregulated Hsp expression and promoted the engulfment of apoptotic bodies by human DCs and subsequent cross presentation of tumor antigens to T cells [209,210].

The results in this study demonstrated all three cancer cell lines had significantly increased ATP secretion following exposure to 3kDa hWJSC-CM concentrates. While ecto-CRT/ecto-Hsp90 is the 'eat-me' signal, other DAMPs such as extracellular ATP from apoptotic cells constituted a 'find-me' signal for the recruitment of DCs and their precursors [189,211]. The secreted ATP binds to both ionotropic (P2X) and metabotropic (P2Y) purinergic receptors which stimulate DCs maturation [190]. During ICD, it have been shown that ATP binds mainly to the P2RX7 receptors and activates NOD-like receptor family, pyrin domain containing 3 inflammasome within DCs or macrophages [212,213] and the release of IL-1b [188] which is a crucial cytokine for propagation of an anti-tumor immune responses [214]. In addition, ATP was shown to mediate the recruitment and differentiation of myeloid DCs to the tumor site after anthracycline treatment *in vivo* [211]. After treatment with chemotherapeutic agents, the secretion of ATP by cancer cells is important for effective antitumor immune responses and small interfering RNA-mediated inhibition that prevented ATP secretion from dying cancer cells and mitigated the antitumor response [215]. Moreover, it has been shown that

autophagy deficient tumors with impaired ATP secretion were less radiosensitive than control tumors in immunocompetent mice and induction of the protective immune response could subsequently be restored by the injection of ecto-ATPases that increases extracellular ATP concentration artificially [216,217].

Lastly, results also demonstrated a significant increased in HMGB1 secretion by all three cancer cell lines after exposure to 3kDa hWJSC-CM concentrates. HMGB1 is a endokine that is a chromatin-binding protein that acts as an intracellular transcription factor and a proinflammatory cytokine when released extracellularly [190,196]. It has been reported that HMGB1 is also associated with late apoptosis and autophagy [218]. Anticancer treatments such as irradiation, anthracyclines and oxaliplatin could induce HMGB1 released by the dying tumor cells which then binds to its receptor TLR4 on DCs [196]. After the binding to TLR4, HMGB1 promotes activation of DCs and triggers its migration *in vitro* [196]. In addition, signaling through TLR4 and its adaptor MyD88 regulates the starting phase of cognate immune responses by regulating phagocytosis and cross-presentation of tumor antigens by DCs [191]. As such, the released of HMGB1 from tumor cells after chemotherapy has been shown to enhance the engulfment of antigenic component by DCs and mediates cross-presentation of tumor antigens into CD4 and CD8 T cells in murine *in vivo* models [196]. Similarly, significant upregulation of HMGB1 within the tumor environment of human cancer patients after preoperative chemoradiotherapy and the increased in local HMGB1 levels was correlated to higher patient survival [219]. The inhibition of HMBG1 in cancer undergoing immunogenic apoptosis in a prophylactic vaccination model mitigate their ability to stimulate an antitumor immunity response [191]. Furthermore, breast cancer patients having a mutation in the TLR4 receptor gene were reported to have early relapse after chemotherapy and radiotherapy treatment [191]. These

observations suggest that HMGB1-related immune response after chemoradiotherapy plays an important role in clinical cancer treatment.

In summary, the results of this chapter indicated for the first time, that all three molecular hallmarks for ICD ecto-CRT/Hsp90, extracellular ATP and HMGB1 were significantly increased in all cancer cell lines after exposure to 3kDa hWJSC-CM concentrates. Moreover, earlier studies reported that hWJSCs secrete large varieties of cytokines and factors like IL-6, IL-8, MCP-1 [8] that have been known to play a role in modulating the innate immune response [58] while the treatment of mammary carcinomas xenograft rat model with rat WJSCs increased CD8+ T cell infiltration in the tumor tissue [53]. This supported the hypothesis that anti-tumorigenic treatment with hWJSCs or its conditioned medium could mount an immunogenic cell death mechanism which consequently could stimulate additional anti-tumor immune response. However, the specific active agents within the 3kDa hWJSC-CM responsible for the induction of immunogenic cell death is still unknown. Future studies should focus on narrowing down and determining the specific molecules or targets that are involved in order to further elucidate the mechanism and their use as a therapeutic drug in the clinics.

Chapter 5: Ex Vivo Expansion of Cord Blood CD34+ Cells Using hWJSCs and hWJSC-CM

5.1 Introduction

Hematopoietic stem cells (HSCs) transplantation has been used for the treatment of malignant and non-malignant hematopoietic diseases such as leukemia, lymphoma and thalassemia. The current sources of HSCs come from the bone marrow (BM), mobilized peripheral blood (mPB) and umbilical cord blood. However, the aspiration of HSCs from the bone marrow is painful with the potential risk of infection and morbidity and rare incidents of rupture of the spleen and sickle cell damage have occurred and the long term safety of the donors following peripheral blood HSCs collection remains unclear [99-102].

To overcome these challenges, HSCs from the human umbilical cord blood (UCB) have been successfully used for the treatment of hematopoietic diseases in children in autologous and allogeneic settings [136,137]. The usage of HSCs from UCB holds many advantages over HSCs isolated from bone marrow or peripheral blood. These advantages includes (i) the ability to collect and store the cord blood HSCs in a repository banks for faster availability to the patients, (ii) the immaturity of the immune cells which the patients now bear lesser risk of graft vs host disease (GVHD), (iii) the less stringent requirement of finding a 'perfect match" sample between donors' cells and recipients' and (iv) the higher proliferation rate, autocrine production of hematopoietic factors and longer telomeres due to their young chronological age [103-105].

However, one major challenge associated with the use of UCB-HSCs for transplantation is the relatively low cell dose available. This has contributed to slower engraftment and increased risk of engraftment failure [220]. It has been reported that the HSC and HPC yielded in UCB was adequate for the treatment

of hematopoietic diseases in children but not adults. It was estimated that for successful engraftment, at least 2.5 x 10^6 CD34+ cells per kg of patient body weight was required [221,222] but a good UCB harvest from a single umbilical cord can generate a total of only about 10 x 10^6 CD34+ cells which is adequate only for a 4 kg child [109].

Ex vivo expansion of hematopoietic stem cells/ its progenitor cells (HSC) would break the obstacle of less cell number and widen its application. Hence optimizing the culture condition for the maintenance and expansion of primitive HSC is important. However, any expansion protocol must attempt to stimulate *in vivo* hematopoiesis while maintaining the stemness properties of HSCs. Human mesenchymal stem cells (MSCs) have been successfully used *in vitro* as a scaffold for stromal support and expansion of HSCs via cell-to-cell contact. This concept was developed on the understanding that the MSCs within the bone marrow *in vivo* act as a natural scaffold on which HSCs interact and proliferate [220]. It is not known whether the mechanisms underlying behind the HSC-MSC interaction that results in HSC proliferation is mediated by diffusible factors released after cell-to-cell contact or through constitutive secretions by MSCs into the immediate microenvironment. To avoid immunological complications, autologous MSCs from the same patient's bone marrow or UCB have been used as a scaffold *in vitro* for expansion of her own HSCs with successful results [109,223,224]. The use of MSCs from UCB for stromal support of autologous HSCs has its own limitations in that the numbers of MSCs in UCB are extremely low and their presence in UCB has been debated [225,226]. In fact Musina et al [227] reported very low counts of UCB MSCs per volume of UCB and showed that such MSCs had low proliferation rates.

These challenges have prompted interest in the study and evaluation of MSCs from other sources such as birth-associated tissues. Large numbers of MSCs with high proliferation rates and low population doubling times have been reported in the Wharton's jelly (hWJSCs) of discarded human umbilical cord [3,4,11,12]. At least 4.6 x 10^6 fresh live hWJSCs per cm of cord without expansion can be obtained and its stemness properties of can last for at least 10 passages *in vitro* [4]. Moreover, they are hypoimmunogenic and are able to be used in both autologous and allogeneic settings without the concerns of graft versus host disease [46] (Weiss et al 2008). Freeze-thaw-survival rates of these hWJSCs after cryopreservation even at the first passage were greater than 90% [4]. Hence, given their abundance we hypothesized that the same patient's hWJSCs can serve as an ideal autologous genetic match for stromal co-culture support for the expansion of her own HSCs. In addition, since the conditioned medium of cultured hWJSCs (hWJSC-CM) has a variety of beneficial growth factors interleukins (IL-6, IL-8), granulocyte macrophage colony stimulating factor (GM-CSF) and granulocyte colony stimulating factor (G-CSF) [49,110] it is possible that the hWJSC-CM can support the expansion of HSCs. Therefore, the aim of this chapter is to evaluate the use of allogeneic and autologous hWJSCs and hWJSC-CM for the *ex vivo* expansion of UCB CD34+ cells.

5.2 Material and Methods

5.2.1 Cell Culture

Human Wharton's jelly stem cells (hWJSCs)

After informed patient consent and approval from the Institutional Domain Specific Review Board (DSRB), hWJSC lines were developed from human umbilical cords. hWJSCs that were previously banked were cultured in hWJSC medium comprising of 80% DMEM, 20% fetal bovine serum (FBS) (Biochrom,

Berlin, Germany), 1% non-essential amino acids, 2 mM L-glutamine, 0.1 mM β-mercaptoethanol, 1% insulin-transferrin-selenium, antibiotic/antimycotic mixture (Invitrogen Life Technologies, Carlsbad, CA) and 16 ng/ml basic fibroblast growth factor (Millipore Bioscience, Temecula, CA).

Commercial Cord Blood CD34+ cells

Approval for purchase and use of commercial cord blood CD34+ cells (HSCs) (StemCell Technologies Vancouver, BC, Canada) was granted by the National University of Singapore Institutional Review Board (NUS-IRB). The cells were thawed as per suppliers' instructions. Briefly, the cells were thawed in 37^{o}C and quickly transferred to 15 ml of Iscove's MDM containing 10% FBS and centrifudged at 200 x g for 15 min at room temperature. The supernatant was decanted and cell pellet seeded separately for experiments.

Isolation of Autologous hWJSCs and CD34+ HSCs

Approval for use of autologous hWJSCs and HSCs was granted by Institutional Domain Specific Review Board (DSRB).

For isolation of hWJSCs, 15-30 cm long of human umbilical cords were collected, cut into pieces and was washed in Hank's balanced salt solution (Invitrogen Life Technologies). Each small piece was slit open with sterile forceps and curved scissors and the Wharton's jelly were inverted face down into a Petri dish containing enzymatic solution comprised of collagenase type I, collagenase type IV and 100IU of hydrluronidase (all Sigma Chemical Co, USA) for 45 min in 37^{o}C, 5% CO2. The detached Wharton's jelly and remaining attached Wharton;s jelly was then separated using blunt surface of a curved forceps and transferred to new Petri dish with fresh DMEM. The gelatinous Wharton's jelly was syringed through an 18G needle to release the hWJSCs. Lastly the solution was centrifuged at 300 x g for 10 min and cell pellets were use for experiments.

For the isolation of autologous CD34+ cells, 100mL of UCB was aspirated from umbilical blood vessels using 50 ml syringes and large bore needles. The UCB CD34+ cells were isolated using Ficoll-Paque (StemCell Technologies) density gradient centrifugation as described by Jaatinen and Laine. Briefly, the UCB was first diluted in PBS/EDTA in the ratio of 1:4 and carefully layered on Ficoll-Paque soultion and centrifuged for 40 min. The buffy coat was then collected, washed and CD34+ cells were enriched by immunomagnetic positive selection using MidiMACS^{TM} system (Mitenyi Biotec, auburn, CA) according to manufacturer's instructions. Briefly, the buffy coat cells were incubated with CD34 microbeads and FcR blocking solution (Mitenyi Biotec) for 30 min at 4^{o}C, washed and added into a MACS LD column attached to a MidiMACS^{TM} magnetic separator. The LD column was then removed from the separator and CD34+ cells were eluted with a plunger. The collected cells were then centrifuged 200 x g and cell pellets used for experiment.

Bone marrow mesenchymal stem cells (hBMMSCs)

Approval for purchase and use of commercial adult hBMMSCs (Lonza, Allendale, NJ, USA) was given by the NUS-IRB. The cells were thawed and cultured in medium consisting of DMEM-high glucose (Invitrogen) supplemented with 10% FBS (Biochrom), 1% antibiotic/antimycotic mixture and 2 mM L-glutamine (Invitrogen).

5.2.2 Preparation of hWJSC conditioned medium (hWJSC-CM)

The preparation of hWJSC-CM was carried out as previously described [8,9,57]. Briefly, early passages of hWJSCs (3P to 5P) were first cultured in hWJSC medium until 70% confluency. The medium was then replaced with basal Stemspan SFEM medium (StemCell Technologies) supplemented with 1%

antibiotic/antimyotic mixture (Invitrogen). After 24h, the hWJSC-CM and was collected, filtered through a 0.22μM filter (Millipore) and stored at -80^{o}C until use.

5.2.3 Immunohistochemistry

hWJSCs and adult BM-MSCs were cultured in a Lab-Tek$^{(R)}$ Chambered #1.0 Borosilicate coverglass system (Thermo Scientific) till confluency. The cells were then fixed in 4% paraformaldehyde for 10 min, permeabilized with 0.1% Triton-X100 for 10 min and then washed with PBS. Non-specific blocking were done with 10% normal goat serum for 10 min. The cells were incubated with primary antibodies CD29, CD44, CD146, VCAM-1, MMP-2, MMP-9, SDF-1a, Laminin and Stro-1 (Biolegends, San Diego, USA) at 4^{o}C overnight. The cells were then incubated with appropriate secondary antibodes (Invitrogen Life Technologies) for 30 min at room temperature in presence of 1mg/mL Hoechst 33342, mounted onto slides with appropriate mounting medium. Images were taken using an Olympus FluoView FV1000 laser scanning confocal microscope (Olympus, Japan).

5.2.4 Cytokine Analysis of hWJSC-CM using the Multiplex Luminex$^{(R)}$ Beads Assay

Differential cytokine analysis of hWJSC-CM and controls was carried out using the Bio-Rad Express assay kit for human group I and II cytokines array (Bio-Rad Laboratories Singapore Pte Ltd, Singapore) based on manufacturers' instruction. The 96 wells plates in the kit were first wetted with 100 μl of wash buffer and 50 μl of beads were added into each well. 50 μl of hWJSC-CM were diulted in equal voulmes of assay diluent and 50 μl of the diluted sample and standards was added to the beads in each well. The plates were then incubated for 1 h at room

temperature in the dark with shaking. After incubation the plates were washed twice in buffer and incubated with 100 μl of secondary biotinylated antibodies (1:10) for 1h in the dark. After washing twice with buffer, 100 μl of streptavidin-PE were then added and incubated for 30 min at room temperature in the dark. Lastly, the wells were washed thrice, loaded with 100 μl of wash buffer and incubated for 2-3 min at room temperature in the dark. The plates were then read on a Bio-plex array reader and data subsequently analyzed using Bio-plex manager software version 3.

5.2.5 Experimental Design

Co-culture of Commercial UCB CD34+ cells with Allogeneic hWJSCs or hWJSC-CM

For co-culture of donor allogeneic hWJSCs with UCB $CD34^+$ cells, hWJSC monolayers (80% confluent) were first inactivated by exposure to 20 μg/mL of mitomycin- C (MMC, NUH Pharmacy, Singapore) and incubated at 37°C for 2.5 h. After incubation the cells were washed thoroughly and then dissociated with TrypLE™ Express (Invitrogen). 25,000 of MMC-treated hWJSCs were seeded per well in 2 different 24-well plates (Nalge Nunc International, Rochester, NY). The next day, 25,000 $CD34^+$ cells were seeded in each well containing the hWJSCs. The two cell types were co-cultured for 9 days at $37\ ^0$C in 5% CO_2 in air in hWJSC-Basal medium **(hWJSC-BM)** [(Stemspan SFEM medium containing bovine serum albumin, recombinant human insulin, human transferrin, 2-mercaptoethanol, Iscove's MDM medium (IMDM) and supplements) (Stem Cell Technologies)

For culture of UCB $CD34^+$ cells in hWJSC-CM, 25,000 $CD34^+$ cells were seeded in each well of 24 well plates and grown separately in 500 μl of hWJSC-CM for 9

days at 37 ^{0}C in 5% CO_2 in air with topping up with 250 μl of hWJSC-CM every 48 h.

Co-culture of Autologous UCB CD34+ cells with autologous hWJSCs

For co-culture of donor autologous hWJSCs with UCB $CD34^+$ cells, autologous hWJSC monolayers (80% confluent) were first inactivated by exposure to 20 μg/mL of mitomycin- C (MMC, NUH Pharmacy, Singapore) and incubated at 37°C for 2.5h. After incubation the cells were washed thoroughly and then dissociated with TrypLE^{TM} Express (Invitrogen). 25,000 of MMC-treated hWJSCs were seeded per well in 24-well plates (Nalge Nunc International, Rochester, NY). The next day, 25,000 autologous $CD34^+$ cells were seeded in each well containing the hWJSCs. The two cell types were co-cultured for 9 days at 37 ^{0}C in 5% CO_2.

5.2.6 Experimental Analysis Test

Phase Contrast and Scanning Electron Microscopy

The interaction of commercial and autologous UCB CD34+ cells with hWJSCs and hWJSC-CM were observed using phase contrast optics and conventional scanning electron microscopy (SEM) during 9 days of culture. Images of the behavior of the cells were captured using Olympus IX70 microscope (Olympus, Japan). For SEM, the cells were first fixed in 3% glutaraldehyde for 3h at room temperature dehydrated through a series of graded alcohol solutions and dried in hexamethyldisilazane overnight. The dried samples were then sputter coated with gold (JEOL JFC-1600 Auto Fine Coaster, Japan) and observed using Field Emission Scanning Electron Microscope (FEI-QUANTA 200 F, Czech Republic) at an accelerating voltage of 10 kV.

Cell viability (MTT assay)

10 µl [3-(4, 5-dimethylthiazolyl-2)-2, 5-diphenyltetrazolium bromide] (MTT, 0.5 mg/ml) (Duchefa Biochemie B.V., Haarlem, Netherlands) was added to the medium for each sample and the tubes were incubated for 4 h at 37^{o}C in 5% CO_2. The cell suspension was then centrifuged at 300 x g for 5 min, medium decanted and 100 µl of DMSO reagent (Sinopharm Chemical Reagent Co.Ltd) added to the cell pellet. The cells were dispensed into 96-well assay plates (NUNC, Rochester, NY) and incubated in the dark at 37^{o}C for 120 min. Absorbance at 570 nm against a reference wavelength of 630 nm was measured using a spectrophotometer microplate reader (mQuant; BioTek, Winooski, VT, USA).

Trypan Blue Vital Cell Counts

Aliquots of the cultured UCB CD34+ cells in all control and experimental arms were taken and stained with 0.4% Trypan Blue (Sigma Chemical Co) for 1 min at room temperature. The number of live cells were counted using a hemocytometer.

CD34+ cells

The cells pellet from Experimental and Control groups were collected and blocked with 10% normal goat serum (NGS) to prevent non-specific binding. The cells were then incubated with primary anti human CD34 antibodies (1:100) (Biolegends, San Diego, USA) for 30 min followed by secondary goat anti-mouse IgG (H+L) Alexa Fluor 488 antibodies (1:750) (Invitrogen Life Technologies) for 30 min in the dark. The cells were washed with PBS, resuspended in 10% NGS, filtered with a 40 µm strainer and analyzed with CyAn^{TM} ADP analyzer (Beckman Coulter, Fullerton, CA, USA).

Colony Forming Unit (CFU)

The cultured CD34+ cells from all control and experimental arms were separated, centrifuged at 300 x g for 5 min. The cell pellets were then seeded into 24 well-plates (Nalge Nunc International) containing 0.5 ml of semisolid methylcellulose in Methocult H4435 medium (StemCell Technologies). The 24-wells plates were incubated at 37^{o}C in a 5% CO_2 in air atmosphere for 14 days. Colonies (CFU) that were formed after 14 days were counted and classified based on morphology as described by the Atlas of Hematopoietic Colonies from Cord Blood. The CFU colonies were imaged using a Inverted phase contrast microscope (Nikon Instruments, Tokyo, Japan). Colony forming unit numbers were then calculated by dividing the number of colonies at day 14 by the number of cells plated and multiplying this value by 10,000 which reflected the colony forming ability of 10,000 cells.

5.2.7 Statistical Analysis

All results were expressed as mean ± SEM and statistical significance between the groups was calculated using the one way ANOVA or two-tailed Student's t-test (SPSS Statistic v 17.0 software package) (SPSS, Inc, IL). The *p*-value of <0.05 was considered as statistically significant.

5.3 Results

5.3.1 Immunohistochemistry

hWJSCs were stained positive for markers like CD29, CD44, CD146, VCAM-1, MMP-2, MMP-9, SDF-1a, laminin and Stro-1 that was shown to help with HSCs homing and migration [Fig. 25 (A-C)].

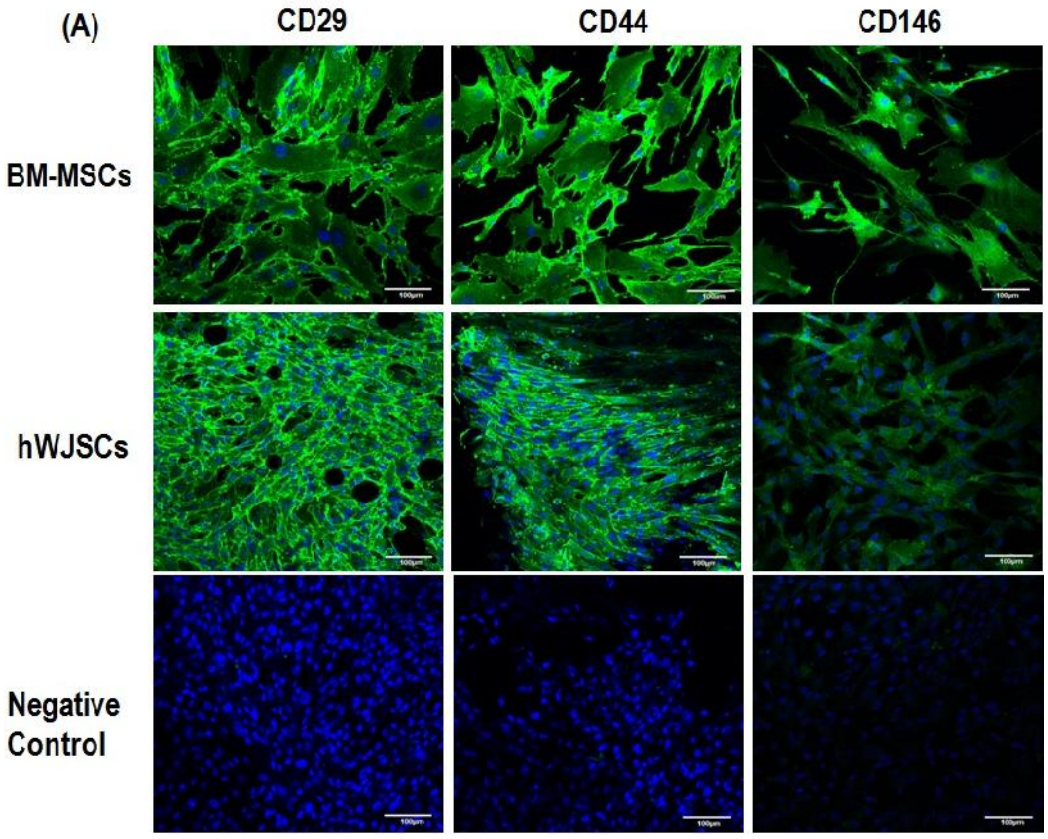

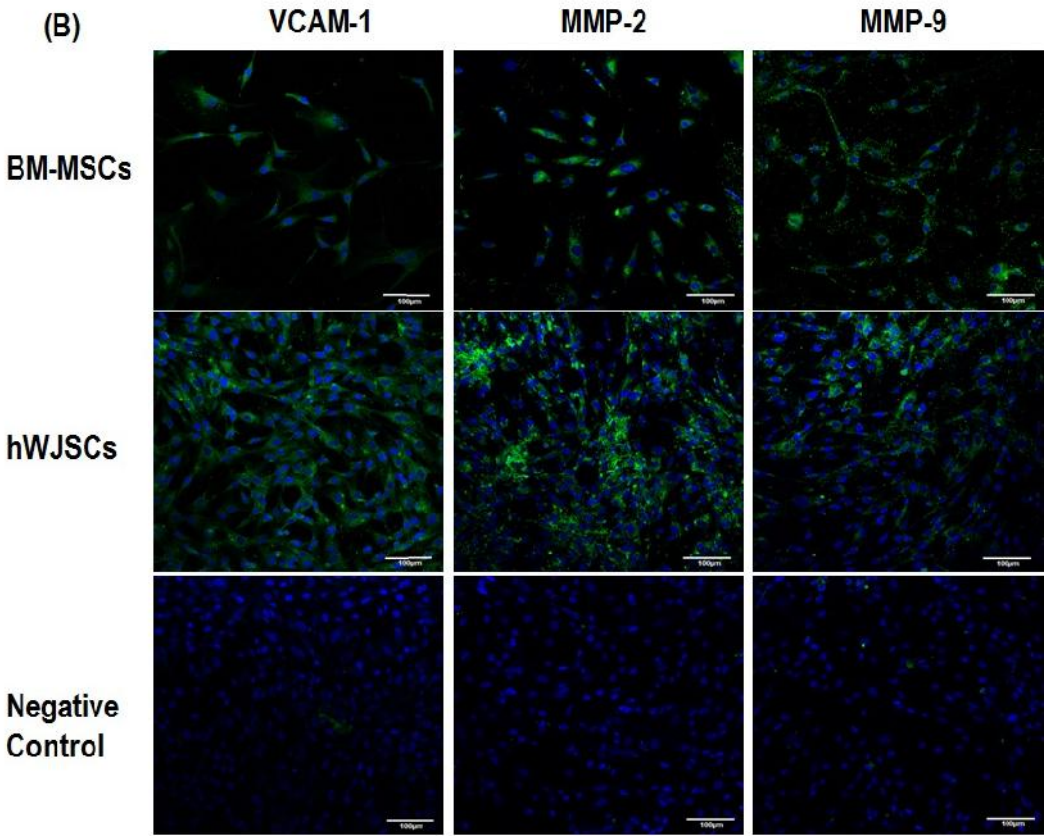
(B)
VCAM-1
MMP-2
MMP-9
BM-MSCs
hWJSCs
Negative Control

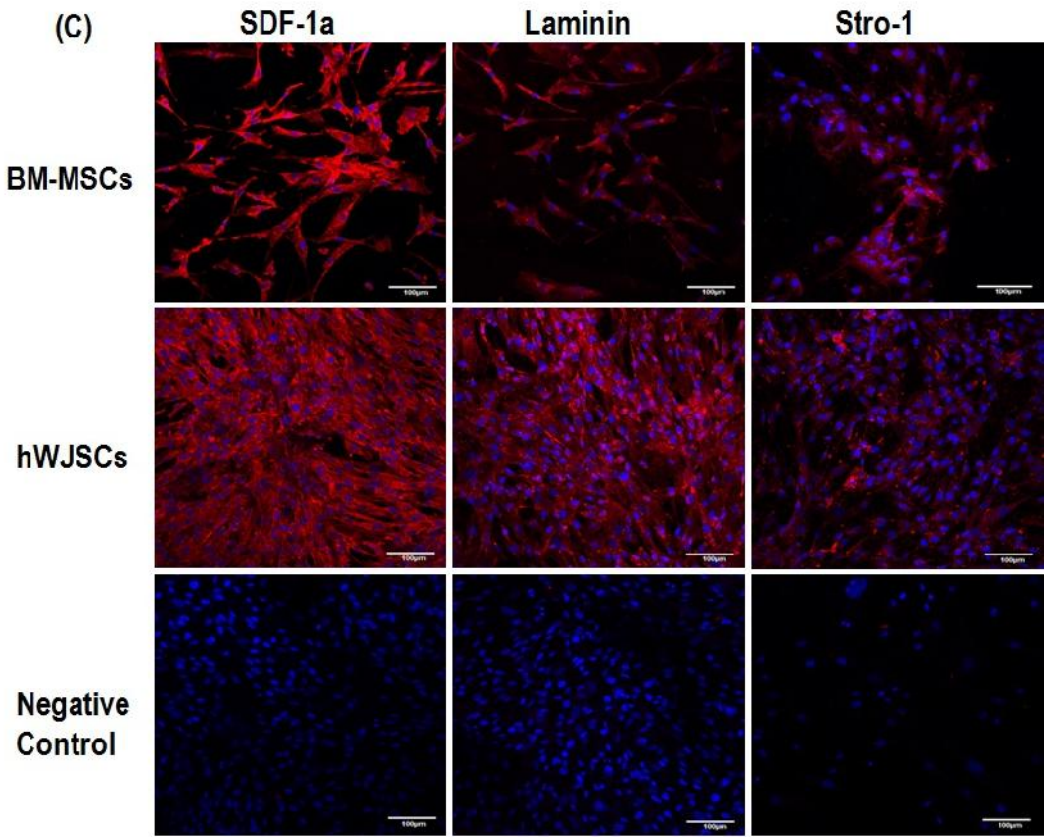
(C)
SDF-1a
Laminin
Stro-1
BM-MSCs
hWJSCs
Negative Control

Figure 25 Immunocytochemistry of BM-MSCs, hWJSCs.

(A-C) Immunocytochemistry of BM-MSCs, hWJSCs. hWJSCs were stained positive for CD29, CD44, CD146, VCAM-1, MMP-2, MMP-9, laminin and Stro-1. Magnification 40X; Scale Bar: 100µM

5.3.2 Proteomic profiles in hWJSC-CM

There were significantly higher level of certain members of interleukins cytokines like IL-1a, IL-6, IL-7 and IL-8, hepatocyte growth factor (HGF), stem cell factor(SCF) , monocyte chemotactic protein-1 (MCP-1) and intercellular adhesion molecule 1 (ICAM-1) in hJWSC-CM compared to basal control media (Fig. 26). Of these factors, the levels of IL-6, IL-8, HGF, SCF and ICAM-1 were extremely high compared to controls. The mean ± SEM concentration level in pg/ml were IL-1a: 4.34 ± 0.02 vs 1.71 ± 0.21; IL-6: 203.82 ± 6.78 vs 0.16 ± 0.01; IL-7: 1.52 ± 0.12 vs 0.635 ± 0.115; IL-8: 1875.94 ± 74.33 vs 4.72 ± 0.14; HGF: 2272.81 ± 5.65 vs 409.05 ± 29.06; SCF: 16390.19 ± 0.15 vs 4.74 ± 0.02; MCP-1: 493.25 ± 27.26 vs 1.695 ± 0.045 and ICAM-1: 118.86 ± 2.09 vs 0 or less than detectable range.

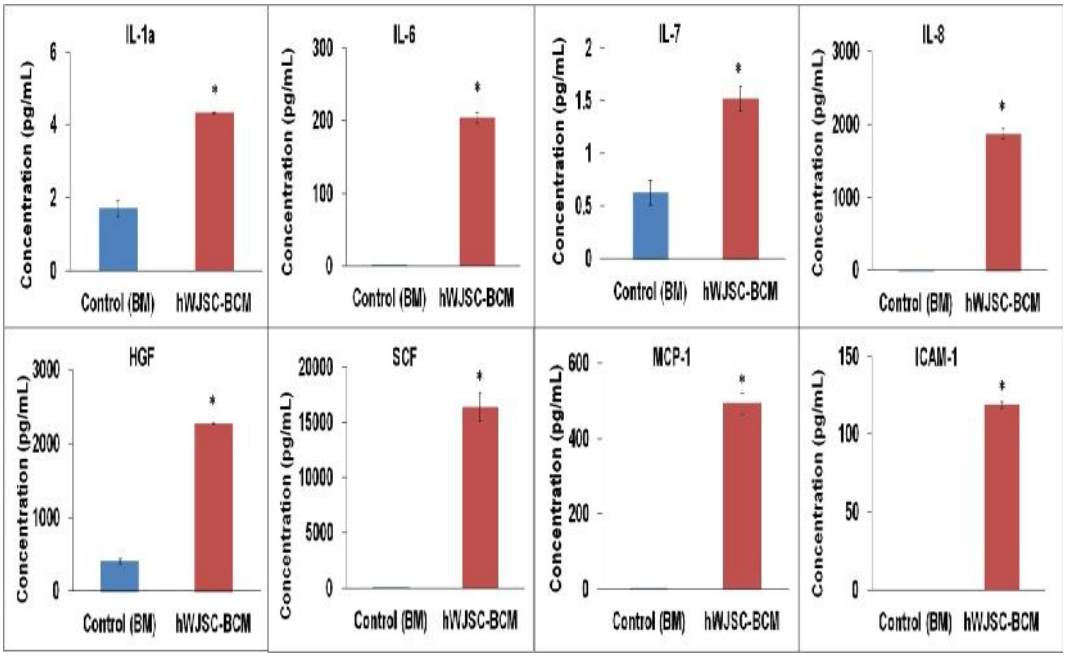

Figure 26 Proteomic analysis of hWJSC-CM

Proteomic analysis of hWJSC-CM. hWJSC-CM showed significantly higherr concentration (pg/ml) of IL-1a, IL-6, IL-7, IL-8, HGF, SCF, MCP-1 and ICAM-1 compared to controls. Asterisk (*) indicates statistical significance of $p<0.05$.

5.3.3 Cell Morphology

Most of the UCB CD34+ cells changed from a circular to an enlogated morphology, put out psedopodia-like outgrowths and migrated towards the bodies of the hWJSCs, loosely attached and undergoing mitosis [Fig. 27(A-B)]. They also became active and showed similar enlongated morphology with pseudopodia-like outgrowths when were exposed to hWJSC-CM (Fig. 27C). Such behavior were not observed in the controls (Fig. 26D). Scanning electron micrographs confirmed the mitotic activity of UCB CD34+ cells on hWJSCs and showed most of the cells attached on the upper surface of the hWJSCs with very few cells migrating beneath [Fig. 27(E-F)].

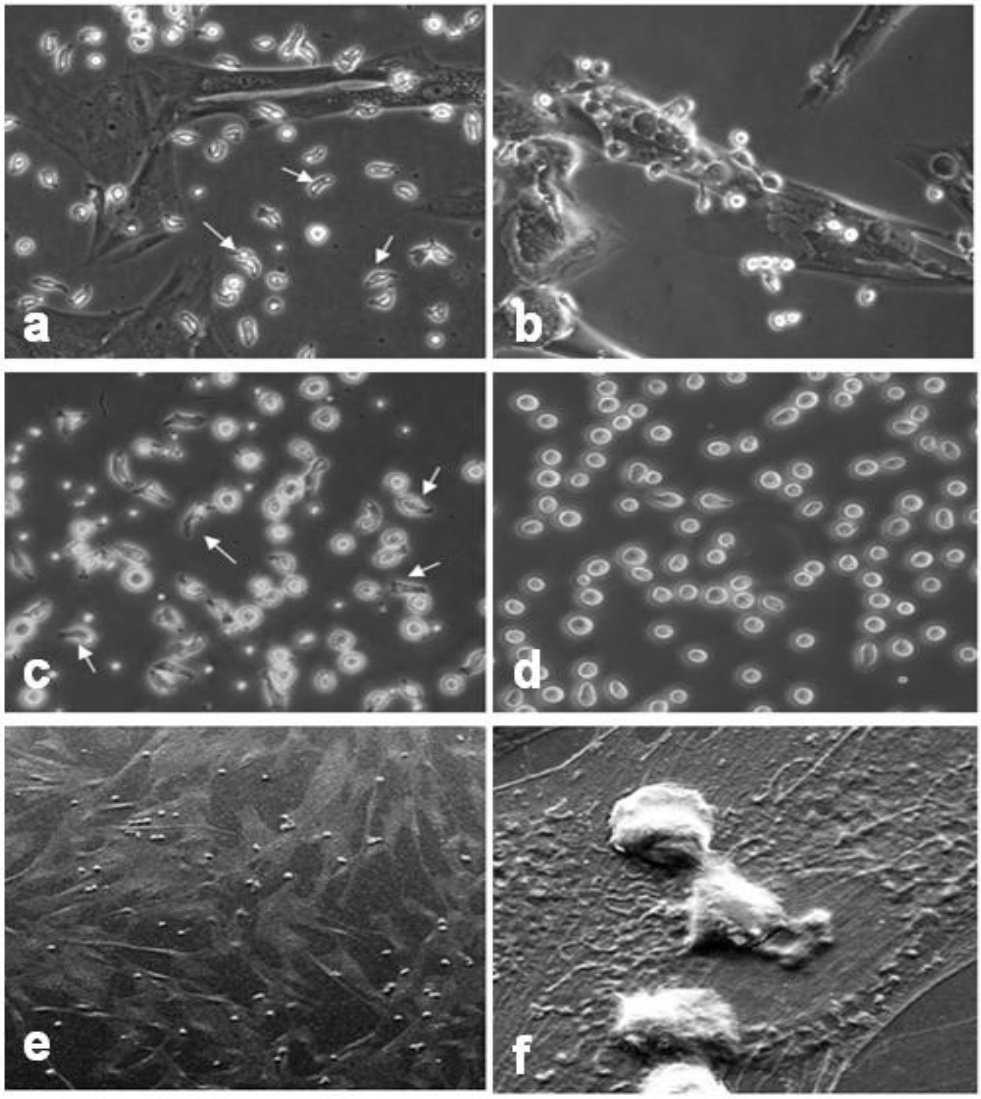

Figure 27 Phase constrast images of UCB CD34+ cells cultured with hWJSC or hWJSC-CM.

(A) UCB CD34+ cells put out pseudopodia-like outgrowths when cultured in hWJSCs (200x). (B) UCB CD34+ cells migrate towards the upper surfaces of hWJSCs, attaching and undergoing multiplication (200x) (C) UCB CD34+ cells putting out pseudopodia-like outgrowths (arrows) in hWJSC-CM which is not seen in control (D). (E) Scanning electron microscopic images indicate the cells attached loosely on the upper surfaces of hWJSCs at low magnification. (F) Scanning electron micrograph showing UCN CD34+ cells undergoing mitosis on surface of hWJSCs.

5.3.4 Cell Viability, Cell Proliferation and CD34+ Analysis

The results showed that there were significant increase in cell viability of UCB CD34+ cells after 9 days of culture with hWJSCs or hWJSC-CM compared to control. The cell viability were 0.03 ± 0.01 (Control), 0.092 ± 0.01 (hWJSCs) and 0.12 ± 0.01 (hWJSC-CM) (Fig. 28A).

There were significant increase in cell proliferation of UCB CD34+ cells after 9 days of culture with hWJSCs or hWJSC-CM compared to control. The fold change on the number of cells (by trypan blue counting) normalized to initial starting number of cells were 0.76 ± 0.04 (Control), 1.8 ± 0.2 (hWJSCs) and 7.6 ± 0.4 (hWJSC-CM) (Fig. 28B).

CD34+ analysis showed that when UCB CD34+ cells were cultured in hWJSCs or hWJSC-CM yield higher percentage of CD34+ cells compared to control. The percentage of CD34+ cells after 9 days of culture were 86.68% (Control), 93.91% (hWJSCs) and 96.91% (hWJSC-CM) (Fig. 28C).

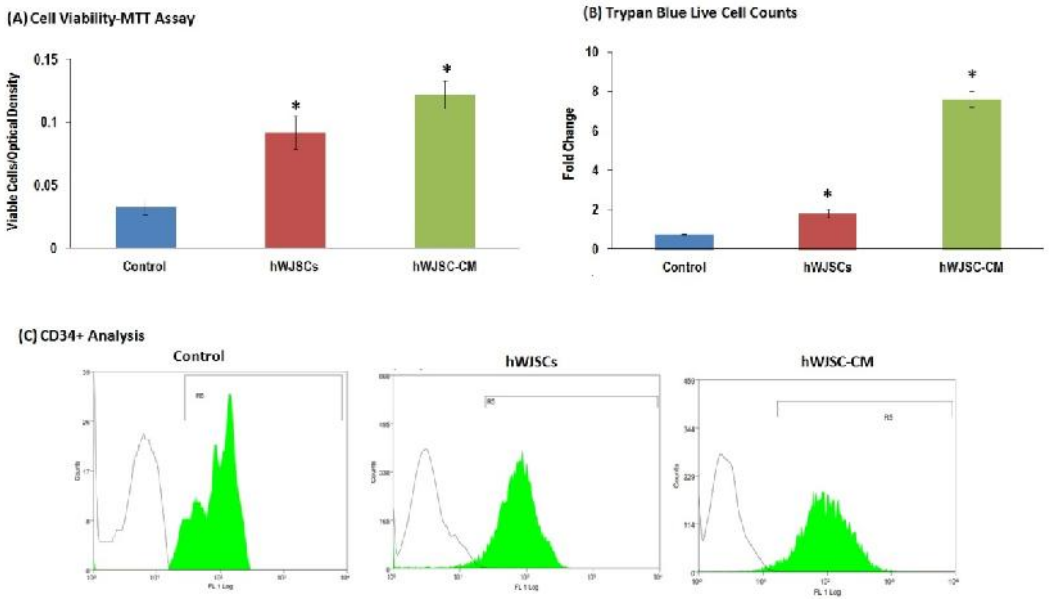

Figure 28 Cell viability, proliferation and percentage CD34+ analysis

Cell viability, proliferation and percentage of CD34+ cells after 9 days of culture with hWJSCs or hWJSC-CM compared to control. (A) Higher mean± SEM of UCB CD34+ cells' cell viability in the presence of allogeneic hWJSCs and hWJSC-CM compared to contol. **(B)** Higher mean ± SEM of UCB CD34+ cells' cell proliferation in the presence of allogeneic hWJSCs and hWJSC-CM compared to contol. **(C)** Contour maps of FACS analysis of UCB CD34+ cells when cultured in the presence of allogeneic hWJSCs and hWJSC-CM. Each contour map represents the percentage of FITC+ CD34 cells against unstained controls. Asterisk (*) indicates statistical significance of $p<0.05$.

5.3.5 Colony Forming Unit Analysis

CFU assay showed that there were an increase in CFU colonies when culturing UCB CD34+ cells with hWJSCs or hWJSC-CM than controls (Fig. 29A). The mean ± SEM CFU unit per 10,000 cells were 304 ± 34 (Control), 688 ± 125 (hWJSCs) and 846 ± 272 (hWJSC-CM) (Fig. 29B). There was an significant increase in CFU-GEMM unit when when culturing UCB CD34+ cells with hWJSCs or hWJSC-CM than controls. The mean ± SEM CFU-GEMM unit per 10,000 cells were 48 ± 11 (Control), 192 ± 23 (hWJSCs) and 208 ± 11 (hWJSC-CM) (Fig. 29C). All six types of colony morphology for normal hematopoiesis were observed in hWJSCs and hWJSC-CM compared to control (Fig. 28D).

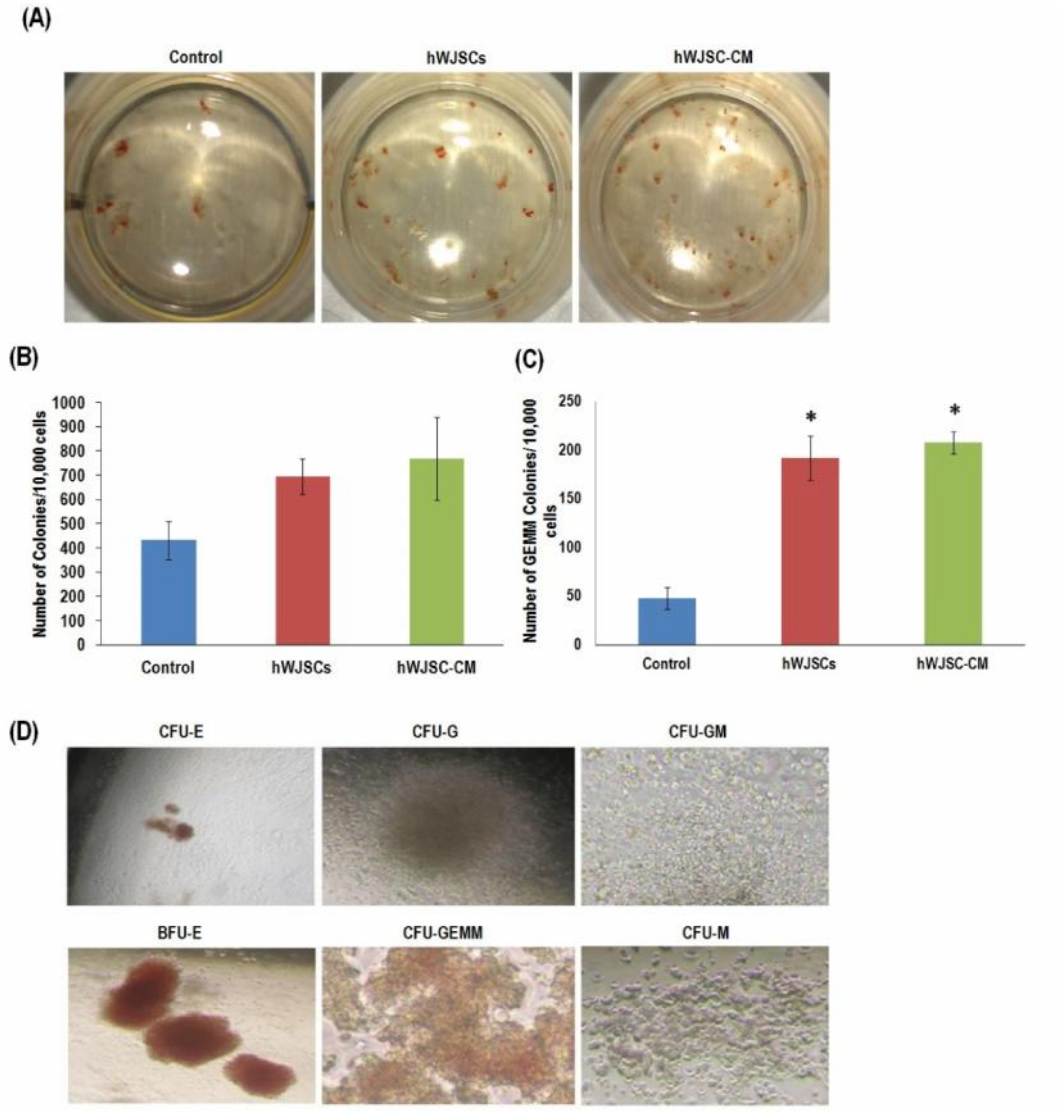

Figure 29 Colony forming unit (CFU) analysis

CFU analysis after 9 days of culture with hWJSCs or hWJSC-CM compared to control. (A) More CFU colonies observed in hWJSCs and hWJSC-CM wells as compared to control **(B)** Higher mean ± SEM CFU unit in the presence of allogeneic hWJSCs and hWJSC-CM compared to control. **(C)** Higher mean ± SEM GEMM colonies in the presence of allogeneic hWJSCs and hWJSC-CM compared to control. **(D)** Six different types of colony morphology observed with UCB CD34+ cells cultured in presence of allogeneic hWJSCs and hWJSC-CM. Asterisk (*) indicates statistical significance of $p<0.05$.

5.3.6 Culture of UCB CD34+ cells with Autologous hWJSCs

When fresh unfrozen autologous UCB CD34+ cells cultured in the presence of its own inactivated umbilical cord for 9 days, significant higher cell viability and higher percentage of CD34+ cells were also observed. The mean ± SEM cell

viability were 0.87 ± 0.01 (Control), 1.04 ± 0.03 (hWJSCs) (Fig. 30A). The mean ± SEM percentage CD34+ cells were 17.2 ± 1.4% (Control), 65.4 ± 0.6% (hWJSCs) (Fig. 30B).

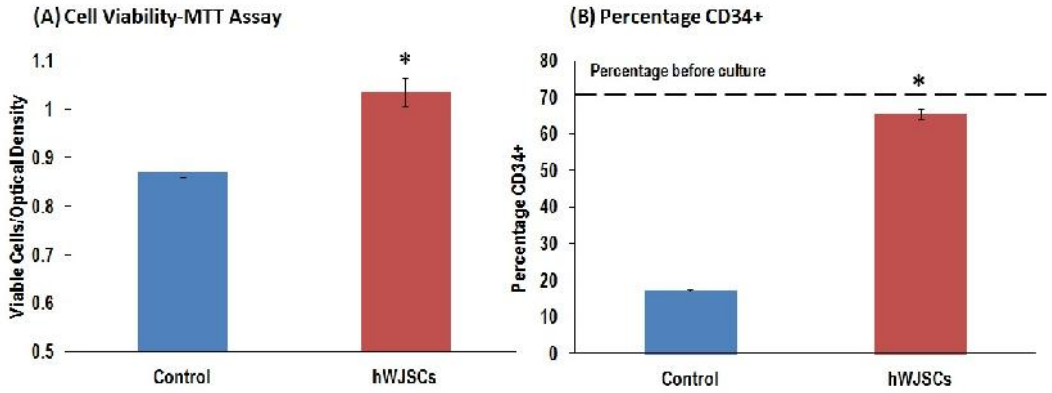

Figure 30 Cell viability and percentage of CD34+ cells of UCB 34+ cells cultured in autologous hWJSCs

(A) Higher mean ± SEM cell viability in the presence of autologous hWJSCs compared to control. **(B)** Higher mean ± SEM percentage CD34 in the presence of autologous hWJSCs to control. Dashed line indicate percentage of CD34+ cells before culture. Asterisk (*) indicates statistical significance of $p<0.05$.

5.4 Discussion

Hematopoietic stem cells from the umbilical cord blood can differentiate into the full spectrum of mature blood lineages and they have been used for the clinical treatment of malignant and non-malignant hematopoietic disorders. However, the low numbers of HSCs present in the UCB together with their low self renewal *in vitro* has limited their use to only small children. One of the therapeutic strategy to help increase UCB HSCs number is to develop reliable *ex vivo* UCB HSCs expansion methods [220].

A variety of stromal cells have been studied as matrices for *ex vivo* expansion of HSCs and these include derived primary monolayers of cells [228], genetically modified cytokine-releasing cells [229], bone marrow MSCs (BM-MSCs) [114] and immortalized BM-MSCs [230]. The mechanism of action of the feeder cell matrices

was to enable a sustained release of molecules to promote HSCs self renewal and proliferation [109]. Fresh patient-aspirated or commercial BM-MSCs have been the cell of choice for stromal support of HSCs as BM-MSCs are the normal resident cells in the bone marrow that provide a natural scaffold for the expansion of neighbouring HSCs *in vivo*. However, there is a need to explore alternative MSCs source due to the pain and risk of infection in harvesting fresh BM-MSCs and its variability to donor age etc. Though UCB-MSCs have been isolated [231-234] , some groups have failed or obtained very low MSCs number in UCB [225,226,235]. In fact, Bieback et al only manage to isolate 29 MSC-like colonies in 17 out of 59 processed cord blood and their optimal cell growth is only reached as late as 20 days in culture [234].

On the other hand, another MSC-like cells like hWJSCs that can be isolated from the Wharton's jelly portion of discarded umbilical cord in abundance is an attractive source for allogeneic or autologous stromal support for HSCs *ex vivo* expansion. Using protocol previously described, the derivation efficiency of hWJSCs was 100% and 4-5 x 10^6 hWJSCs/cm of the umbilical cord can be consistently isolated [3,4]. Such MSCs numbers with serial culture are very much higher than what is available in bone marrow or UCB.

Phase contrast images and SEM images showed that in the presence of hWJSCs or hWJSC-CM, the HSCs began to put out pseudopodia-like outgrowth to help them migrate towards the surface of the stromal hWJSCs niche, to attach and proliferate. Such outgrowths have been previously described as "fleet fleet" [236] or uropods [223]. Direct contact of HSCs with MSCs have been shown to affect migratory behavior and gene expression profiles of CD133+ HSCs during *ex vivo* expansion [223]. It was hypotheisized that specific stem cell niches within the stromal cell monolayers played a role in HSCs migration and proliferation and the

MSCs surface was the predominant site for HSCs proliferation while the compartments beneath the MSCs layer mimicked the stem cell niche [224]. In addition, the immunocytochemistry staining of hWJSCs in this chapter indicate that similar to BM-MSCs, hWJSCs also expresses molecules like CXCR4, CD44, CD146, CD29, VCAM-1, MMP-2, MMP-9, hyaluronan, laminin, Stro-1 that is required for HSCs migration and homing.

hWJSCs have been shown to secrete a wide variety of factors of the interleukin family, glycosaminoglycans (GAGs), hyaluronic acid (HA), cell membrane proteins, cell adhesion molecules, cadherins and growth factors [7,112]. The results of the proteomic analysis in this chapter were consistent with these observations. The members of the interleukins family specifically IL-6 and IL-8 and the growth factors (SCF, HGF) were secreted at extremely high level and may be important for CD34+ cells *ex vivo* expansion. IL-6 has been reposted to stimulate hematopoiesis [237] and IL-8 enhances proliferation [238]. SCF and HGF were shown to be effective in their maintenance [239]. hWJSCs also secreted high levels of HA and GAGs which are the building blocks of the extracellular matrix [14]. Interestingly, it was recently shown that when heparan sulfate was administered alone to CD34+ cells it helped to expand and maintain blood lineages *in vitro* [240]. While others reported the use of bone marrow stromal conditioned medium supplemented with IL-3 and MIP-1a are required for expansion of long-term culture-initiating cells and CFC [241], hWJSC-CM is naturally rich in these specific agents and other additional useful interleukins, growth factors to bring about an even greater desirable effects.

The logistical limitations using BM-MSCs from a family member of the patient as stromal support for ex vivo expansion of HSCs included (1) the appropriate family member not being available for donation and (2) the long time taken to not only

generate sufficent BM-MSCs but also to carry out co-culture expansion to provide sufficient HSCs since the disease progression was rapid in some leukemic patients [220]. The availability of "off-the-shelf" GMP compliant allogeneic MSCs for immediate use to alleviate this logistic problem have been recommended. The results of this chapter supported these suggestions and hWJSCs could be an alternative "off-the-shelf" allogeneic MSCs source. Moreover, hWJSCs in general are considered hypoimmunogenic [46].

The results of the present study also demonstrated that autologous hWJSCs harvested from the same umbilical cord can also provide a useful source for stromal support for cord blood HSCs expansion. The feasibility to store autologous hWJSCs have immense benefits as it has also been demonstrated that the major histocompatibility complex (MHC) restriction exists between HSCs and stromal cells both *in vitro* and *in vivo* [242,243]. Significant reductions in both cobblestone colonies of murine HSCs and bone marrow engraftments were observed with MHC-mismatched stromal cells as compared to MHC-matched stromal cells in *vitro* and *in vivo* respectively [242,243]. Likewise, there is also preferential expansion of UCB CD34+ cells when co-cultured with MHC-matched amnion-derived MSCs [244]. As the harvesting of hWJSCs only take a few hours [3,4], it is possible to freeze and store UCB-HSCs and hWJSCs from the same umbilical cord on the same day in a dual chamber blood collection bag. When the HSCs are needed, the hWJSCs could be thawed and used for HSCs expansion of HSCs if the number were inadequate. Moreover, co-transplantation of hWJSCs with UCB CD34+ cells could accelerate hematopoietic recovery in NOD/SCID mice even when limited numbers of UCB CD34+ cells were infused [112]. As such, the use of autologous hWJSCs cell source together with cord blood HSCs would to help improve the HSC tranplantation engraftment efficiencies greatly, and therefore we propose to co-bank hWJSCs with their corresponding

cord blood stem cells in the cord blood bank. This approach will avoid the need for discarding precious HSCs samples that are low in numbers as it is practiced by cord blood banks today.

Chapter 6: hWJSC-CM Enhances Cord Blood CD34+ Cells Freeze Thaw Survival

6.1 Introduction

Since the introduction of bone marrow hematopoietic stem cells (HSCs) transplantation, HSCs have been used in the treatment of hematopoietic diseases such as leukemia, lymphoma, thalassemia and autoimmune disorders. HSC transplantation has also been shown to produce promising results for the treatment of chronic liver failure and acquired immunodeficiency syndrome [95,96].

HSCs can be obtained from many different sources such as bone marrow (BM), peripheral blood (PB) and umbilical cord blood (UCB). HSCs isolated from the UCB have several advantages for transplantation therapy compared to the BM and PB [103-105]. They are easily collected and stored in cord blood banks, have lesser risk of graft versus host disease (GVHD) in transplant recipients due to their immune naivety and require less stringent criteria for donor-recipient matching. Additionally they have high proliferation rates, autocrine production of hematopoietic factors and longer telomere lengths due to their younger chronological age.

However, a major limitation to their use in transplantation is the low cell numbers collected in a single UCB unit. The typical yield of HSCs from a single freeze-thawed UCB unit is about 1.0×10^7 cells [109]. This number is far from enough than the recommended cell numbers range of 2.5 to 5×10^6 CD34+ cells/kg for a successful engraftment [245,246]. As such, single unit UCB-derived HSC transplantation is often a challenge for the treatment of adults [109]. Two of the strategies for successful transplantation in adult humans are (i) the use of double UCB unit transplantation and (ii) *ex vivo* expansion of the single UCB unit. However, double UCB transplantation has been associated with delayed

engraftment and elevated engraftment failure and usually one UCB unit ultimately predominates over the other [220]. Since there is a threshold dose below which cord blood transplantation recipients have engraftment failure, the *ex vivo* expansion of HSC numbers from single UCB units for the treatment of adults is a more plausible approach to successful transplantation therapy. Thus, attempts were made to increase HSC numbers in single UCB units. One such method is the refinement of existing cryopreservation protocols so as to increase freeze-thaw survival cell numbers.

For most types of cells, slow programmed freezing gives optimum freeze-thaw survival results compared to rapid or ultra-rapid methods because of the slow ice crystal formation helping in its preservation. However, existing slow freezing protocols for HSCs are far from ideal as there is significant cell death and loss of CD34+ cell populations after freeze-thaw [247]. This is because the slow freezing process results in nutrient deprivation, cellular dehydration, stress changes to structure, and physiology of HSCs and these effects compromise the post-thaw survival rate of stem cells [248]. Cryoinjury-induced apoptosis has also been reported as one of the main reasons for the loss of viability after cryopreservation [249]. Post-thaw apoptosis of CD34+ cells has also been shown to affect the recovery of viable CD34+ cells required for transplantation therapy [250,251]. It has been reported that the post-thaw apoptosis of CD34+ cells was mediated by the mitochondria and activated caspase 3 activity [252]. Previous studies used catalase and trehalose additives to provide cryoprotection by preventing apoptotic cell death [253]. The ROCK inhibitor Y-27632 was shown to enhance post-thaw survival and recovery of human embryonic stem cells and induced pluripotent stem cells [254,255], human mesenchymal stem cells (hMSCs) [249] and human umbilical cord Wharton's jelly stem cells (hWJSCs) [256]. However, it was shown to impair the survival, recovery and expansion of cryopreserved CD34+ cells [247]. Currently,

novel methods are being explored to improve the freeze-thaw viability and numbers of cryopreserved UCB-HSCs [105]. An optimal protocol for cryopreservation of HSCs that could overcome cryopreservation-induced damage needs to be developed to support HSC transplantation [257].

Chapter 5 showed that the secretions in the culture medium conditioned by hWJSCs over 24h had potent molecules that had strong anticancer effects and also supported the expansion of HSCs *ex vivo* [8]. When UCB-HSCs were exposed to hWJSC conditioned medium (hWJSC-CM) they were motile immediately, put out pseudopodia-like projections and underwent proliferation. With increase culture time, augmentation of CD34+ cell numbers and colony forming units resulted and eventually generated all the lineages of normal hematopoiesis [8]. A proteomic analysis of the hWJSC-CM showed high concentrations of several families of important agents such as interleukins, growth factors, glycosaminoglycans and cell adhesion molecules which were attributed the spontaneous activity and expansion of the HSCs to [8]. Given the potent actions and potential therapeutic value of the agents in hWJSC-CM, the aim of this chapter is to explore whether the incorporation of hWJSC-CM as a supplement in freezing and thawing media in cryopreservation protocols and in post-thaw culture would enhance freeze-thaw survival and subsequent increase of CD34+ cell numbers.

6.2 Material and Methods

6.2.1 Cell Culture

Human Wharton's jelly stem cells (hWJSCs)

After informed patient consent and approval from the Institutional Domain Specific Review Board (DSRB), hWJSC lines were developed from human

umbilical cords. hWJSCs were cultured in hWJSC medium comprising of 80% DMEM, 20% fetal bovine serum (FBS) (Biochrom, Berlin, Germany), 1% non-essential amino acids, 2 mM L-glutamine, 0.1 mM β-mercaptoethanol, 1% insulin-transferrin-selenium, antibiotic/antimycotic mixture (Invitrogen Life Technologies, Carlsbad, CA) and 16 ng/ml basic fibroblast growth factor (Millipore Bioscience, Temecula, CA).

Cord Blood CD34+ cells

Approval for purchase and use of commercial cord blood CD34+ cells (HSCs) (StemCell Technologies Vancouver, BC, Canada) was granted by the National University of Singapore Institutional Review Board (NUS-IRB). The cell lines were thawed and expanded in StemSpan SFEM medium (StemCell Technologies) supplemented with 2mM L-glutamine, 1% antibiotic/antimyotic mixture (Invitrogen Life Technologies) and cytokines cocktail CC110 for 3 days before use for freeze-thaw survival experiments (StemCell Technologies).

6.2.2 Preparation of hWJSC conditioned medium (hWJSC-CM)

The preparation of hWJSC-CM was carried out as previously described [8,9,57]. Briefly, early passages of hWJSCs (3P to 5P) were first cultured in hWJSC medium until 70% confluency. The medium was then replaced with basal StemSpan SFEM (StemSpan Technologies) supplemented with 1% antibiotic/antimyotic mixture (Invitrogen). After 24h, the medium (hWJSC-CM) was collected, filtered through a 0.22μM filter (Millipore) and stored at -80^{o}C until use.

6.2.3 Experimental Design

Freezing of cord blood CD34+ cells

The expanded cord blood CD34+ cells were divided into 2 equal groups. Cells in the control group (Group A) were frozen in Freezing Medium (Control) (FMC) comprising of 50% StemSpan SFEM (StemCell Technologies Vancouver, BC) supplemented with 2 mM L-glutamine, 1% antibiotic/antimyotic mixture (Invitrogen Life Technologies), 40% FBS (HyClone Thermo Fisher Scientific, Rochester, NY) and 10% DMSO (Sinopharm Chemical Reagent Co.Ltd, Shanghai, China). Cells in the experimental group (Group B) were frozen in 24h-50% hWJSC-CM supplemented with 2 mM L- glutamine, 1% antibiotic/antimyotic mixture (Invitrogen Life Technologies, Carlsbad, CA), 40% FBS (HyClone Thermo Scientific) and 10% DMSO (Sinopharm Chemical Reagent Co Ltd). Both groups of cells were frozen using slow programmed freezing in a controlled rate freezing machine (Kryo10 Series II) from room temperature at a freezing rate of -1^{o}C per minute to -120^{o}C as previously described [258]. The cryovials were removed at -120^{o}C and plunged into liquid nitrogen (-196^{0}C) in a tank for at least 2 weeks before analysis.

Thawing of cord blood CD34+ cells

Frozen CD34+ cells from Groups A and B were thawed rapidly within 1-2 min in a 37^{o}C water bath and added to thawing medium [IMDM (Invitrogen Life Technologies) supplemented with 20% FBS (HyClone Thermo Fisher Scientific), 2 mM L-glutamine, 1% antibiotic/antimyotic mixture (Invitrogen Life Technologies)] and centrifuged. The cell pellets from each of Groups A and B were divided into 2 Subgroups, with each Subgroup having Experimental and Control arms. Subgroup 1: *0 h post- thaw analysis* (Analysis done immediately after thawing) (Experimental arm: hWJSC-CM; Control arm: control).

Subgroup 2: *72 h post-thaw analysis* (Analysis done 72 hours after thawing). Thawed cells grown for 72 h in 24h-50% hWJSC-CM supplemented with 20% FBS (HyClone Thermo Fisher Scientific, 2mM L-glutamine and 1% antibiotic/antimyotic mixture (Invitrogen Life Technologies) in the Experimental group while in the Control group, thawed cells grown for 72 h in basal StemSpan SFEM supplemented with 20% FBS (HyClone Thermo Fisher Scientific), 2mM L-glutamine and 1% antibiotic/antimyotic mixture (Invitrogen Life Technologies).

The cells were then analyzed for cell morphology, cell proliferation assay, CD34+ cell analysis, CFU assay, Annexin V-FITC/PI assay, Live/Dead® Viability assay and cell cycle assay.

6.2.4 Experimental Analysis Test

Cell Morphology

Cell pellets from Experimental and Control arms from both subgroups were placed in their respective media and the cell morphology imaged with Olympus IX70 Inverted fluorescence microscope (Olympus Corporation, Tokyo, Japan).

Cell viability (MTT assay)

The cells from Experimental and Control groups collected, washed once with PBS (-), centrifuged at 300 x g and then re-suspended in 100 μL growth media. 10 μl [3-(4, 5-dimethylthiazolyl-2)-2, 5-diphenyltetrazolium bromide] (MTT, 0.5 mg/ml) (Duchefa Biochemie B.V., Haarlem, Netherlands) was added to the medium for each sample and the tubes were incubated overnight at 37^{o}C in 5% CO_2. The cell suspension was then centrifuged at 1,500 x g for 5 min, medium decanted and 100 μl of DMSO reagent (Sinopharm Chemical Reagent Co.Ltd) added to the cell pellet. The cells were dispensed into 96-well assay plates (NUNC, Rochester, NY) and incubated in the dark at 37^{o}C for 10 min.

Absorbance at 570 nm against a reference wavelength of 630 nm was measured using a spectrophotometer microplate reader (mQuant; BioTek, Winooski, VT, USA).

CD34+ cells

The cells pellet from Experimental and Control groups were collected and blocked with 10% normal goat serum (NGS) to prevent non-specific binding. The cells were then incubated with primary anti human CD34 antibodies (1:100) (Biolegends, San Diego, USA) for 30 min followed by secondary goat anti-mouse IgG (H+L) Alexa Fluor 488 antibodies (Invitrogen Life Technologies) for 30 min in the dark. The cells were washed with PBS, resuspended in 10% NGS, filtered with a 40 μm strainer and analyzed with CyAn^{TM} ADP analyzer (Beckman Coulter, Fullerton, CA, USA).

Colony Forming Unit (CFU)

Cell pellets from Experimental and Control arms were re-suspended in 1 mL of IMDM medium supplemented with 20% FBS, L-glutamine and antibiotic/antimycotic mixture. 50 μl of the cell suspension from each group was seeded into each well of a 24-well plate containing 0.5 mL in MethoCult^{R} H4435 medium (StemCell Technologies). The 24-wells plates were incubated at 37^{o}C in a 5% CO_2 in air atmosphere for 12 days. Colonies (CFU) that were formed after 12 days were classified based on morphology as described by the Atlas of Hematopoietic Colonies from Cord Blood. The CFU colonies were imaged using an inverted phase contrast microscope (Nikon Instruments, Tokyo, Japan). The CFU colonies were later quantified using the CytoSelect^{TM} Hematopoietic Colony Forming assay (Cell Biolabs, Inc., San Diego, CA). Briefly, the cells were collected and resuspended in 250 μL IMDM medium supplemented with 20%

FBS, L-glutamine and antibiotic/antimycotic mixture (Invitrogen Life Technologies). 50 μl of 4X Lysis Buffer/CyQuant® GR dye solution (1:75 dilution) was then added to each sample, mixed, and incubated for 30 min at room temperature. 100 μl of the mixture was added to each well in the 96 well plate and readings were taken with a 485 nm/535 nm filter set using TECAN GENios (TECAN Austria GmBH, Salzburg, Austria).

Annexin V/PI assay

The cell pellet from Experimental and Control groups were collected, washed once with PBS (-), centrifuged and then resuspended with 500 μL of 1X Annexin V binding buffer (BioVision, Inc., Mountain View, CA). The cells were then stained with 1 μL of Annexin V- FITC (BioVision) and counterstained with 1 μL of propidium iodide (PI, Invitrogen), at room temperature for 15 min, filtered with a 40 μm nylon strainer and analyzed using a CyAn^{TM} ADP analyzer (Beckman Coulter, Fullerton, CA, USA).

Live/Dead cell assay

The live/dead cell assay was performed on the cell pellets from Experimental and Control groups using the Live/Dead® Viability/Cytotoxicity Kit for mammalian cells (Invitrogen). A working solution of component A (included in the kit) was first made by adding 1 μl of component A into 79 μl of DMSO (Sinopharm Chemical Reagent Co.Ltd). 1 μL of this component A working solution and 2 μL of component B (supplied in the kit) were added to 500 μl of PBS (-) to make the staining solution.

The cells were later collected, washed once with PBS (-), centrifuged and resuspended in 500 μl of staining solution and then incubated for 15 min in the

dark. The cell suspension was filtered with a 40 µm nylon strainer and analyzed using a CyAn^{TM} ADP analyzer (Beckman).

Cell cycle analysis

The cell pellets from the Experimental and Control groups were collected, washed once with PBS (-), then fixed in cold 70% ethanol at -20^{o}C overnight. The cells were later washed with PBS (-) once before adding 20 µg/mL PI, 100 µg/mL RNase A (AppliChem GmbH, Garmstadt, Germany) to each sample and then incubated for 15 min at 37^{o}C in 5% CO_2. The cell suspension was then filtered using a 40 µm nylon strainer to remove any cell clumps before analysis using a CyAn^{TM} ADP analyser (Beckman).

6.2.5 Statistical Analysis

All results were expressed as mean (fold change) ± SEM and statistical significance between the groups was calculated using the one way ANOVA or two-tailed Student's t-test (SPSS Statistic v 17.0 software package) (SPSS, Inc, IL). The *p*-value of <0.05 was considered as statistically significant.

6.3 Results

6.3.1 Cell Morphology

No distinct morphological differences were observed in the UCB CD34+ cells between the Control and Experimental groups with cells in both groups showing their characteristic spherical shape and size immediately after thawing [Fig. 31(a, b)]. There are more cellular debris was observed after 72 h culture in the Control compared to the Experimental group [Fig. 31(c-f)].

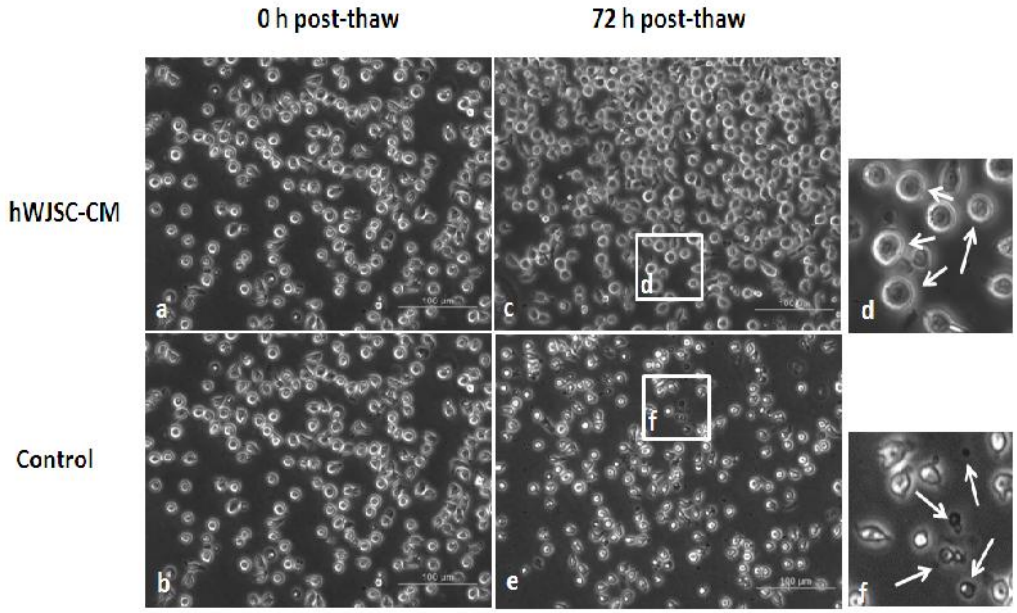

Figure 31 Morphology of CD34+

(a, b): Morphology of CD34+ cells frozen in hWJSC-CM, thawed and analysed immediately (0 h post-thaw). Note the thawed CD34+ cells that were frozen in hWJSC-CM having similar healthy circular morphology as controls. **(c-f): Morphology of CD34+ cells frozen in hWJSC-CM, thawed and then grown in hWJSC-CM for 72 h (72 h post-thaw). (c, d):** Note low and high magnification of healthy CD34+ cells (arrows) **(e, f):** Controls showing greater cell death (cell debris) (arrows). Scale bar: 100 μm.

6.3.2 Cell Viability and CD34+ analysis

Cord blood CD34+ cells had significant greater cell viability in hWJSC-CM compared to controls immediately after thawing. The cell viability rates increased by 2.08 ± 0.3 fold (Fig. 32A) in samples frozen in hWJSC-CM immediately after thawing. Cord blood CD34+ cells then had significantly greater cell viability of CD34+ cells were observed when they were frozen in hWJSC-CM and cultured after thawing for 72 h in hWJSC-CM compared to controls. The cell viability rates increased by 2.28 ± 0.17 fold (normalized to control) (Fig. 32B) in samples frozen in hWJSC-CM and cultured in hWJSC-CM after thawing. Cord blood CD34+ cells showed higher percentages of CD34+ in hWJSC-CM compared to the controls immediately after thawing. The percentages of CD34+ for control and hWJSC-CM were 94.84 ± 2.42% and 96.63 ± 1.43% respectively (Fig. 32C) immediately

after thawing. Cord blood CD34+ cells then showed significantly greater percentages of CD34+ cells when they were frozen in hWJSC-CM and cultured after thawing for 72 h in hWJSC-CM compared to controls. The percentages of CD34+ for control and hWJSC-CM were 65.23 ± 1.69% and 77.57 ± 0.54% (Fig. 32D) 72 h after thawing.

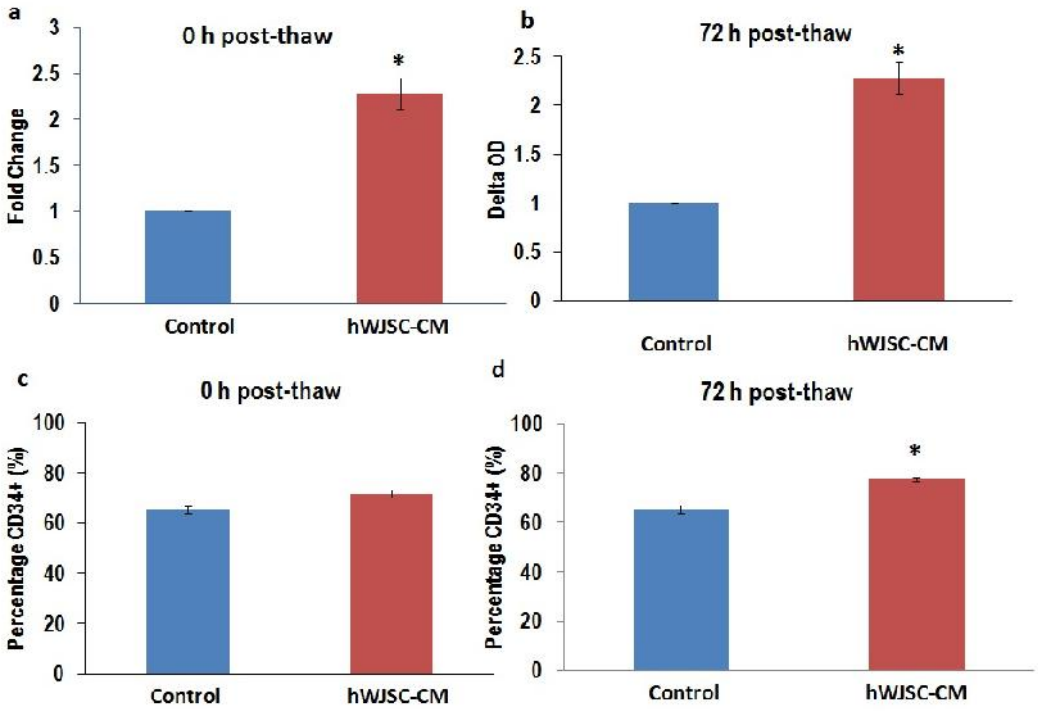

Figure 32 Cell viability rate of CD34+ cells frozen in hWJSC-CM, thawed and grown in hWJSC-CM for 72h.

(a): Note greater fold increases (normalised to respective controls) of CD34+ cells frozen in hWJSC-CM, thawed and analysed immediately (0 h post-thaw) and; **(b):** Note greater fold increases of CD34+ cells after thawing and growing in hWJSC-CM for 72 h (72 h post-thaw). **(c):** Higher percentaged of CD34+ cells were observed when CD34+ were frozen in hWJSC-CM, thawed and analysed immediately (0 h post-thaw); and **(d)** Higher percentage of CD34+ cells were observed when CD34+cells were frozen in hWJSC-CM, thawed and grown in hWJSC-CM for 72. Values are mean ± SEM of 3 different experiments. Asterisk (*): $p<0.05$.

6.3.3 Colony Forming Unit (CFU) Assay

Cord blood CD34+ cells from all groups displayed typical GEMM CFU morphology as described by the Atlas of Hematopoietic Colonies from Cord Blood [Fig 33 (A-D)]. When the CFU colonies were quantified using the CytoSelect™ Hematopoietic Colony Forming assay, cells that were frozen in hWJSC-CM produced more CFUs compared to controls (1.07 ± 0.02) immediately after thawing (Fig. 33E). Cord blood CD34+ cells had produced more CFUs when they were frozen in hWJSC-CM and cultured after thawing for 72 h in hWJSC-CM compared to the controls. The CFU unit increased 1.6 ± 0.17 fold (normalized to control) (Fig. 33F) in samples frozen in hWJSC-CM and cultured in hWJSC-CM after thawing.

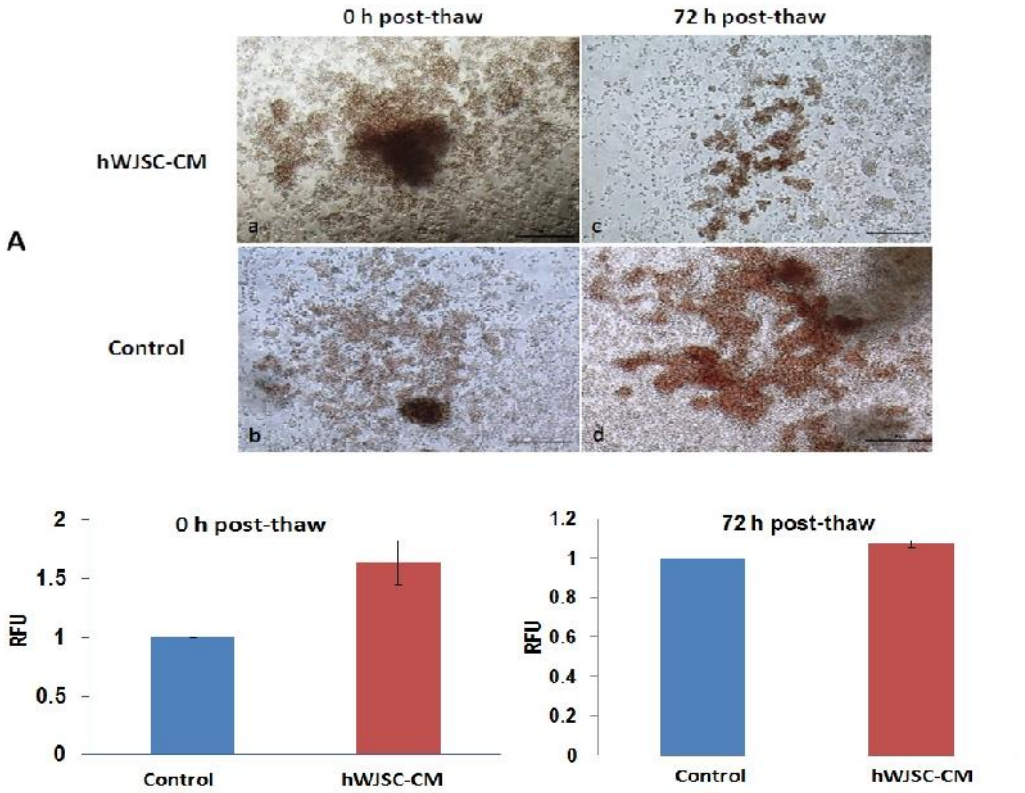

Figure 33 CFU assay of CD34+ cells frozen in hWJSC-CM, thawed and grown in hWJSC-CM for 72 h.

(a): CD34+ cells frozen in hWJSC-CM, thawed and grown on methylcellulose for 12 days showed typical GEMM colonies, **(b):** Parallel controls showed similar GEMM colonies. **(c):** Similar GEMM colonies were observed for CD34+ cells frozen in hWJSC-CM, thawed and then grown in hWJSC-CM for 72 h. **(d):** Parallel controls showed similar GEMM colonies. **(e):** Greater number of colonies (normalised to controls) were observed when CD34+ cells were frozen in hWJSC-CM, thawed and grown on methylcellulose; and **(f):** Greater number of colonies (normalised to controls) were observed when CD34+ cells were frozen in hWJSC-CM, thawed, grown in hWJSC-CM for 72 h and then grown on methylcellulose. Values are mean ± SEM of 3 different experiments.

6.3.4 Annexin V-FITC/PI Assay

Cord blood CD34+ cells had lower percentages of Annexin V+ cells in hWJSC-CM compared to controls immediately after thawing. The percentages of Annexin V+ for control and hWJSC-CM were 15.36 ± 0.59% and 14.00 ± 0.95% respectively (Fig. 34A) immediately after thawing. Likewise cord blood CD34+ had lower percentages of PI+ cells in hWJSC-CM compared to the controls immediately after thawing. The percentages of PI+ for control and hWJSC-CM

were 11.45 ± 0.23% and 11.45 ± 0.23% receptectively (Fig. 34B) immediately after thawing.

Cord blood CD34+ cells then had significantly lower percentages of Annexin V+ and PI+ cells when they were frozen in hWJSC-CM and cultured after thawing for 72 h in hWJSC-CM compared to the controls. The mean ± SEM percentages for Annexin V+ for control and hWJSC-CM were 18.92 ± 0.1% and 8.68 ± 0.57% (Fig. 34C) respectively 72 h after thawing. The mean ± SEM percentages for PI+ cells for control and hWJSC-CM were 12.39 ± 0.35% and 7.19 ± 0.34% respectively (Fig. 34D) 72 h after thawing.

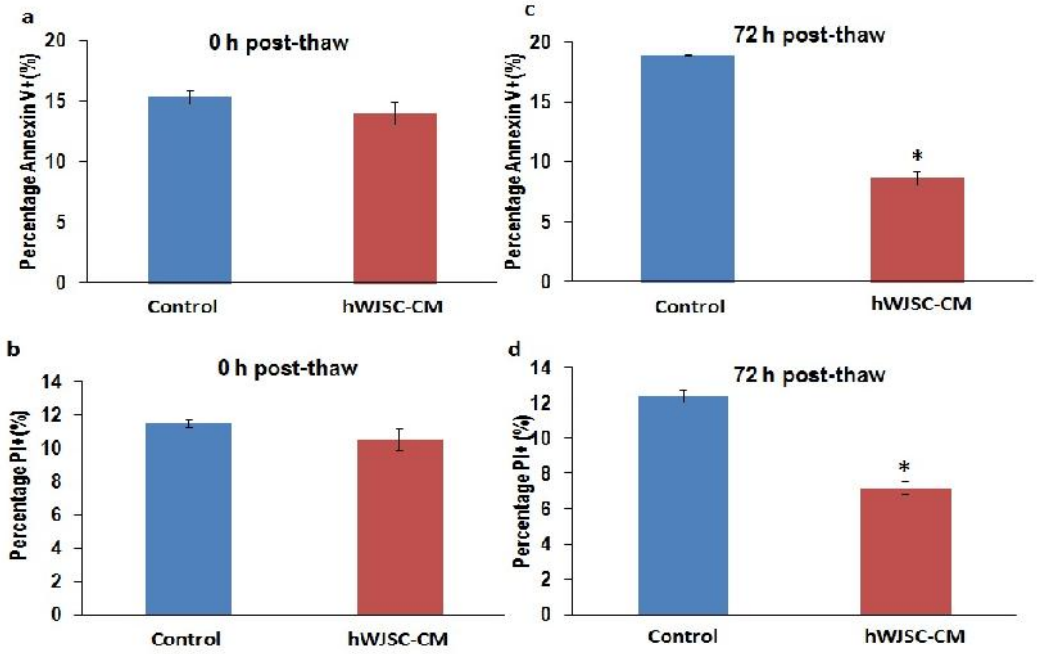

Figure 34 Annexin V/PI assay of CD34+ cells frozen in hWJSC-CM, thawed and grown in hWJSC-CM for 72 h.

(a): Lower percentages of apoptotic cells (Annexin V+) were observed when CD34+ cells were frozen in hWJSC-CM, thawed and analysed immediately (0 h post-thaw). **(b):** Lower percentages of necrotic cells (PI+) were observed when CD34+ cells were frozen in hWJSC-CM, thawed and analysed immediately (0 h post-thaw). **(c):** Lower percentages of apoptotic cells (Annexin V+) were observed when CD34+ cells were frozen in hWJSC-CM, thawed and grown in hWJSC-CM for 72 h (72 h post-thaw). **(d):** Lower percentages of necrotic cells (PI+) were observed when CD34+ cells were frozen in hWJSC-CM, thawed and grown in hWJSC-CM for 72 h (72 h post-thaw). Values are mean ± SEM of 3 samples with 3 different experiments. Asterisk (*): $p<0.05$.

6.3.5 Live/Dead and Cell Cycle Assay

Cord blood CD34+ cells showed greater percentages of live cells in hWJSC-CM compared to the controls immediately after thawing. The percentages of live cells for control and hWJSC-CM were 81.2 ± 0.58% and 83.07 ± 1.73% respectively (Fig. 35A) immediately after thawing. Similarly, cord blood CD34+ showed lower percentages of dead cells in hWJSC-CM compared to controls immediately after thawing. The percentages of dead cells for control and hWJSC-CM were 17.07 ± 1.93% and 16.18 ± 1.34% respectively (Fig. 35B) immediately after thawing.

Cord blood CD34+ cells then had higher percentages of live cells when they were frozen in hWJSC-CM and cultured after thawing for 72 h in hWJSC-CM compared to controls. The mean ± SEM percentages for live cells for control and hWJSC-CM were 68.05 ± 0.84% and 74.75 ± 3.43% (Fig. 35C) respectively 72 h after thawing.

Likewise cord blood CD34+ had lower percentages of dead cells when they were frozen in hWJSC-CM and cultured after thawing for 72 h in hWJSC-CM compared to controls. The mean ± SEM percentages for dead cells for control and hWJSC-CM were 22.02 ± 0.49% and 20.05 ± 2.1% respectively (Fig. 35D) 72 h after thawing.

Cell cycle analysis had lesser percentage of cord blood CD34+ cells with fragmented DNA (Sub-G1 phase) in samples frozen in hWJSC-CM compared to the controls. The percentages of sub-G1 for control and hWJSC-CM were 4.47 ± 1.89% and 3.24 ± 0.63% respectively (Fig. 35E) immediately after thawing. In addition, cord blood CD34+ had significantly lower percentages of cells with fragmented DNA dead when they were frozen in hWJSC-CM and cultured after thawing for 72 h in hWJSC-CM compared to controls. The mean ± SEM percentages for sub-G1 cells for control and hWJSC-CM were 10.65 ± 0.27% and 3.10 ± 0.69% respectively (Fig. 35F) 72 h after thawing.

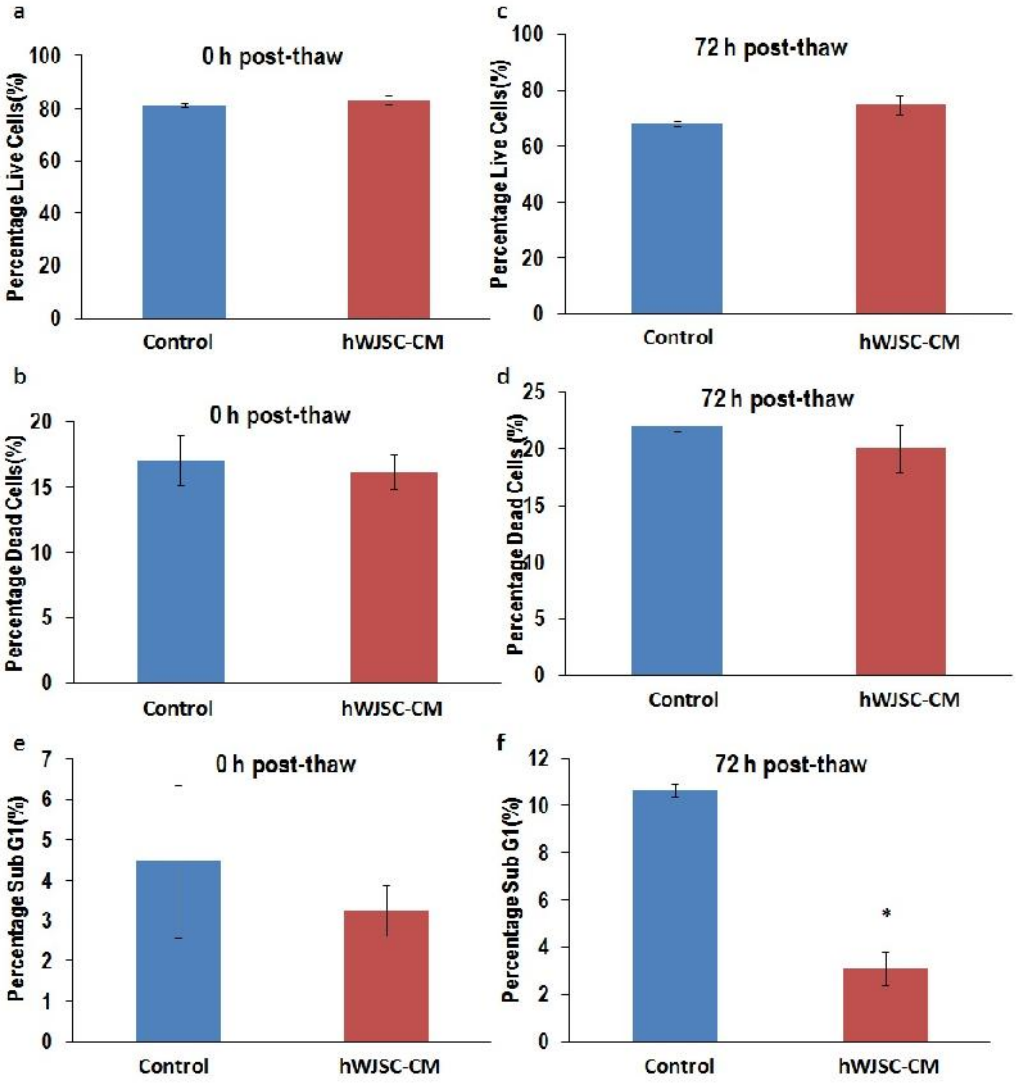

Figure 35 Live/Dead viability and cell cycle analysis of CD34+ cells frozen in hWJSC-CM, thawed and grown in hWJSC-CM for 72 h.

(a): Higher percentages of live cells were observed when CD34+ cells were frozen in hWJSC-CM, thawed and analysed immediately (0 h post-thaw). **(b):** Lower percentages of dead cells were observed when CD34+ cells were frozen in hWJSC-CM thawed and analysed immediately (0 h post-thaw).**(c):** Higher percentages of live cells were observed when CD34+ cells were frozen in hWJSC-CM, thawed and grown in hWJSC-CM for 72 h (72 h post-thaw). **(d):** Lower percentages of dead cells were observed when CD34+ cells were frozen in hWJSC-CM, thawed and grown in hWJSC-CM for 72 h (72 h post-thaw). **(e):** Lower percentages of cells with fragmented DNA (sub G1 phase) were observed when CD34+ cells were frozen in hWJSC-CM, thawed and analysed immediately (0 h post-thaw); and **(f):** Lower percentages of cells with fragmented DNA (sub G1 phase) were observed when CD34+ cells were frozen in hWJSC-CM, thawed and grown in hWJSC-CM for 72 h (72 h post-thaw). Values are mean ± SEM of 3 different experiments. Asterisk (*): $p<0.05$.

6.4 Discussion

hWJSCs are mesenchymal stem cells (MSCs) that can be harvested painlessly in large numbers from discarded umbilical cords without ethical constraints and served as an attractive alternative to bone marrow MSCs for cell based therapies [3,4]. *In vivo*, MSCs served as a natural scaffold within the bone marrow for the expansion of HSCs. They are similar to a pharmacy that dispense molecules for the maturation and proliferation of CD34+ cells that eventually produced all the blood lineages in the general circulation. Such expansion of CD34+ cells is mediated via cell-to-cell attachment and migration into the niches of the MSC scaffold or via the molecules secreted by the MSCs. hWJSCs are of the same embryological origin as bone marrow MSCs [5], but they are different in terms of their nature, properties and concentrations of the unique bioactive molecules they release [259]. hWJSCs appear to provide the three dimensional architecture mimicking physiological conditions *ex vivo.* We reported in chapter 5 that HSCs multiply in large numbers *in vitro* when in the presence of hWJSCs or hWJSC-CM and postulated that such effects may be cell-to-cell contact mediated or via molecules such as interleukins, growth factors, glycosaminoglycans and growth adhesion factors released in high concentrations into hWJSC-CM [8]. The present study demonstrated that the members of these interleukin, interferon, GAGs and cell adhesion molecule families are secreted in high concentrations by hWJSCs and they singly or in combination may be the important players involved in enhanced CD34+ survival and proliferation. These same agents may be playing a role in the increased freeze-thaw survival and subsequent enhanced growth of CD34+ cells observed in this chapter. The cell adhesion molecules in particular may be helping to preserve the cell membrane integrity of the CD34+ cells during the freezing process while the growth factors and interleukins may enhance mitosis of the cells during the 72 h after freeze-thawing.

Studies aimed at improving the cryopreservation of HSCs are focused mainly in two areas (1) refinement of the freezing media and (2) improvement of the freezing and storage procedures [260]. DMSO at a concentration of 10% is the conventional cryoprotectant used for the freezing of HSCs in cord blood banks. However, clinically, DMSO has been known to be associated with significant side effects that include nausea, vomiting and abdominal cramps in addition to other systemic disturbances in patients receiving HSC transplantation. Therefore reducing the concentration of DMSO or buffering its effects is of vital importance in improved cryopreservation protocols for HSCs. Additionally, cryopreservation using the current conventional recipes of DMSO + freezing media results in a significant proportion of collected stem cells (20-30%) becoming non-viable due to early irreversible apoptosis [261]. Various additives were able to improve the post-thaw recovery of CD34+ cells. Low levels of trehalose and catalase were shown to reduce post-thaw apoptosis in murine HSCs [262]. Freezing solutions supplemented with membrane stabilisers such as taurine, ascorbic acid and α-tocopheryl acetate also showed improved post-thaw recovery [263]. These reports confirmed that supplements in the freezing medium can help to protect CD34+ cells from the cryoinjuries of freezing and thawing. The results of the present study using hWJSC-CM in the freezing medium showed greater post-thaw recovery of CD34+ cells as compared to the use of such additives. This improvement is perhaps due to a combined effect of the interleukins, GAGs, growth factors and cell adhesion molecules present in hWJSC-CM. It was reported that the addition of certain selected interleukins to cultures of CD34+ cells induced the expansion and differentiation of these cells [264]. Hyaluronic acid which is an important member of the GAGs family was shown to stimulate the growth of CD34+ selected UCB cells into specifically differentiated mature eosinophils. This process was modulated by the CD44 receptor on the progenitor

cell population [265]. Interleukin 11 stimulated the proliferation of human hematopoietic CD34+ and CD34+CD33-DR- cells and synergized with stem cell factor, interleukin-3, and granulocyte-macrophage colony-stimulating factor [266]. Cryopreservation results in a combination of physical and biological stresses that damages cells leading to post-thaw apoptosis [257]. CD34+ cells appear to be more vulnerable to cryoinjury compared to other somatic cells. Cryoinjury-induced apoptosis is one of the main reasons for the loss of viability after cryopreservation and such post-thaw loss of viability of CD34+ cells has been the major contributing factor that influences the cell numbers required for successful HSC engraftment [249-251]. Although the use of UCB-HSCs in transplantation therapy has become increasingly popular, its application has been confined to transplantation for children because of limited viable CD34+ cell numbers [267]. Previous cryopreservation studies which examined vehicle solution, serum and protein addition, cryoprotectant and freezing curve focused only on improving the physical parameters without taking into consideration how to prevent these biological stresses [268]. Studies from adherent stem cell populations such as bone marrow MSCs and hWJSCs postulated that by inhibiting the p160-Rho-associated coiled-coil kinase signaling pathway, post-thaw apoptosis could be prevented, hence improving cell recovery and survival [256]. However, the same inhibitor failed to exhibit a similar protective effect on non-adherent UCB CD34+ cells suggesting that cell death may be occurring via a different signaling pathway [247]. The exact mechanisms as to how hWJSC-CM influences freeze-thaw survival and expansion of CD34+ cells are still unclear. Preliminary results from detailed proteomic and microRNA studies on hWJSC and/or hWJSC-CM conducted previously suggested that there is a down regulation of miR-146 which in turn resulted in an increase in prostaglandin E2 (PGE_2) production (Unpublished data). Recently, there appeared to be increasing evidence

suggesting that PGE_2 is crucial for the regulation of hematopoiesis and HSC engraftment [269]. It was reported that both mouse and human HSCs express PGE_2 receptors and short term *ex-vivo* exposure to PGE_2 enhanced the expansion, homing and survival of HSCs [270]. Hence the presence of PGE_2 in the hWJSC-CM may have also prevented cryoinjury-induced apoptosis by increasing intracellular survivin levels.

hWJSCs and hWJSC-CM support the expansion of HSCs and hWJSC-CM also helped to enhance CD34+ thaw-survival viability and further cell proliferation after thawing, we proposed that cord blood banks derive and store hWJSCs at the same time as UCB collection. An autologous supply of the same patient's hWJSCs will be an ideal adjuvant that can not only be used for cell based therapies after differentiation into a desirable lineage but can also be useful for improved freezing and expansion *ex vivo*. An autologous source has the added advantage of being matched to the same patient avoiding any immunorejection problems. Additionally, since hWJSCs have been reported to be hypoimmunogenic [46], allogeneic sources from other donor umbilical cords could also be stored in cord blood banks as 'off-the-shelf' cells for the same purpose. Up to 4-5 x 10^6 live fresh hWJSCs could be obtained from 1 cm of umbilical cord and they are highly proliferative with short population doubling times [3,4]. As such, frozen hWJSCs could be thawed and confluent monolayers established very fast for stromal support as well as for preparation of 24 h hWJSC-CM. Storage of hWJSCs or hWJSC-CM could be easily carried out in the second chamber of a dual chamber blood bag (first chamber: UCB) and the freezing protocol with or without hWJSC-CM could be the same for the contents of both chambers. To meet this objective we also proposed that hWJSC lines and hWJSC-CM be developed under current good manufacturing practice (cGMP) conditions that will be safe for the patients.

Chapter 7: General Discussion

7.1 Hypotheses

Numerous independent reports have confirmed the hWJSCs paradoxical tumoricidal properties *in vitro* and *in vivo* on solid tumors of mammary adenocarcinoma, ovarian carcinoma, osteosarcoma, and cholangiocarcinoma and bladder carcinoma. hWJSCs could also provide the structural and physiological support for self renewal, expansion and homing of HSCs as reported by several authors. Furthermore, hWJSCs express and secrete high level of adhesion molecules, extracellular matrix components like glycosaminoglycans, osteopontin, MCP-1 and ICAM-1 which are inherent constituents of the hematopoietic stem cell niche that help to regulate the expansion and maintenance of HSCs. As such, this thesis hypothesized that hWJSCs and/or its extracts can be used to enhance the treatment of hematological malignancies and blood disorders. The approach to the hypothesis was to evaluate (1) the tumoricidal effect of hWJSCs or its extracts on malignant hematological malignancies and (2) to use hWJSCs or its extracts to enhance the numbers and freeze thaw survival of hematopoietic stem cells (HSC) (Fig. 36).

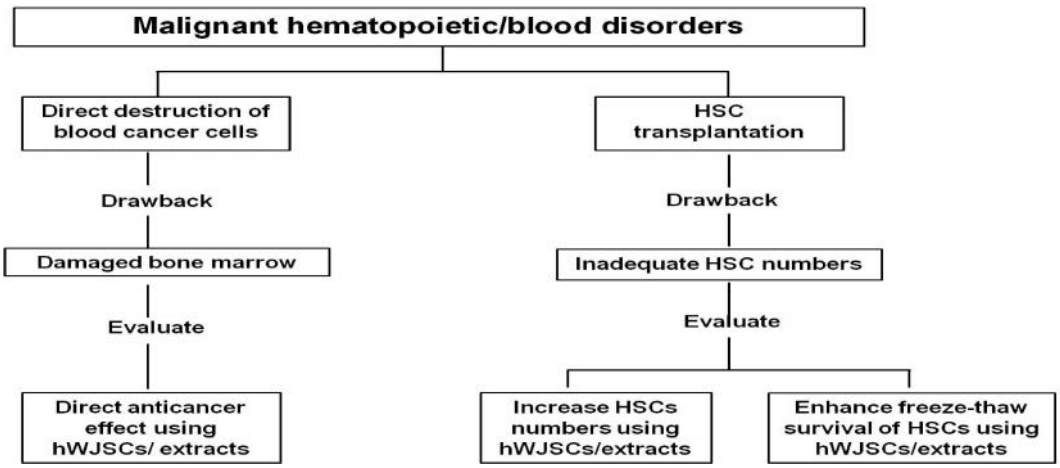

Figure 36 Approach to the hypothesis

hWJSCs or its extracts were evaluated for their anti-tumorigenic effect on hematological malignancies, enhancement of HSC numbers and freeze-thaw survival.

7.2 Findings, Implications and Limitations

7.2.1 Direct anti-cancer effects of hWJSCs and hWJSC-CM

The bone marrow microenvironment which is made up of mesenchymal stem cells (MSCs) and extracellular matrix (ECM) serves as an important hematopoietic niche which influences the abilities of hematopoietic stem cells (HSCs) or hematopoietic progenitor cells (HPCs) to home, engraft, self-renew and differentiate via direct cell-cell contact and secretion of hematopoietic growth factors. The use of aggressive chemotherapeutic agents or radiation-conditioning regimes prior to HSC transplantation often cause damage to the bone marrow microenvironment and have a profound influence on HSC engraftment kinetics and the outcome of patient treatment.

This thesis uses a primitive stromal cell from the Wharton's jelly compartment of the human umbilical cord with high expression of MSC CD markers and low level expression of human embryonic stem cell (hESC) markers. They are hypoimmunogenic, do not form tumor associated fibroblasts and do not induce tumorigenesis in laboratory animals, primates and humans. Moreover, there are numerous reports that have confirmed their tumoricidal properties both *in vitro* and *in vivo* on solid tumors. Likewise, results from this thesis have demonstrated for the first time that these hWJSCs have tumoricidal effects on non-solid hematopoietic malignant cells as well. The mechanism whereby the hWJSCs inhibit the growth of the lymphoma cells appeared to be via secretions from the hWJSCs because hWJSC-CM have inhibited lymphoma cell growth. Exposing lymphoma cells to a 3kDa molecular weight cut-off (MWCO) concentrate of hWJSC-CM induced the most cell death in the cancer cells compared to other molecular weight cut-offs. Further analysis suggested that the bioactive molecules were larger than 3kDa as lymphoma cell viability significant decreased

with the 3kDa hWJSC-CM concentrates fraction and not with the flow through (FT) fraction. The results also showed a mechanism of lymphoma cell death induced by hWJSC-CM via the oxidative stress pathway by alteration of antioxidant enzymes. Exposing lymphoma cells to 3kDa hWJSC-CM concentrates showed an increase in functional activity of H_2O_2-generating SOD enzymes and concomitant decrease in functional activity of all three H_2O_2-catabolic antioxidative enzymes (GPx, catalase and TPx). Significant increases in H_2O_2 levels in both lymphoma cell lines were also observed after treatment with the 3kDa MWCO concentrates. Though numerous studies previously have suggested that the high level of intracellular H_2O_2 induced cancer cell death, direct administration of H_2O_2 to cancer patients was never seen as an appropriate therapeutic strategy as both the safety and effectiveness were yet to be ascertained. The thesis suggested a method of inducing cancer cell death by increasing intracellular H_2O_2 using hWJSC-CM.

In addition, most chemotherapy or radiation treatment regimens administered to lymphoma patients often result in damage to the bone marrow, gastrointestinal tract, heart, brain and kidney. The non-specific inhibition of growth of normal cells by such regimens is an unwanted side effect. Previous studies also indicated that aggressive chemotherapeutic or radiation conditioning regimens prior to HSC transplantation often caused irreversible damage to the stromal cells in the hematopoietic microenvironment ultimately affecting HSC engraftment and reconstitution after transplantation. The control fibroblast and adult hBMMSCs in this thesis were minimally affected by hWJSCs, hWJSC-CM or 3kDa MWCO concentrates. Therefore the use of hWJSC-CM as a potential therapy for lymphoma patients may be a safe option in the future as the hematopoietic niche remains intact.

Lastly, the results in the thesis also indicated that all three molecular hallmarks for ICD namely ecto-CRT/Hsp90, extracellular ATP and HMGB1 were

significantly increased in all tested cancer cell lines exposed to 3kDa hWJSC-CM concentrates. Moreover, earlier studies reported that hWJSCs secrete large varieties of cytokines and factors like IL-6, IL-8, and MCP-1 that have been known to play a role in modulating the innate immune response. Treatment of mammary carcinoma xenograft rat model with rat WJSCs increased CD8+ T cell infiltration in the tumor tissue. This further strengthens the hypothesis that anti-tumorigenic treatment with hWJSCs or its conditioned medium could also mount an immunogenic cell death response. Recent growing evidence indicates that the patient's immune competence is crucial in determining efficacy of chemotherapeutic and radio-therapeutic treatments and the discoveries of chemotherapeutic and radiotherapeutic treatment strategies that induce immunogenic cell death in tumors have resulted in many long-term successful therapeutic options for tumor eradication. Therefore, the upregulation of molecular DAMPs seen in all cancer cell lines in this thesis shows that hWJSCs or hWJSC-CM could mount a dual anti-cancer attack in (1) directly killing cancer cells and (2) activating an immunogenic cancer cell death response which could unlock a sequence of events leading to development of anti-tumor immunity.

Though the thesis demonstrated the tumoricidal and immunogenic cell death potential of hWJSCs and hWJSC-CM, one of the limitations is that the specific active agents present in hWJSC-CM that are responsible for its tumoricidal effect or induction of immunogenic cell death were not extensively pursued in the thesis. Future studies will involve in the narrowing down and determining the specific molecules or targets in hWJSCs or hWJSC-CM that are involved. The possible anti-tumorigenic agents in the hWJSC-CM includes the proteins, miRNAs, mRNAs and microvesicles present. Untargeted metabolomics or proteomics using high performance liquid chromatography and mass spectrometry could be used to determine the moelcules and proteins within the 3kDa MWCO hWJSC-CM concentrates. Likewise, mRNA or miRNA-PCR array could be performed to

determine the miRNAs present in the 3kDa MWCO hWJSC-CM concentrates. Furthermore, microvesicles could also be isolated and used directly to analyze their anti-tumorigenic properties on lymphoma cells. With the results, the immunogenic tumoricidal effects of specific agents within the 3kDa MWCO hWJSC-CM concentrates or hWJSCs could be further evaluated by knocking down, blocking or neutralizing the mRNA, miRNA, proteins or microvesicles in order to narrow down the candidate active agents as future therapeutics. The tumoricidal effects of the candidate agents could first be evaluated in a primary patient-derived cancer cells *in vitro* system and subsequently evaluated in a humanized pre-clinical *in vivo* animal model.

7.2.2 Increasing hematopoietic stem cell number for transplantation

Bone marrow hematopoietic stem cell (HSC) transplantation has been used for the treatment of malignant and non-malignant hematopoietic diseases such as leukemia, lymphoma and thalassemia. HSCs from the human umbilical cord blood (UCB) have been successfully used for the treatment of hematopoietic diseases in children in autologous and allogeneic settings. UCB contains HSCs and hematopoietic progenitor cells (HPCs) that appear to have higher proliferation rates and immunological tolerance compared to those in bone marrow. However, one major challenge associated with the use of UCB-HSCs for transplantation is the relatively low cell numbers available. It has been reported that the HSC and HPC yields in UCB was adequate for the treatment of hematopoietic diseases in children and not adults as it is estimated that for successful engraftment, at least 2.5 x 10^6 CD34+ cells per kg of patient body weight is required. However, a good UCB harvest from a single umbilical cord generates a total of only about 10 x 10^6 CD34+ cells. Moreover, preexisting slow freezing protocols for HSCs are far from ideal as there is significant cell death

and loss of CD34+ cell populations after freeze-thaw. Cryoinjury-induced apoptosis has also been reported as one of the main reasons for the loss of viability after cryopreservation. Post-thaw apoptosis of CD34+ cells has also been shown to affect the recovery of viable CD34+ cells required for transplantation therapy. As such, the thesis evaluated the use hWJSCs or its extracts to increase the numbers of cord blood CD34+ cells by *ex vivo* expansion and improve their freeze thaw survival of hematopoietic stem cells

In this thesis, phase contrast images and SEM images showed that in the presence of hWJSCs or hWJSC-CM, the HSCs began to put out pseudopodia-like outgrowth to help them migrate towards the surface of the stromal hWJSCs niche, to attach and proliferate. In addition, secretions in the culture medium conditioned by hWJSCs over 24-72h had potent molecules supported the expansion of HSCs *ex vivo*. When UCB-HSCs were exposed to hWJSC conditioned medium (hWJSC-CM) they immediately became motile, put out pseudopodia-like projections and underwent proliferation. With increased culture time, there were more CD34+ cell numbers and colony forming units which eventually generated all the lineages of normal hematopoiesis. A proteomic analysis of the hWJSC-CM showed high concentrations of several families of important agents such as interleukins, growth factors, glycosaminoglycans and cell adhesion molecules to which the spontaneous activity and expansion of the HSCs were attributed. Moreover, adding hWJSC-CM in the freezing medium showed greater post-thaw recovery of CD34+ cells compared to the use of such additives.

The logistical limitations of using BM-MSCs from a family member of the patient as stromal support for ex vivo expansion of HSCs or improvement in HSCs freeze-thaw survival include (1) the appropriate family member not being available for donation and (2) the long time taken to not only generate sufficient

BM-MSCs but also to carry out co-culture expansion to provide sufficient HSCs since the disease progression was rapid in some leukemic patients. The availability of "off-the-shelf" GMP compliant allogeneic and hypoimmunogenic MSCs like hWJSCs for immediate use to alleviate this logistical problem are recommended. In addition, the thesis also demonstrated that autologous hWJSCs harvested from the same umbilical cord can also provide a useful source for stromal support for cord blood HSCs expansion. The feasibility to store autologous hWJSCs have immense benefits as it has also been demonstrated that the major histocompatibility complex (MHC) restriction existde between HSCs and stromal cells *in vitro* and *in vivo.* As the harvesting of hWJSCs only take a few hours, it is possible to freeze and store UCB-HSCs and hWJSCs from the same umbilical cord on the same day in a dual chamber blood collection bag. When the HSCs are needed, the hWJSCs could be thawed and used for HSCs expansion of HSCs if the number were inadequate. As such, the use of autologous hWJSCs cell source together with cord blood HSCs would help improve the HSC transplantation engraftment efficiencies, and therefore this thesis proposes to co-bank hWJSCs with their corresponding cord blood stem cells in the cord blood bank. This approach will avoid the need for discarding precious HSC samples that are low in numbers as is practiced by cord blood banks today.

However, one limitation to the thesis was that all evaluations of the expanded cord blood CD34+ cells were performed using *in vitro* assays and no evaluations were done using the *in vivo* HSCs repopulating mouse model. Therefore, it is still not known whether CD34+ cells expanded after autologous or allogeneic hWJSC stromal support or after enhancement in freeze-thaw protocol are adequate to bring about improvement in engraftment *in vivo*. As it is paramount to evaluate *in vivo* engraftment in the animal model to confirm the enhancement in CD34+ cells

HSCs repopulating capabilties using hWJSCs or hWJSC-CM, future studies need to be centered in proving the improved functional engrafment outcome of the cord blood CD34+ HSCs after hWJSCs co-culture or hWJSC-CM supplement in an *in vivo* animal model. The expanded CD34+ HSCs could be transplanted into sub-lethally irradiated NOD-SCID IL2Rg null mice via the tail vein and the positive positive engraftment of the human cells (at least 0.1% of CD45+ cells) in the bone marrow will be analysed twelve weeks after the transplantation. In addition, the presence of primitive and differentiated human HSCs markers like CD34, CD45, CD13, CD19 and CD3 in the mice bone marrow, spleen and peripheral blood could be evaluated .

7.3 Conclusion

The results from this thesis demonstrated that hWJSCs or hWJSC extracts (namely hWJSC-CM) can be derived from commonly discarded umbilical cord and used as a direct anti-tumorigenic agent on lymphoma cells or used as supplements in increasing cord blood HSCs numbers by *ex vivo* expansion or improving their freeze-thaw survival rates. However, further studies will include experiments to determinate the tumorigenic active agents within hWJSCs or hWJSC-CM, the evaluation of the anti-tumorigenic effect on patient-derived lymphoma cells and in an *in vivo* experimental model. Likewise, an *in vivo* experimental system is needed to evaluate the cord blood HSCs that have been expanded *ex vivo* using hWJSCs/hWJSC-CM or freeze in hWJSC-CM. Nevertheless, the findings in the thesis would encourage the storage of commonly discarded hWJSCs in public cord blood banks and these cells could subsequently be used to help improve the efficiency in the management of hematological malignancies and blood disorders clinically in the future.

Chapter 8: Bibliography

1 Bongso, A. & Fong, C. Y. The therapeutic potential, challenges and future clinical directions of stem cells from the Wharton's jelly of the human umbilical cord. *Stem cell reviews* **9**, 226-240, doi:10.1007/s12015-012-9418-z (2013).

2 McElreavey, K. D., Irvine, A. I., Ennis, K. T. & McLean, W. H. Isolation, culture and characterisation of fibroblast-like cells derived from the Wharton's jelly portion of human umbilical cord. *Biochemical Society transactions* **19**, 29S (1991).

3 Fong, C. Y., Richards, M., Manasi, N., Biswas, A. & Bongso, A. Comparative growth behaviour and characterization of stem cells from human Wharton's jelly. *Reproductive biomedicine online* **15**, 708-718 (2007).

4 Fong, C. Y. *et al.* Derivation efficiency, cell proliferation, freeze-thaw survival, stem-cell properties and differentiation of human Wharton's jelly stem cells. *Reproductive biomedicine online* **21**, 391-401, doi:10.1016/j.rbmo.2010.04.010 (2010).

5 Wang, X. Y. *et al.* Identification of mesenchymal stem cells in aorta-gonad-mesonephros and yolk sac of human embryos. *Blood* **111**, 2436-2443, doi:10.1182/blood-2007-07-099333 (2008).

6 Taghizadeh, R. R., Cetrulo, K. J. & Cetrulo, C. L. Wharton's Jelly stem cells: future clinical applications. *Placenta* **32 Suppl 4**, S311-315, doi:10.1016/j.placenta.2011.06.010 (2011).

7 Angelucci, S. *et al.* Proteome analysis of human Wharton's jelly cells during in vitro expansion. *Proteome science* **8**, 18, doi:10.1186/1477-5956-8-18 (2010).

8 Fong, C. Y. *et al.* Human umbilical cord Wharton's jelly stem cells and its conditioned medium support hematopoietic stem cell expansion ex vivo. *Journal of cellular biochemistry* **113**, 658-668, doi:10.1002/jcb.23395 (2012).

9 Gauthaman, K. *et al.* Human umbilical cord Wharton's jelly stem cell (hWJSC) extracts inhibit cancer cell growth in vitro. *Journal of cellular biochemistry* **113**, 2027-2039, doi:10.1002/jcb.24073 (2012).

10 Dominici, M. *et al.* Minimal criteria for defining multipotent mesenchymal stromal cells. The International Society for Cellular Therapy position statement. *Cytotherapy* **8**, 315-317, doi:10.1080/14653240600855905 (2006).

11 Wang, H. S. *et al.* Mesenchymal stem cells in the Wharton's jelly of the human umbilical cord. *Stem cells* **22**, 1330-1337, doi:10.1634/stemcells.2004-0013 (2004).

12 Troyer, D. L. & Weiss, M. L. Wharton's jelly-derived cells are a primitive stromal cell population. *Stem cells* **26**, 591-599, doi:10.1634/stemcells.2007-0439 (2008).

13 Gauthaman, K. *et al.* Osteogenic differentiation of human Wharton's jelly stem cells on nanofibrous substrates in vitro. *Tissue engineering. Part A* **17**, 71-81, doi:10.1089/ten.TEA.2010.0224 (2011).

14 Fong, C. Y. *et al.* Human umbilical cord Wharton's jelly stem cells undergo enhanced chondrogenic differentiation when grown on nanofibrous scaffolds and in a sequential two-stage culture medium environment. *Stem cell reviews* **8**, 195-209, doi:10.1007/s12015-011-9289-8 (2012).

15 Fong, C. Y. *et al.* Human Wharton's jelly stem cells have unique transcriptome profiles compared to human embryonic stem cells and other mesenchymal stem cells. *Stem cell reviews* **7**, 1-16, doi:10.1007/s12015-010-9166-x (2011).

16 Carlin, R., Davis, D., Weiss, M., Schultz, B. & Troyer, D. Expression of early transcription factors Oct-4, Sox-2 and Nanog by porcine umbilical cord (PUC) matrix cells. *Reproductive biology and endocrinology : RB&E* **4**, 8, doi:10.1186/1477-7827-4-8 (2006).

17 Nekanti, U. *et al.* Long-term expansion and pluripotent marker array analysis of Wharton's jelly-derived mesenchymal stem cells. *Stem cells and development* **19**, 117-130, doi:10.1089/scd.2009.0177 (2010).

18 Hoynowski, S. M. *et al.* Characterization and differentiation of equine umbilical cord-derived matrix cells. *Biochemical and biophysical research communications* **362**, 347-353, doi:10.1016/j.bbrc.2007.07.182 (2007).

19 Chao, Y. H. *et al.* Cotransplantation of umbilical cord MSCs to enhance engraftment of hematopoietic stem cells in patients with severe aplastic anemia. *Bone marrow transplantation* **46**, 1391-1392, doi:10.1038/bmt.2010.305 (2011).

20 Hu, J. *et al.* Long term effects of the implantation of Wharton's jelly-derived mesenchymal stem cells from the umbilical cord for newly-onset type 1 diabetes mellitus. *Endocrine journal* **60**, 347-357 (2013).

21 Dalous, J., Larghero, J. & Baud, O. Transplantation of umbilical cord-derived mesenchymal stem cells as a novel strategy to protect the central nervous system: technical aspects, preclinical studies, and clinical perspectives. *Pediatric research* **71**, 482-490, doi:10.1038/pr.2011.67 (2012).

22 Chen, H. *et al.* Human umbilical cord Wharton's jelly stem cells: immune property genes assay and effect of transplantation on the immune cells of heart failure patients. *Cellular immunology* **276**, 83-90, doi:10.1016/j.cellimm.2012.03.012 (2012).

23 Wu, K. H. *et al.* Cotransplantation of umbilical cord-derived mesenchymal stem cells promote hematopoietic engraftment in cord blood transplantation: a pilot study. *Transplantation* **95**, 773-777, doi:10.1097/TP.0b013e31827a93dd (2013).

24 Ma, L. *et al.* Immunosuppressive function of mesenchymal stem cells from human umbilical cord matrix in immune thrombocytopenia patients. *Thrombosis and haemostasis* **107**, 937-950, doi:10.1160/TH11-08-0596 (2012).

25 Wu, K. H. *et al.* Effective treatment of severe steroid-resistant acute graft-versus-host disease with umbilical cord-derived mesenchymal stem cells. *Transplantation* **91**, 1412-1416, doi:10.1097/TP.0b013e31821aba18 (2011).

26 Fan, C. G., Zhang, Q. J. & Zhou, J. R. Therapeutic potentials of mesenchymal stem cells derived from human umbilical cord. *Stem cell reviews* **7**, 195-207, doi:10.1007/s12015-010-9168-8 (2011).

27 Mitchell, K. E. *et al.* Matrix cells from Wharton's jelly form neurons and glia. *Stem cells* **21**, 50-60, doi:10.1634/stemcells.21-1-50 (2003).

28 Fu, Y. S. *et al.* Conversion of human umbilical cord mesenchymal stem cells in Wharton's jelly to dopaminergic neurons in vitro: potential therapeutic application for Parkinsonism. *Stem cells* **24**, 115-124, doi:10.1634/stemcells.2005-0053 (2006).

29 Matsuse, D. *et al.* Human umbilical cord-derived mesenchymal stromal cells differentiate into functional Schwann cells that sustain peripheral nerve regeneration. *Journal of neuropathology and experimental neurology* **69**, 973-985, doi:10.1097/NEN.0b013e3181eff6dc (2010).

30 Peng, J. *et al.* Human umbilical cord Wharton's jelly-derived mesenchymal stem cells differentiate into a Schwann-cell phenotype and promote neurite outgrowth in vitro. *Brain research bulletin* **84**, 235-243, doi:10.1016/j.brainresbull.2010.12.013 (2011).

31 Xu, Q. *et al.* In vitro and in vivo magnetic resonance tracking of Sinerem-labeled human umbilical mesenchymal stromal cell-derived Schwann cells. *Cellular and molecular neurobiology* **31**, 365-375, doi:10.1007/s10571-010-9628-3 (2011).

32 Weiss, M. L. *et al.* Human umbilical cord matrix stem cells: preliminary characterization and effect of transplantation in a rodent model of Parkinson's disease. *Stem cells* **24**, 781-792, doi:10.1634/stemcells.2005-0330 (2006).

33 Koh, S. H. *et al.* Implantation of human umbilical cord-derived mesenchymal stem cells as a neuroprotective therapy for ischemic stroke in rats. *Brain research* **1229**, 233-248, doi:10.1016/j.brainres.2008.06.087 (2008).

34 Ding, D. C. *et al.* Enhancement of neuroplasticity through upregulation of beta1-integrin in human umbilical cord-derived stromal cell implanted stroke model. *Neurobiology of disease* **27**, 339-353, doi:10.1016/j.nbd.2007.06.010 (2007).

35 Yang, C. C. *et al.* Transplantation of human umbilical mesenchymal stem cells from Wharton's jelly after complete transection of the rat spinal cord. *PloS one* **3**, e3336, doi:10.1371/journal.pone.0003336 (2008).

36 Dongmei, H. *et al.* Clinical analysis of the treatment of spinocerebellar ataxia and multiple system atrophy-cerebellar type with umbilical cord mesenchymal stromal cells. *Cytotherapy* **13**, 913-917, doi:10.3109/14653249.2011.579958 (2011).

37 Lv, Y. T. *et al.* Transplantation of human cord blood mononuclear cells and umbilical cord-derived mesenchymal stem cells in autism. *Journal of translational medicine* **11**, 196, doi:10.1186/1479-5876-11-196 (2013).

38 Chao, K. C., Chao, K. F., Fu, Y. S. & Liu, S. H. Islet-like clusters derived from mesenchymal stem cells in Wharton's Jelly of the human umbilical cord for transplantation to control type 1 diabetes. *PloS one* **3**, e1451, doi:10.1371/journal.pone.0001451 (2008).

39 Anzalone, R. *et al.* New emerging potentials for human Wharton's jelly mesenchymal stem cells: immunological features and hepatocyte-like differentiative capacity. *Stem cells and development* **19**, 423-438, doi:10.1089/scd.2009.0299 (2010).

40 Campard, D., Lysy, P. A., Najimi, M. & Sokal, E. M. Native umbilical cord matrix stem cells express hepatic markers and differentiate into hepatocyte-like cells. *Gastroenterology* **134**, 833-848, doi:10.1053/j.gastro.2007.12.024 (2008).

41 Zhang, Y. N., Lie, P. C. & Wei, X. Differentiation of mesenchymal stromal cells derived from umbilical cord Wharton's jelly into hepatocyte-like cells. *Cytotherapy* **11**, 548-558, doi:10.1080/14653240903051533 (2009).

42 Zhao, Q. *et al.* Differentiation of human umbilical cord mesenchymal stromal cells into low immunogenic hepatocyte-like cells. *Cytotherapy* **11**, 414-426, doi:10.1080/14653240902849754 (2009).

43 Tsai, P. C. *et al.* The therapeutic potential of human umbilical mesenchymal stem cells from Wharton's jelly in the treatment of rat liver fibrosis. *Liver transplantation : official publication of the American Association for the Study of Liver Diseases and the International Liver Transplantation Society* **15**, 484-495, doi:10.1002/lt.21715 (2009).

44 Shi, M. *et al.* Human mesenchymal stem cell transfusion is safe and improves liver function in acute-on-chronic liver failure patients. *Stem cells translational medicine* **1**, 725-731, doi:10.5966/sctm.2012-0034 (2012).

45 Zhang, Z. *et al.* Human umbilical cord mesenchymal stem cells improve liver function and ascites in decompensated liver cirrhosis patients. *Journal of gastroenterology and hepatology* **27 Suppl 2**, 112-120, doi:10.1111/j.1440-1746.2011.07024.x (2012).

46 Weiss, M. L. *et al.* Immune properties of human umbilical cord Wharton's jelly-derived cells. *Stem cells* **26**, 2865-2874, doi:10.1634/stemcells.2007-1028 (2008).

47 Prasanna, S. J., Gopalakrishnan, D., Shankar, S. R. & Vasandan, A. B. Pro-inflammatory cytokines, IFNgamma and TNFalpha, influence immune properties of human bone marrow and Wharton jelly mesenchymal stem cells differentially. *PloS one* **5**, e9016, doi:10.1371/journal.pone.0009016 (2010).

48 La Rocca, G. *et al.* Isolation and characterization of Oct-4+/HLA-G+ mesenchymal stem cells from human umbilical cord matrix: differentiation potential and detection of new markers. *Histochemistry and cell biology* **131**, 267-282, doi:10.1007/s00418-008-0519-3 (2009).

49 Tipnis, S., Viswanathan, C. & Majumdar, A. S. Immunosuppressive properties of human umbilical cord-derived mesenchymal stem cells: role of B7-H1 and IDO. *Immunology and cell biology* **88**, 795-806, doi:10.1038/icb.2010.47 (2010).

50 Kikuchi-Taura, A. *et al.* Human umbilical cord provides a significant source of unexpanded mesenchymal stromal cells. *Cytotherapy* **14**, 441-450, doi:10.3109/14653249.2012.658911 (2012).

51 Rachakatla, R. S., Marini, F., Weiss, M. L., Tamura, M. & Troyer, D. Development of human umbilical cord matrix stem cell-based gene therapy for experimental lung tumors. *Cancer gene therapy* **14**, 828-835, doi:10.1038/sj.cgt.7701077 (2007).

52 Ayuzawa, R. *et al.* Naive human umbilical cord matrix derived stem cells significantly attenuate growth of human breast cancer cells in vitro and in vivo. *Cancer letters* **280**, 31-37, doi:10.1016/j.canlet.2009.02.011 (2009).

53 Ganta, C. *et al.* Rat umbilical cord stem cells completely abolish rat mammary carcinomas with no evidence of metastasis or recurrence 100 days post-tumor cell inoculation. *Cancer research* **69**, 1815-1820, doi:10.1158/0008-5472.CAN-08-2750 (2009).

54 Matsuzuka, T. *et al.* Human umbilical cord matrix-derived stem cells expressing interferon-beta gene significantly attenuate bronchioloalveolar carcinoma xenografts in SCID mice. *Lung cancer* **70**, 28-36, doi:10.1016/j.lungcan.2010.01.003 (2010).

55 Maurya, D. K. *et al.* Therapy with un-engineered naive rat umbilical cord matrix stem cells markedly inhibits growth of murine lung adenocarcinoma. *BMC cancer* **10**, 590, doi:10.1186/1471-2407-10-590 (2010).

56 Chao, K. C., Yang, H. T. & Chen, M. W. Human umbilical cord mesenchymal stem cells suppress breast cancer tumourigenesis through direct cell-cell contact and internalization. *Journal of cellular and molecular medicine* **16**, 1803-1815, doi:10.1111/j.1582-4934.2011.01459.x (2012).

57 Gauthaman, K. *et al.* Human Wharton's jelly stem cell conditioned medium and cell-free lysate inhibit human osteosarcoma and mammary carcinoma cell growth in vitro and in xenograft mice. *Journal of cellular biochemistry* **114**, 366-377, doi:10.1002/jcb.24367 (2013).

58 Kawabata, A. *et al.* Naive rat umbilical cord matrix stem cells significantly attenuate mammary tumor growth through modulation of endogenous immune responses. *Cytotherapy* **15**, 586-597, doi:10.1016/j.jcyt.2013.01.006 (2013).

59 Liu, J., Han, G., Liu, H. & Qin, C. Suppression of cholangiocarcinoma cell growth by human umbilical cord mesenchymal stem cells: a possible role of Wnt and Akt signaling. *PloS one* **8**, e62844, doi:10.1371/journal.pone.0062844 (2013).

60 Ma, Y., Hao, X., Zhang, S. & Zhang, J. The in vitro and in vivo effects of human umbilical cord mesenchymal stem cells on the growth of breast cancer cells. *Breast cancer research and treatment* **133**, 473-485, doi:10.1007/s10549-011-1774-x (2012).

61 Wu, S., Ju, G. Q., Du, T., Zhu, Y. J. & Liu, G. H. Microvesicles derived from human umbilical cord Wharton's jelly mesenchymal stem cells attenuate bladder tumor cell growth in vitro and in vivo. *PloS one* **8**, e61366, doi:10.1371/journal.pone.0061366 (2013).

62 De Coppi, P. *et al.* Isolation of amniotic stem cell lines with potential for therapy. *Nature biotechnology* **25**, 100-106, doi:10.1038/nbt1274 (2007).

63 Bongso, A., Fong, C. Y., Ng, S. C. & Ratnam, S. Isolation and culture of inner cell mass cells from human blastocysts. *Human reproduction* **9**, 2110-2117 (1994).

64 Thomson, J. A. *et al.* Embryonic stem cell lines derived from human blastocysts. *Science* **282**, 1145-1147 (1998).

65 Bunnell, B. A., Flaat, M., Gagliardi, C., Patel, B. & Ripoll, C. Adipose-derived stem cells: isolation, expansion and differentiation. *Methods* **45**, 115-120, doi:10.1016/j.ymeth.2008.03.006 (2008).

66 Pittenger, M. F. *et al.* Multilineage potential of adult human mesenchymal stem cells. *Science* **284**, 143-147 (1999).

67 Walenda, T. *et al.* Co-culture with mesenchymal stromal cells increases proliferation and maintenance of haematopoietic progenitor cells. *Journal of cellular and molecular medicine* **14**, 337-350, doi:10.1111/j.1582-4934.2009.00776.x (2010).

68 Laurent, L. C. *et al.* Dynamic changes in the copy number of pluripotency and cell proliferation genes in human ESCs and iPSCs during reprogramming and time in culture. *Cell stem cell* **8**, 106-118, doi:10.1016/j.stem.2010.12.003 (2011).

69 Ben-David, U. & Benvenisty, N. The tumorigenicity of human embryonic and induced pluripotent stem cells. *Nature reviews. Cancer* **11**, 268-277, doi:10.1038/nrc3034 (2011).

70 Fong, C. Y., Gauthaman, K. & Bongso, A. Teratomas from pluripotent stem cells: A clinical hurdle. *Journal of cellular biochemistry* **111**, 769-781, doi:10.1002/jcb.22775 (2010).

71 Fujikawa, T. *et al.* Teratoma formation leads to failure of treatment for type I diabetes using embryonic stem cell-derived insulin-producing cells. *The American journal of pathology* **166**, 1781-1791, doi:10.1016/S0002-9440(10)62488-1 (2005).

72 Cao, F. *et al.* In vivo visualization of embryonic stem cell survival, proliferation, and migration after cardiac delivery. *Circulation* **113**, 1005-1014, doi:10.1161/CIRCULATIONAHA.105.588954 (2006).

73 Gauthaman, K. *et al.* Extra-embryonic human Wharton's jelly stem cells do not induce tumorigenesis, unlike human embryonic stem cells. *Reproductive biomedicine online* **24**, 235-246, doi:10.1016/j.rbmo.2011.10.007 (2012).

74 Wang, Y. *et al.* A toxicity study of multiple-administration human umbilical cord mesenchymal stem cells in cynomolgus monkeys. *Stem cells and development* **21**, 1401-1408, doi:10.1089/scd.2011.0441 (2012).

75 Houghton, J. *et al.* Gastric cancer originating from bone marrow-derived cells. *Science* **306**, 1568-1571, doi:10.1126/science.1099513 (2004).

76 Tolar, J. *et al.* Sarcoma derived from cultured mesenchymal stem cells. *Stem cells* **25**, 371-379, doi:10.1634/stemcells.2005-0620 (2007).

77 Amariglio, N. *et al.* Donor-derived brain tumor following neural stem cell transplantation in an ataxia telangiectasia patient. *PLoS medicine* **6**, e1000029, doi:10.1371/journal.pmed.1000029 (2009).

78 Zhu, W. *et al.* Mesenchymal stem cells derived from bone marrow favor tumor cell growth in vivo. *Experimental and molecular pathology* **80**, 267-274, doi:10.1016/j.yexmp.2005.07.004 (2006).

79 Yu, J. M., Jun, E. S., Bae, Y. C. & Jung, J. S. Mesenchymal stem cells derived from human adipose tissues favor tumor cell growth in vivo. *Stem cells and development* **17**, 463-473, doi:10.1089/scd.2007.0181 (2008).

80 Cardone, A., Tolino, A., Zarcone, R., Borruto Caracciolo, G. & Tartaglia, E. Prognostic value of desmoplastic reaction and lymphocytic infiltration in the management of breast cancer. *Panminerva medica* **39**, 174-177 (1997).

81 Bissell, M. J. & Radisky, D. Putting tumours in context. *Nature reviews. Cancer* **1**, 46-54, doi:10.1038/35094059 (2001).

82 Blankenstein, T. The role of tumor stroma in the interaction between tumor and immune system. *Current opinion in immunology* **17**, 180-186, doi:10.1016/j.coi.2005.01.008 (2005).

83 Mishra, P. J. *et al.* Carcinoma-associated fibroblast-like differentiation of human mesenchymal stem cells. *Cancer research* **68**, 4331-4339, doi:10.1158/0008-5472.CAN-08-0943 (2008).

84 Karnoub, A. E. *et al.* Mesenchymal stem cells within tumour stroma promote breast cancer metastasis. *Nature* **449**, 557-563, doi:10.1038/nature06188 (2007).

85 Spaeth, E. L. *et al.* Mesenchymal stem cell transition to tumor-associated fibroblasts contributes to fibrovascular network expansion and tumor progression. *PloS one* **4**, e4992, doi:10.1371/journal.pone.0004992 (2009).

86 Jodele, S. *et al.* The contribution of bone marrow-derived cells to the tumor vasculature in neuroblastoma is matrix metalloproteinase-9 dependent. *Cancer research* **65**, 3200-3208, doi:10.1158/0008-5472.CAN-04-3770 (2005).

87 Paunescu, V. *et al.* Tumour-associated fibroblasts and mesenchymal stem cells: more similarities than differences. *Journal of cellular and molecular medicine* **15**, 635-646, doi:10.1111/j.1582-4934.2010.01044.x (2011).

88 Subramanian, A. *et al.* Human umbilical cord Wharton's jelly mesenchymal stem cells do not transform to tumor-associated fibroblasts in the presence of breast and ovarian cancer cells unlike bone marrow mesenchymal stem cells. *Journal of cellular biochemistry* **113**, 1886-1895, doi:10.1002/jcb.24057 (2012).

89 Zhao, T., Zhang, Z. N., Rong, Z. & Xu, Y. Immunogenicity of induced pluripotent stem cells. *Nature* **474**, 212-215, doi:10.1038/nature10135 (2011).

90 Guha, P., Morgan, J. W., Mostoslavsky, G., Rodrigues, N. P. & Boyd, A. S. Lack of immune response to differentiated cells derived from syngeneic induced pluripotent stem cells. *Cell stem cell* **12**, 407-412, doi:10.1016/j.stem.2013.01.006 (2013).

91 Medicetty, S., Bledsoe, A. R., Fahrenholtz, C. B., Troyer, D. & Weiss, M. L. Transplantation of pig stem cells into rat brain: proliferation during the first 8 weeks. *Experimental neurology* **190**, 32-41, doi:10.1016/j.expneurol.2004.06.023 (2004).

92 Di Nicola, M. *et al.* Human bone marrow stromal cells suppress T-lymphocyte proliferation induced by cellular or nonspecific mitogenic stimuli. *Blood* **99**, 3838-3843 (2002).

93 Aggarwal, S. & Pittenger, M. F. Human mesenchymal stem cells modulate allogeneic immune cell responses. *Blood* **105**, 1815-1822, doi:10.1182/blood-2004-04-1559 (2005).

94 Najar, M. *et al.* Mesenchymal stromal cells promote or suppress the proliferation of T lymphocytes from cord blood and peripheral blood: the importance of low cell ratio and role of interleukin-6. *Cytotherapy* **11**, 570-583, doi:10.1080/14653240903079377 (2009).

95 Salama, H. *et al.* Autologous hematopoietic stem cell transplantation in 48 patients with end-stage chronic liver diseases. *Cell transplantation* **19**, 1475-1486, doi:10.3727/096368910X514314 (2010).

96 Krishnan, A. & Forman, S. J. Hematopoietic stem cell transplantation for AIDS-related malignancies. *Current opinion in oncology* **22**, 456-460, doi:10.1097/CCO.0b013e32833d2cf0 (2010).

97 Wengler, G. S. *et al.* In-utero transplantation of parental CD34 haematopoietic progenitor cells in a patient with X-linked severe combined immunodeficiency (SCIDXI). *Lancet* **348**, 1484-1487 (1996).

98 Flake, A. W. *et al.* Treatment of X-linked severe combined immunodeficiency by in utero transplantation of paternal bone marrow. *The New England journal of medicine* **335**, 1806-1810, doi:10.1056/NEJM199612123352404 (1996).

99 Becker, P. S. *et al.* Spontaneous splenic rupture following administration of granulocyte colony-stimulating factor (G-CSF): occurrence in an allogeneic donor of peripheral blood stem cells. *Biology of blood and marrow transplantation : journal of the American Society for Blood and Marrow Transplantation* **3**, 45-49 (1997).

100 Falzetti, F., Aversa, F., Minelli, O. & Tabilio, A. Spontaneous rupture of spleen during peripheral blood stem-cell mobilisation in a healthy donor. *Lancet* **353**, 555, doi:10.1016/S0140-6736(99)00268-8 (1999).

101 Nuamah, N. M., Goker, H., Kilic, Y. A., Dagmoura, H. & Cakmak, A. Spontaneous splenic rupture in a healthy allogeneic donor of peripheral-blood stem cell following the administration of granulocyte colony-stimulating factor (g-csf). A case report and review of the literature. *Haematologica* **91**, ECR08 (2006).

102 Adler, B. K. *et al.* Fatal sickle cell crisis after granulocyte colony-stimulating factor administration. *Blood* **97**, 3313-3314 (2001).

103 Gluckman, E. *et al.* Outcome of cord-blood transplantation from related and unrelated donors. Eurocord Transplant Group and the European Blood and Marrow Transplantation Group. *The New England journal of medicine* **337**, 373-381, doi:10.1056/NEJM199708073370602 (1997).

104 Gluckman, E. & Rocha, V. Cord blood transplantation: state of the art. *Haematologica* **94**, 451-454, doi:10.3324/haematol.2009.005694 (2009).

105 Broxmeyer, H. E. Insights into the biology of cord blood stem/progenitor cells. *Cell proliferation* **44 Suppl 1**, 55-59, doi:10.1111/j.1365-2184.2010.00728.x (2011).

106 Rocha, V. & Broxmeyer, H. E. New approaches for improving engraftment after cord blood transplantation. *Biology of blood and marrow transplantation : journal of the American Society for Blood and Marrow Transplantation* **16**, S126-132, doi:10.1016/j.bbmt.2009.11.001 (2010).

107 Ramirez, P., Brunstein, C. G., Miller, B., Defor, T. & Weisdorf, D. Delayed platelet recovery after allogeneic transplantation: a predictor of increased treatment-related mortality and poorer survival. *Bone marrow transplantation* **46**, 981-986, doi:10.1038/bmt.2010.218 (2011).

108 Solh, M., Brunstein, C., Morgan, S. & Weisdorf, D. Platelet and red blood cell utilization and transfusion independence in umbilical cord blood and allogeneic peripheral blood hematopoietic cell transplants. *Biology of blood and marrow transplantation : journal of the American Society for Blood and Marrow Transplantation* **17**, 710-716, doi:10.1016/j.bbmt.2010.08.017 (2011).

109 Zhang, Y., Chai, C., Jiang, X. S., Teoh, S. H. & Leong, K. W. Co-culture of umbilical cord blood CD34+ cells with human mesenchymal stem cells. *Tissue engineering* **12**, 2161-2170, doi:10.1089/ten.2006.12.2161 (2006).

110 Bakhshi, T. *et al.* Mesenchymal stem cells from the Wharton's jelly of umbilical cord segments provide stromal support for the maintenance of cord blood hematopoietic stem cells during long-term ex vivo culture. *Transfusion* **48**, 2638-2644, doi:10.1111/j.1537-2995.2008.01926.x (2008).

111 Lu, L. L. *et al.* Isolation and characterization of human umbilical cord mesenchymal stem cells with hematopoiesis-supportive function and other potentials. *Haematologica* **91**, 1017-1026 (2006).

112 Friedman, R. *et al.* Umbilical cord mesenchymal stem cells: adjuvants for human cell transplantation. *Biology of blood and marrow transplantation : journal of the American Society for Blood and Marrow Transplantation* **13**, 1477-1486, doi:10.1016/j.bbmt.2007.08.048 (2007).

113 Koc, O. N. *et al.* Rapid hematopoietic recovery after coinfusion of autologous-blood stem cells and culture-expanded marrow mesenchymal stem cells in advanced breast cancer patients receiving high-dose chemotherapy. *Journal of clinical oncology : official journal of the American Society of Clinical Oncology* **18**, 307-316 (2000).

114 Noort, W. A. *et al.* Mesenchymal stem cells promote engraftment of human umbilical cord blood-derived CD34(+) cells in NOD/SCID mice. *Experimental hematology* **30**, 870-878 (2002).

115 Angelopoulou, M. *et al.* Cotransplantation of human mesenchymal stem cells enhances human myelopoiesis and megakaryocytopoiesis in NOD/SCID mice. *Experimental hematology* **31**, 413-420 (2003).

116 Lazarus, H. M. *et al.* Cotransplantation of HLA-identical sibling culture-expanded mesenchymal stem cells and hematopoietic stem cells in hematologic malignancy patients. *Biology of blood and marrow transplantation : journal of the American Society for Blood and Marrow Transplantation* **11**, 389-398, doi:10.1016/j.bbmt.2005.02.001 (2005).

117 Le Blanc, K. *et al.* Transplantation of mesenchymal stem cells to enhance engraftment of hematopoietic stem cells. *Leukemia* **21**, 1733-1738, doi:10.1038/sj.leu.2404777 (2007).

118 Baron, F. *et al.* Cotransplantation of mesenchymal stem cells might prevent death from graft-versus-host disease (GVHD) without abrogating graft-versus-tumor effects after HLA-mismatched allogeneic transplantation following nonmyeloablative conditioning. *Biology of blood and marrow transplantation : journal of the American Society for Blood and Marrow Transplantation* **16**, 838-847, doi:10.1016/j.bbmt.2010.01.011 (2010).

119 Carrancio, S. *et al.* Bone marrow mesenchymal stem cells for improving hematopoietic function: an in vitro and in vivo model. Part 2: Effect on bone marrow microenvironment. *PloS one* **6**, e26241, doi:10.1371/journal.pone.0026241 (2011).

120 Bartsch, K. *et al.* Mesenchymal stem cells remain host-derived independent of the source of the stem-cell graft and conditioning regimen used. *Transplantation* **87**, 217-221, doi:10.1097/TP.0b013e3181938998 (2009).

121 Muguruma, Y. *et al.* Reconstitution of the functional human hematopoietic microenvironment derived from human mesenchymal stem cells in the murine bone marrow compartment. *Blood* **107**, 1878-1887, doi:10.1182/blood-2005-06-2211 (2006).

122 Karp, J. M. & Leng Teo, G. S. Mesenchymal stem cell homing: the devil is in the details. *Cell stem cell* **4**, 206-216, doi:10.1016/j.stem.2009.02.001 (2009).

123 Villaron, E. M. *et al.* Mesenchymal stem cells are present in peripheral blood and can engraft after allogeneic hematopoietic stem cell transplantation. *Haematologica* **89**, 1421-1427 (2004).

124 Horvat-Karajz, K. *et al.* In vitro effect of carboplatin, cytarabine, paclitaxel, vincristine, and low-power laser irradiation on murine mesenchymal stem cells. *Lasers in surgery and medicine* **41**, 463-469, doi:10.1002/lsm.20791 (2009).

125 Spyridonidis, A. *et al.* Reduced intensity conditioning compared to standard conditioning preserves the in vitro growth capacity of bone marrow stroma, which remains of host origin. *Stem cells and development* **14**, 213-222, doi:10.1089/scd.2005.14.213 (2005).

126 Kemp, K. *et al.* Chemotherapy-induced mesenchymal stem cell damage in patients with hematological malignancy. *Annals of hematology* **89**, 701-713, doi:10.1007/s00277-009-0896-2 (2010).

127 Liu, Y. *et al.* Reconstruction of hematopoietic inductive microenvironment after transplantation of VCAM-1-modified human umbilical cord blood stromal cells. *PloS one* **7**, e31741, doi:10.1371/journal.pone.0031741 (2012).

128 Di, G. H. *et al.* Human umbilical cord mesenchymal stromal cells mitigate chemotherapy-associated tissue injury in a pre-clinical mouse model. *Cytotherapy* **14**, 412-422, doi:10.3109/14653249.2011.646044 (2012).

129 Wu, K. H. *et al.* Human Application of Ex-Vivo Expanded Umbilical Cord-Derived Mesenchymal Stem Cells: Enhance Hematopoiesis after Cord Blood Transplantation. *Cell transplantation*, doi:10.3727/096368913X663523 (2013).

130 O'Flaherty, E., Sparrow, R. & Szer, J. Bone marrow stromal function from patients after bone marrow transplantation. *Bone marrow transplantation* **15**, 207-212 (1995).

131 Guest, I. & Uetrecht, J. Drugs toxic to the bone marrow that target the stromal cells. *Immunopharmacology* **46**, 103-112 (2000).

132 Tauchmanova, L. *et al.* High prevalence of endocrine dysfunction in long-term survivors after allogeneic bone marrow transplantation for hematologic diseases. *Cancer* **95**, 1076-1084, doi:10.1002/cncr.10773 (2002).

133 Tauchmanova, L. *et al.* Long-lasting bone damage detected by dual-energy x-ray absorptiometry, phalangeal osteosonogrammetry, and in vitro growth of marrow stromal cells after allogeneic stem cell transplantation. *The Journal of clinical endocrinology and metabolism* **87**, 5058-5065 (2002).

134 Lo Celso, C., Wu, J. W. & Lin, C. P. In vivo imaging of hematopoietic stem cells and their microenvironment. *Journal of biophotonics* **2**, 619-631, doi:10.1002/jbio.200910072 (2009).

135 Gillette, J. M. & Lippincott-Schwartz, J. Hematopoietic progenitor cells regulate their niche microenvironment through a novel mechanism of cell-cell communication. *Communicative & integrative biology* **2**, 305-307 (2009).

136 Rubinstein, P. *et al.* Outcomes among 562 recipients of placental-blood transplants from unrelated donors. *The New England journal of medicine* **339**, 1565-1577, doi:10.1056/NEJM199811263392201 (1998).

137 Laughlin, M. J. *et al.* Hematopoietic engraftment and survival in adult recipients of umbilical-cord blood from unrelated donors. *The New England journal of medicine* **344**, 1815-1822, doi:10.1056/NEJM200106143442402 (2001).

138 Fritz, V. & Jorgensen, C. Mesenchymal stem cells: an emerging tool for cancer targeting and therapy. *Current stem cell research & therapy* **3**, 32-42 (2008).

139 Prockop, D. J. Repair of tissues by adult stem/progenitor cells (MSCs): controversies, myths, and changing paradigms. *Molecular therapy : the journal of the American Society of Gene Therapy* **17**, 939-946, doi:10.1038/mt.2009.62 (2009).

140 Wong, R. S. Mesenchymal stem cells: angels or demons? *Journal of biomedicine & biotechnology* **2011**, 459510, doi:10.1155/2011/459510 (2011).

141 Maestroni, G. J., Hertens, E. & Galli, P. Factor(s) from nonmacrophage bone marrow stromal cells inhibit Lewis lung carcinoma and B16 melanoma growth in mice. *Cellular and molecular life sciences : CMLS* **55**, 663-667 (1999).

142 Ohlsson, L. B., Varas, L., Kjellman, C., Edvardsen, K. & Lindvall, M. Mesenchymal progenitor cell-mediated inhibition of tumor growth in vivo and in vitro in gelatin matrix. *Experimental and molecular pathology* **75**, 248-255 (2003).

143 Khakoo, A. Y. *et al.* Human mesenchymal stem cells exert potent antitumorigenic effects in a model of Kaposi's sarcoma. *The Journal of experimental medicine* **203**, 1235-1247, doi:10.1084/jem.20051921 (2006).

144 Zhang, T. *et al.* Bone marrow-derived mesenchymal stem cells promote growth and angiogenesis of breast and prostate tumors. *Stem cell research & therapy* **4**, 70, doi:10.1186/scrt221 (2013).

145 Secchiero, P. *et al.* Human bone marrow mesenchymal stem cells display anti-cancer activity in SCID mice bearing disseminated non-Hodgkin's lymphoma xenografts. *PloS one* **5**, e11140, doi:10.1371/journal.pone.0011140 (2010).

146 Fonseka, M., Ramasamy, R., Yip, W. K., Tan, B. C. & Seow, H. F. Human Umbilical Cord Blood-Derived Mesenchymal Stem Cells (hUCB-MSC) Inhibits the Proliferation of K562 (Human Erythromyeloblastoid Leukemic Cell Line). *Cell biology international*, doi:10.1042/CBI20110595 (2012).

147 Yang, H. T. & Chao, K. C. Foetal defence against cancer: a hypothesis. *Journal of cellular and molecular medicine* **17**, 1096-1098, doi:10.1111/jcmm.12095 (2013).

148 Alexander, A. *et al.* Metastatic melanoma in pregnancy: risk of transplacental metastases in the infant. *Journal of clinical oncology : official journal of the American Society of Clinical Oncology* **21**, 2179-2186, doi:10.1200/JCO.2003.12.149 (2003).

149 Dildy, G. A., 3rd, Moise, K. J., Jr., Carpenter, R. J., Jr. & Klima, T. Maternal malignancy metastatic to the products of conception: a review. *Obstetrical & gynecological survey* **44**, 535-540 (1989).

150 Jackisch, C. *et al.* Lung cancer during pregnancy involving the products of conception and a review of the literature. *Archives of gynecology and obstetrics* **268**, 69-77, doi:10.1007/s00404-002-0356-x (2003).

151 Liu, J. & Guo, L. Intraplacental choriocarcinoma in a term placenta with both maternal and infantile metastases: a case report and review of the literature. *Gynecologic oncology* **103**, 1147-1151, doi:10.1016/j.ygyno.2006.08.007 (2006).

152 Potter, J. F. & Schoeneman, M. Metastasis of maternal cancer to the placenta and fetus. *Cancer* **25**, 380-388 (1970).

153 Henry, F., Bretaudeau, L., Barbieux, I., Meflah, K. & Gregoire, M. Induction of antigen presentation by macrophages after phagocytosis of tumour apoptotic cells. *Research in immunology* **149**, 673-679 (1998).

154 Barker, R. N. *et al.* Antigen presentation by macrophages is enhanced by the uptake of necrotic, but not apoptotic, cells. *Clinical and experimental immunology* **127**, 220-225 (2002).

155 Takemura, G. & Fujiwara, H. Doxorubicin-induced cardiomyopathy from the cardiotoxic mechanisms to management. *Progress in cardiovascular diseases* **49**, 330-352, doi:10.1016/j.pcad.2006.10.002 (2007).

156 Takimoto, C. H. *et al.* Severe neurotoxicity following 5-fluorouracil-based chemotherapy in a patient with dihydropyrimidine dehydrogenase deficiency. *Clinical cancer research : an official journal of the American Association for Cancer Research* **2**, 477-481 (1996).

157 Vogelzang, N. J. Nephrotoxicity from chemotherapy: prevention and management. *Oncology* **5**, 97-102, 105; disc 105, 109-111 (1991).

158 Chamberlin, W., Barone, J., Kedo, A. & Fried, W. Lack of recovery of murine hematopoietic stromal cells after irradiation-induced damage. *Blood* **44**, 385-392 (1974).

159 Galotto, M. *et al.* Stromal damage as consequence of high-dose chemo/radiotherapy in bone marrow transplant recipients. *Experimental hematology* **27**, 1460-1466 (1999).

160 Gibson, L. F. *et al.* Disruption of bone marrow stromal cell function by etoposide. *Biology of blood and marrow transplantation : journal of the American Society for Blood and Marrow Transplantation* **3**, 122-132 (1997).

161 Wolf, N. S. Dissecting the hematopoietic microenvironment. V: limitations of repair following damage to the hematopoietic support stroma. *Experimental hematology* **10**, 108-118 (1982).

162 Lee, S. H. *et al.* Co-transplantation of third-party umbilical cord blood-derived MSCs promotes engraftment in children undergoing unrelated umbilical cord blood transplantation. *Bone marrow transplantation* **48**, 1040-1045, doi:10.1038/bmt.2013.7 (2013).

163 Lopez-Lazaro, M. Dual role of hydrogen peroxide in cancer: possible relevance to cancer chemoprevention and therapy. *Cancer letters* **252**, 1-8, doi:10.1016/j.canlet.2006.10.029 (2007).

164 Davicino, R., Manuele, M. G., Turner, S., Ferraro, G. & Anesini, C. Antiproliferative activity of Larrea divaricata Cav. on lymphoma cell line: participation of hydrogen peroxide in its action. *Cancer investigation* **28**, 13-22, doi:10.3109/07357900902849665 (2010).

165 Polytarchou, C., Hatziapostolou, M. & Papadimitriou, E. Hydrogen peroxide stimulates proliferation and migration of human prostate cancer cells through activation of activator protein-1 and up-regulation of the heparin affin regulatory peptide gene. *The Journal of biological chemistry* **280**, 40428-40435, doi:10.1074/jbc.M505120200 (2005).

166 Park, S., You, X. & Imlay, J. A. Substantial DNA damage from submicromolar intracellular hydrogen peroxide detected in Hpx- mutants of Escherichia coli. *Proceedings of the National Academy of Sciences of the United States of America* **102**, 9317-9322, doi:10.1073/pnas.0502051102 (2005).

167 Hunt, C. R. *et al.* Genomic instability and catalase gene amplification induced by chronic exposure to oxidative stress. *Cancer research* **58**, 3986-3992 (1998).

168 del Bello, B., Paolicchi, A., Comporti, M., Pompella, A. & Maellaro, E. Hydrogen peroxide produced during gamma-glutamyl transpeptidase activity is involved in prevention of apoptosis and maintainance of proliferation in U937 cells. *FASEB journal : official publication of the Federation of American Societies for Experimental Biology* **13**, 69-79 (1999).

169 Qian, Y. *et al.* Hydrogen peroxide formation and actin filament reorganization by Cdc42 are essential for ethanol-induced in vitro angiogenesis. *The Journal of biological chemistry* **278**, 16189-16197, doi:10.1074/jbc.M207517200 (2003).

170 Ahmad, K. A., Iskandar, K. B., Hirpara, J. L., Clement, M. V. & Pervaiz, S. Hydrogen peroxide-mediated cytosolic acidification is a signal for mitochondrial translocation of Bax during drug-induced apoptosis of tumor cells. *Cancer research* **64**, 7867-7878, doi:10.1158/0008-5472.CAN-04-0648 (2004).

171 Hirpara, J. L., Clement, M. V. & Pervaiz, S. Intracellular acidification triggered by mitochondrial-derived hydrogen peroxide is an effector mechanism for drug-induced apoptosis in tumor cells. *The Journal of biological chemistry* **276**, 514-521, doi:10.1074/jbc.M004687200 (2001).

172 Lin, H. D., Fong, C. Y., Biswas, A., Choolani, M. & Bongso, A. Human Wharton's Jelly Stem Cells, its Conditioned Medium and Cell-Free Lysate Inhibit the Growth of Human Lymphoma Cells. *Stem cell reviews*, doi:10.1007/s12015-014-9514-3 (2014).

173 Oberley, L. W. Anticancer therapy by overexpression of superoxide dismutase. *Antioxidants & redox signaling* **3**, 461-472, doi:10.1089/15230860152409095 (2001).

174 Bakan, N. *et al.* Glutathione peroxidase, glutathione reductase, Cu-Zn superoxide dismutase activities, glutathione, nitric oxide, and malondialdehyde concentrations in serum of patients with chronic lymphocytic leukemia. *Clinica chimica acta; international journal of clinical chemistry* **338**, 143-149 (2003).

175 Bewick, M., Coutie, W. & Tudhope, G. R. Superoxide dismutase, glutathione peroxidase and catalase in the red cells of patients with malignant lymphoma. *British journal of haematology* **65**, 347-350 (1987).

176 Jaramillo, M. C., Frye, J. B., Crapo, J. D., Briehl, M. M. & Tome, M. E. Increased manganese superoxide dismutase expression or treatment with manganese porphyrin potentiates dexamethasone-induced apoptosis in lymphoma cells. *Cancer research* **69**, 5450-5457, doi:10.1158/0008-5472.CAN-08-4031 (2009).

177 Rodriguez, A. M., Carrico, P. M., Mazurkiewicz, J. E. & Melendez, J. A. Mitochondrial or cytosolic catalase reverses the MnSOD-dependent inhibition of proliferation by enhancing respiratory chain activity, net ATP production, and decreasing the steady state levels of H(2)O(2). *Free radical biology & medicine* **29**, 801-813 (2000).

178 Li, S., Yan, T., Yang, J. Q., Oberley, T. D. & Oberley, L. W. The role of cellular glutathione peroxidase redox regulation in the suppression of tumor cell growth by manganese superoxide dismutase. *Cancer research* **60**, 3927-3939 (2000).

179 Jeffree, G. M. Hydrogen peroxide and cancer. *Nature* **182**, 892 (1958).

180 Nathan, C. F. & Cohn, Z. A. Antitumor effects of hydrogen peroxide in vivo. *The Journal of experimental medicine* **154**, 1539-1553 (1981).

181 Questionable methods of cancer management: hydrogen peroxide and other 'hyperoxygenation' therapies. *CA: a cancer journal for clinicians* **43**, 47-56 (1993).

182 Chen, Q. *et al.* Pharmacologic ascorbic acid concentrations selectively kill cancer cells: action as a pro-drug to deliver hydrogen peroxide to tissues. *Proceedings of the National Academy of Sciences of the United States of America* **102**, 13604-13609, doi:10.1073/pnas.0506390102 (2005).

183 Padayatty, S. J. *et al.* Intravenously administered vitamin C as cancer therapy: three cases. *CMAJ : Canadian Medical Association journal = journal de l'Association medicale canadienne* **174**, 937-942, doi:10.1503/cmaj.050346 (2006).

184 Tome, M. E., Jaramillo, M. C. & Briehl, M. M. Hydrogen peroxide signaling is required for glucocorticoid-induced apoptosis in lymphoma cells. *Free radical biology & medicine* **51**, 2048-2059, doi:10.1016/j.freeradbiomed.2011.09.002 (2011).

185 Poh, T. W. & Pervaiz, S. LY294002 and LY303511 sensitize tumor cells to drug-induced apoptosis via intracellular hydrogen peroxide production independent of the phosphoinositide 3-kinase-Akt pathway. *Cancer research* **65**, 6264-6274, doi:10.1158/0008-5472.CAN-05-0152 (2005).

186 MacMillan-Crow, L. A. & Crow, J. P. Does more MnSOD mean more hydrogen peroxide? *Anti-cancer agents in medicinal chemistry* **11**, 178-180 (2011).

187 Bracci, L., Schiavoni, G., Sistigu, A. & Belardelli, F. Immune-based mechanisms of cytotoxic chemotherapy: implications for the design of novel and rationale-based combined treatments against cancer. *Cell death and differentiation* **21**, 15-25, doi:10.1038/cdd.2013.67 (2014).

188 Inoue, H. & Tani, K. Multimodal immunogenic cancer cell death as a consequence of anticancer cytotoxic treatments. *Cell death and differentiation* **21**, 39-49, doi:10.1038/cdd.2013.84 (2014).

189 Martins, I. *et al.* Molecular mechanisms of ATP secretion during immunogenic cell death. *Cell death and differentiation* **21**, 79-91, doi:10.1038/cdd.2013.75 (2014).

190 Garg, A. D., Martin, S., Golab, J. & Agostinis, P. Danger signalling during cancer cell death: origins, plasticity and regulation. *Cell death and differentiation* **21**, 26-38, doi:10.1038/cdd.2013.48 (2014).

191 Apetoh, L. *et al.* Toll-like receptor 4-dependent contribution of the immune system to anticancer chemotherapy and radiotherapy. *Nature medicine* **13**, 1050-1059, doi:10.1038/nm1622 (2007).

192 Fukunaga, A. *et al.* CD8+ tumor-infiltrating lymphocytes together with CD4+ tumor-infiltrating lymphocytes and dendritic cells improve the prognosis of patients with pancreatic adenocarcinoma. *Pancreas* **28**, e26-31 (2004).

193 Zhang, L. *et al.* Intratumoral T cells, recurrence, and survival in epithelial ovarian cancer. *The New England journal of medicine* **348**, 203-213, doi:10.1056/NEJMoa020177 (2003).

194 Sato, E. *et al.* Intraepithelial CD8+ tumor-infiltrating lymphocytes and a high CD8+/regulatory T cell ratio are associated with favorable prognosis in ovarian cancer. *Proceedings of the National Academy of Sciences of the United States of America* **102**, 18538-18543, doi:10.1073/pnas.0509182102 (2005).

195 Tomsova, M., Melichar, B., Sedlakova, I. & Steiner, I. Prognostic significance of CD3+ tumor-infiltrating lymphocytes in ovarian carcinoma. *Gynecologic oncology* **108**, 415-420, doi:10.1016/j.ygyno.2007.10.016 (2008).

196 Kono, K., Mimura, K. & Kiessling, R. Immunogenic tumor cell death induced by chemoradiotherapy: molecular mechanisms and a clinical translation. *Cell death & disease* **4**, e688, doi:10.1038/cddis.2013.207 (2013).

197 Igney, F. H. & Krammer, P. H. Death and anti-death: tumour resistance to apoptosis. *Nature reviews. Cancer* **2**, 277-288, doi:10.1038/nrc776 (2002).

198 Thompson, C. B. Apoptosis in the pathogenesis and treatment of disease. *Science* **267**, 1456-1462 (1995).

199 Kroemer, G., Galluzzi, L., Kepp, O. & Zitvogel, L. Immunogenic cell death in cancer therapy. *Annual review of immunology* **31**, 51-72, doi:10.1146/annurev-immunol-032712-100008 (2013).

200 Obeid, M. *et al.* Calreticulin exposure dictates the immunogenicity of cancer cell death. *Nature medicine* **13**, 54-61, doi:10.1038/nm1523 (2007).

201 Tesniere, A. *et al.* Immunogenic death of colon cancer cells treated with oxaliplatin. *Oncogene* **29**, 482-491, doi:10.1038/onc.2009.356 (2010).

202 Zitvogel, L. *et al.* Immunogenic tumor cell death for optimal anticancer therapy: the calreticulin exposure pathway. *Clinical cancer research : an official journal of the American Association for Cancer Research* **16**, 3100-3104, doi:10.1158/1078-0432.CCR-09-2891 (2010).

203 Sukkurwala, A. Q. *et al.* Immunogenic calreticulin exposure occurs through a phylogenetically conserved stress pathway involving the chemokine CXCL8. *Cell death and differentiation* **21**, 59-68, doi:10.1038/cdd.2013.73 (2014).

204 Zappasodi, R. *et al.* Improved clinical outcome in indolent B-cell lymphoma patients vaccinated with autologous tumor cells experiencing immunogenic death. *Cancer research* **70**, 9062-9072, doi:10.1158/0008-5472.CAN-10-1825 (2010).

205 Chao, M. P. *et al.* Calreticulin is the dominant pro-phagocytic signal on multiple human cancers and is counterbalanced by CD47. *Science translational medicine* **2**, 63ra94, doi:10.1126/scitranslmed.3001375 (2010).

206 Fucikova, J. *et al.* Human tumor cells killed by anthracyclines induce a tumor-specific immune response. *Cancer research* **71**, 4821-4833, doi:10.1158/0008-5472.CAN-11-0950 (2011).

207 Spisek, R. *et al.* Bortezomib enhances dendritic cell (DC)-mediated induction of immunity to human myeloma via exposure of cell surface heat shock protein 90 on dying tumor cells: therapeutic implications. *Blood* **109**, 4839-4845, doi:10.1182/blood-2006-10-054221 (2007).

208 Spisek, R. & Dhodapkar, M. V. Towards a better way to die with chemotherapy: role of heat shock protein exposure on dying tumor cells. *Cell cycle* **6**, 1962-1965 (2007).

209 Buttiglieri, S., Galetto, A., Forno, S., De Andrea, M. & Matera, L. Influence of drug-induced apoptotic death on processing and presentation of tumor antigens by dendritic cells. *International journal of cancer. Journal international du cancer* **106**, 516-520, doi:10.1002/ijc.11243 (2003).

210 Galetto, A. *et al.* Drug- and cell-mediated antitumor cytotoxicities modulate cross-presentation of tumor antigens by myeloid dendritic cells. *Anti-cancer drugs* **14**, 833-843, doi:10.1097/01.cad.0000097711.69687.64 (2003).

211 Ma, Y. *et al.* Anticancer chemotherapy-induced intratumoral recruitment and differentiation of antigen-presenting cells. *Immunity* **38**, 729-741, doi:10.1016/j.immuni.2013.03.003 (2013).

212 Ayna, G. *et al.* ATP release from dying autophagic cells and their phagocytosis are crucial for inflammasome activation in macrophages. *PloS one* **7**, e40069, doi:10.1371/journal.pone.0040069 (2012).

213 Zitvogel, L., Kepp, O., Galluzzi, L. & Kroemer, G. Inflammasomes in carcinogenesis and anticancer immune responses. *Nature immunology* **13**, 343-351, doi:10.1038/ni.2224 (2012).

214 Ghiringhelli, F. *et al.* Activation of the NLRP3 inflammasome in dendritic cells induces IL-1beta-dependent adaptive immunity against tumors. *Nature medicine* **15**, 1170-1178, doi:10.1038/nm.2028 (2009).

215 Michaud, M. *et al.* Autophagy-dependent anticancer immune responses induced by chemotherapeutic agents in mice. *Science* **334**, 1573-1577, doi:10.1126/science.1208347 (2011).

216 Ko, A. *et al.* Autophagy inhibition radiosensitizes in vitro, yet reduces radioresponses in vivo due to deficient immunogenic signalling. *Cell death and differentiation* **21**, 92-99, doi:10.1038/cdd.2013.124 (2014).

217 Mandapathil, M. *et al.* Generation and accumulation of immunosuppressive adenosine by human CD4+CD25highFOXP3+ regulatory T cells. *The Journal of biological chemistry* **285**, 7176-7186, doi:10.1074/jbc.M109.047423 (2010).

218 Bell, C. W., Jiang, W., Reich, C. F., 3rd & Pisetsky, D. S. The extracellular release of HMGB1 during apoptotic cell death. *American journal of physiology. Cell physiology* **291**, C1318-1325, doi:10.1152/ajpcell.00616.2005 (2006).

219 Suzuki, Y. *et al.* Immunogenic tumor cell death induced by chemoradiotherapy in patients with esophageal squamous cell carcinoma. *Cancer research* **72**, 3967-3976, doi:10.1158/0008-5472.CAN-12-0851 (2012).

220 Robinson, S. N. *et al.* Mesenchymal stem cells in ex vivo cord blood expansion. *Best practice & research. Clinical haematology* **24**, 83-92, doi:10.1016/j.beha.2010.11.001 (2011).

221 Rocha, V. *et al.* Graft-versus-host disease in children who have received a cord-blood or bone marrow transplant from an HLA-identical sibling. Eurocord and International Bone Marrow Transplant Registry Working Committee on Alternative Donor and Stem Cell Sources. *The New England journal of medicine* **342**, 1846-1854, doi:10.1056/NEJM200006223422501 (2000).

222 Paulin, T. Importance of bone marrow cell dose in bone marrow transplantation. *Clinical transplantation* **6**, 48-54 (1992).

223 Alakel, N. *et al.* Direct contact with mesenchymal stromal cells affects migratory behavior and gene expression profile of CD133+ hematopoietic stem cells during ex vivo expansion. *Experimental hematology* **37**, 504-513, doi:10.1016/j.exphem.2008.12.005 (2009).

224 Jing, D. *et al.* Hematopoietic stem cells in co-culture with mesenchymal stromal cells--modeling the niche compartments in vitro. *Haematologica* **95**, 542-550, doi:10.3324/haematol.2009.010736 (2010).

225 Mareschi, K. *et al.* Isolation of human mesenchymal stem cells: bone marrow versus umbilical cord blood. *Haematologica* **86**, 1099-1100 (2001).

226 Wexler, S. A. *et al.* Adult bone marrow is a rich source of human mesenchymal 'stem' cells but umbilical cord and mobilized adult blood are not. *British journal of haematology* **121**, 368-374 (2003).

227 Musina, R. A., Bekchanova, E. S., Belyavskii, A. V., Grinenko, T. S. & Sukhikh, G. T. Umbilical cord blood mesenchymal stem cells. *Bulletin of experimental biology and medicine* **143**, 127-131 (2007).

228 Breems, D. A. *et al.* Stroma-contact prevents loss of hematopoietic stem cell quality during ex vivo expansion of CD34+ mobilized peripheral blood stem cells. *Blood* **91**, 111-117 (1998).

229 Balduini, A., Braun, S. E., Cornetta, K., Lyman, S. & Broxmeyer, H. E. Comparative effects of retroviral-mediated gene transfer into primary human stromal cells of Flt3-ligand, interleukin 3 and GM-CSF on production of cord blood progenitor cells in long-term culture. *Stem cells* **16 Suppl 1**, 37-49, doi:10.1002/stem.5530160807 (1998).

230 Nishioka, K. *et al.* Immortalization of bone marrow-derived human mesenchymal stem cells by removable simian virus 40T antigen gene: analysis of the ability to support expansion of cord blood hematopoietic progenitor cells. *International journal of oncology* **23**, 925-932 (2003).

231 Erices, A., Conget, P. & Minguell, J. J. Mesenchymal progenitor cells in human umbilical cord blood. *British journal of haematology* **109**, 235-242 (2000).

232 Goodwin, H. S. *et al.* Multilineage differentiation activity by cells isolated from umbilical cord blood: expression of bone, fat, and neural markers. *Biology of blood and marrow transplantation : journal of the American Society for Blood and Marrow Transplantation* **7**, 581-588 (2001).

233 Lee, O. K. *et al.* Isolation of multipotent mesenchymal stem cells from umbilical cord blood. *Blood* **103**, 1669-1675, doi:10.1182/blood-2003-05-1670 (2004).

234 Bieback, K., Kern, S., Kluter, H. & Eichler, H. Critical parameters for the isolation of mesenchymal stem cells from umbilical cord blood. *Stem cells* **22**, 625-634, doi:10.1634/stemcells.22-4-625 (2004).

235 Romanov, Y. A., Svintsitskaya, V. A. & Smirnov, V. N. Searching for alternative sources of postnatal human mesenchymal stem cells: candidate MSC-like cells from umbilical cord. *Stem cells* **21**, 105-110, doi:10.1634/stemcells.21-1-105 (2003).

236 Frimberger, A. E. *et al.* The fleet feet of haematopoietic stem cells: rapid motility, interaction and proteopodia. *British journal of haematology* **112**, 644-654 (2001).

237 Patchen, M. L., MacVittie, T. J., Williams, J. L., Schwartz, G. N. & Souza, L. M. Administration of interleukin-6 stimulates multilineage hematopoiesis and accelerates recovery from radiation-induced hematopoietic depression. *Blood* **77**, 472-480 (1991).

238 Corre, I., Pineau, D. & Hermouet, S. Interleukin-8: an autocrine/paracrine growth factor for human hematopoietic progenitors acting in synergy with colony stimulating factor-1 to promote monocyte-macrophage growth and differentiation. *Experimental hematology* **27**, 28-36 (1999).

239 Weimar, I. S. *et al.* Hepatocyte growth factor/scatter factor (HGF/SF) affects proliferation and migration of myeloid leukemic cells. *Leukemia* **12**, 1195-1203 (1998).

240 Bramono, D. S., Rider, D. A., Murali, S., Nurcombe, V. & Cool, S. M. The effect of human bone marrow stroma-derived heparan sulfate on the ex vivo expansion of human cord blood hematopoietic stem cells. *Pharmaceutical research* **28**, 1385-1394, doi:10.1007/s11095-010-0352-y (2011).

241 Bhatia, R. *et al.* A clinically suitable ex vivo expansion culture system for LTC-IC and CFC using stroma-conditioned medium. *Experimental hematology* **25**, 980-991 (1997).

242 Hashimoto, F., Sugiura, K., Inoue, K. & Ikehara, S. Major histocompatibility complex restriction between hematopoietic stem cells and stromal cells in vivo. *Blood* **89**, 49-54 (1997).

243 Sugiura, K. *et al.* Major histocompatibility complex restriction between hematopoietic stem cells and stromal cells in vitro. *Stem cells* **19**, 46-58, doi:10.1634/stemcells.19-1-46 (2001).

244 Mizokami, T. *et al.* Preferential expansion of human umbilical cord blood-derived CD34-positive cells on major histocompatibility complex-matched amnion-derived mesenchymal stem cells. *Haematologica* **94**, 618-628, doi:10.3324/haematol.2008.004705 (2009).

245 Rebulla, P. Cord blood banking 2002: 112,010 of 7,914,773 chances. *Transfusion* **42**, 1246-1248 (2002).

246 Berz, D., McCormack, E. M., Winer, E. S., Colvin, G. A. & Quesenberry, P. J. Cryopreservation of hematopoietic stem cells. *American journal of hematology* **82**, 463-472, doi:10.1002/ajh.20707 (2007).

247 Bueno, C., Montes, R. & Menendez, P. The ROCK inhibitor Y-27632 negatively affects the expansion/survival of both fresh and cryopreserved cord blood-derived CD34+ hematopoietic progenitor cells: Y-27632 negatively affects the expansion/survival of CD34+HSPCs. *Stem cell reviews* **6**, 215-223, doi:10.1007/s12015-010-9118-5 (2010).

248 Welch, W. J., Kang, H. S., Beckmann, R. P. & Mizzen, L. A. Response of mammalian cells to metabolic stress; changes in cell physiology and structure/function of stress proteins. *Current topics in microbiology and immunology* **167**, 31-55 (1991).

249 Heng, B. C. Effect of Rho-associated kinase (ROCK) inhibitor Y-27632 on the post-thaw viability of cryopreserved human bone marrow-derived mesenchymal stem cells. *Tissue & cell* **41**, 376-380, doi:10.1016/j.tice.2009.01.004 (2009).

250 de Boer, F. *et al.* Early apoptosis largely accounts for functional impairment of CD34+ cells in frozen-thawed stem cell grafts. *Journal of hematotherapy & stem cell research* **11**, 951-963, doi:10.1089/152581602321080619 (2002).

251 de Boer, F. *et al.* Extensive early apoptosis in frozen-thawed CD34-positive stem cells decreases threshold doses for haematological recovery after autologous peripheral blood progenitor cell transplantation. *Bone marrow transplantation* **29**, 249-255, doi:10.1038/sj.bmt.1703357 (2002).

252 Stroh, C. *et al.* The role of caspases in cryoinjury: caspase inhibition strongly improves the recovery of cryopreserved hematopoietic and other cells. *FASEB journal : official publication of the Federation of American Societies for Experimental Biology* **16**, 1651-1653, doi:10.1096/fj.02-0034fje (2002).

253 Sasnoor, L. M., Kale, V. P. & Limaye, L. S. Prevention of apoptosis as a possible mechanism behind improved cryoprotection of hematopoietic cells by catalase and trehalose. *Transplantation* **80**, 1251-1260 (2005).

254 Baharvand, H., Salekdeh, G. H., Taei, A. & Mollamohammadi, S. An efficient and easy-to-use cryopreservation protocol for human ES and iPS cells. *Nature protocols* **5**, 588-594, doi:10.1038/nprot.2009.247 (2010).

255 Gauthaman, K., Fong, C. Y. & Bongso, A. Effect of ROCK inhibitor Y-27632 on normal and variant human embryonic stem cells (hESCs) in vitro: its benefits in hESC expansion. *Stem cell reviews* **6**, 86-95, doi:10.1007/s12015-009-9107-8 (2010).

256 Gauthaman, K., Fong, C. Y., Subramanian, A., Biswas, A. & Bongso, A. ROCK inhibitor Y-27632 increases thaw-survival rates and preserves stemness and differentiation potential of human Wharton's jelly stem cells after cryopreservation. *Stem cell reviews* **6**, 665-676, doi:10.1007/s12015-010-9184-8 (2010).

257 Fleming, K. K. & Hubel, A. Cryopreservation of hematopoietic and non-hematopoietic stem cells. *Transfusion and apheresis science : official journal of the World Apheresis Association : official journal of the European Society for Haemapheresis* **34**, 309-315, doi:10.1016/j.transci.2005.11.012 (2006).

258 Hayakawa, J. *et al.* 5% dimethyl sulfoxide (DMSO) and pentastarch improves cryopreservation of cord blood cells over 10% DMSO. *Transfusion* **50**, 2158-2166, doi:10.1111/j.1537-2995.2010.02684.x (2010).

259 Huang, Y. C., Parolini, O., La Rocca, G. & Deng, L. Umbilical cord versus bone marrow-derived mesenchymal stromal cells. *Stem cells and development* **21**, 2900-2903, doi:10.1089/scd.2012.0216 (2012).

260 Hanna, J. & Hubel, A. Preservation of stem cells. *Organogenesis* **5**, 134-137 (2009).

261 Al-Anazi, K. A. Autologous Hematopoietic Stem Cell Transplantation for Multiple Myeloma without Cryopreservation. *Bone marrow research* **2012**, 917361, doi:10.1155/2012/917361 (2012).

262 Sasnoor, L. M., Kale, V. P. & Limaye, L. S. Supplementation of conventional freezing medium with a combination of catalase and trehalose results in better protection of surface molecules and functionality of hematopoietic cells. *Journal of hematotherapy & stem cell research* **12**, 553-564, doi:10.1089/152581603322448268 (2003).

263 Limaye, L. S. & Kale, V. P. Cryopreservation of human hematopoietic cells with membrane stabilizers and bioantioxidants as additives in the conventional freezing medium. *Journal of hematotherapy & stem cell research* **10**, 709-718, doi:10.1089/152581601753193931 (2001).

264 Garin, M. I., Apperley, J. F. & Melo, J. V. Ex vivo expansion and characterisation of CD34+ cells derived from chronic myeloid leukaemia bone marrow and peripheral blood, and from normal bone marrow and mobilised peripheral blood. *European journal of haematology* **64**, 85-92 (2000).

265 Hamann, K. J., Dowling, T. L., Neeley, S. P., Grant, J. A. & Leff, A. R. Hyaluronic acid enhances cell proliferation during eosinopoiesis through the CD44 surface antigen. *Journal of immunology* **154**, 4073-4080 (1995).

266 Lemoli, R. M. *et al.* Interleukin-11 stimulates the proliferation of human hematopoietic CD34+ and CD34+CD33-DR- cells and synergizes with stem cell factor, interleukin-3, and granulocyte-macrophage colony-stimulating factor. *Experimental hematology* **21**, 1668-1672 (1993).

267 Sasnoor, L. M., Kale, V. P. & Limaye, L. S. A combination of catalase and trehalose as additives to conventional freezing medium results in improved cryoprotection of human hematopoietic cells with reference to in vitro migration and adhesion properties. *Transfusion* **45**, 622-633, doi:10.1111/j.0041-1132.2005.04288.x (2005).

268 Clarke, D. M., Yadock, D. J., Nicoud, I. B., Mathew, A. J. & Heimfeld, S. Improved post-thaw recovery of peripheral blood stem/progenitor cells using a novel intracellular-like cryopreservation solution. *Cytotherapy* **11**, 472-479, doi:10.1080/14653240902887242 (2009).

269 Durand, E. M. & Zon, L. I. Newly emerging roles for prostaglandin E2 regulation of hematopoiesis and hematopoietic stem cell engraftment. *Current opinion in hematology* **17**, 308-312, doi:10.1097/MOH.0b013e32833a888c (2010).

270 Hoggatt, J., Singh, P., Sampath, J. & Pelus, L. M. Prostaglandin E2 enhances hematopoietic stem cell homing, survival, and proliferation. *Blood* **113**, 5444-5455, doi:10.1182/blood-2009-01-201335 (2009).